

Anduaem Damtew Hamza

Analysis of the potential of nonlinear solvent gradients in preparative chromatography



Fakultät für Verfahrens- und Systemtechnik
Otto-von-Guericke-Universität Magdeburg

Analysis of the potential of nonlinear solvent gradients in preparative chromatography

Dissertation

zur Erlangung des akademischen Grades

**Doktoringenieur
(Dr.-Ing.)**

von MSc. **Anduaem Damtew Hamza**

geb. am 17/08/1975 in Dessie, Äthiopien

genehmigt durch die Fakultät für Verfahrens- und Systemtechnik
der Otto-von-Guericke-Universität Magdeburg

Gutachter:

Prof. Dr.-Ing. Andreas Seidel-Morgenstern
Prof. Dr. rer. nat. Franziska Scheffler

Promotionskolloquium am 04. June 2010

Abstract

In this thesis the potential of modulating solvent composition during chromatographic separation is investigated theoretically and experimentally. Hereby main focus is set on evaluating the potential of nonlinear gradient profiles in preparative liquid elution chromatography. As a case study was analysed the isolation of the second eluting component from a ternary mixture. Based on an experimental investigation, the changing thermodynamic equilibria and the effect of the gradient profiles on the shape of the elution profiles were studied theoretically. A reversed phase system was used with binary solvent mixtures of water and methanol to form the gradients. Thereby simulation and experimental verification of applying nonlinear gradients for the separation of ternary mixtures were performed.

To quantify the isolation of components in the middle of an elution train, a careful selection of the cut times is required. In order to fulfil this task, a suitable procedure was developed in this study. The separation of the middle component of a ternary mixture resembles a more general separation problem of multi-component mixtures, where the target component needs to be separated from neighbouring components. Thus, the results of this study can be easily extended to optimize separations of multi-component mixtures.

In the course of the work, at first adsorption isotherm parameters were estimated for a ternary mixture of three cycloketones considered as a model system. The effect of solvent compositions on these parameters was described mathematically. Gradient profiles were described mathematically as a function of time and a gradient shape factor. Four cases, differing by the number of free parameters, were considered to investigate the potential of nonlinear solvent gradients. The Craig equilibrium stage model was used to predict the band profiles and to quantify and compare different modes of operation (isocratic and various variants of gradient elution). Optimal operating conditions were identified theoretically for the production of cyclohexanone. The strong impact of the shape of gradients on process performance was elucidated. In the optimizations an artificial neural network method was used successfully. Finally, selected predictions were validated experimentally for optimal cases.

Zusammenfassung

In der vorliegenden Arbeit wurde das Potential der gezielten Modulation der Lösungsmittelzusammensetzung während chromatographischer Trennprozesse theoretisch und experimentell untersucht. Der Schwerpunkt wurde hierbei auf die Beurteilung des Potentials nichtlinearer Gradientenprofile in der präparativen Flüssigchromatographie gesetzt. Als Fallstudie wurde die Isolierung der als zweites eluierenden Komponente in einem ternären Gemisch analysiert. Aufbauend auf experimentellen Untersuchungen wurden sowohl die sich ändernden thermodynamischen Gleichgewichte als auch der Effekt der Gradienten auf die Elutionsprofile theoretisch studiert. Zur Ausbildung der Gradienten wurde ein so genanntes „reversed phase system“ unter Verwendung von binären Lösungsmittelgemischen bestehend aus Wasser und Methanol verwendet. Auf diese Weise wurden sowohl Simulationen wie auch experimentelle Verifizierungen bezüglich der Anwendung nichtlinearer Gradienten für die Trennung ternärer Gemische durchgeführt.

Zur Quantifizierung der Isolierung von mittleren Komponenten in einer Elutionsfolge ist eine sorgfältige Wahl der Fraktionierzeitpunkte erforderlich. Zu deren Bestimmung wurde in der vorliegenden Studie ein geeignetes Verfahren entwickelt. Die Trennung einer Mittelkomponente in einem ternären Gemisch ähnelt dem allgemeineren Trennungsproblem in einem Mehrkomponentengemisch, in dem die Zielkomponente von Nachbarkomponenten abgetrennt werden muss. Die Ergebnisse der vorliegenden Studie können daher einfach erweitert werden, um auch die Trennung von Mehrkomponentenmischungen zu optimieren.

Im Verlauf der Arbeit wurden zunächst die Parameter der Adsorptionsisothermen eines ternären Modellsystems bestehend aus drei Cycloketonen bestimmt. Der Einfluss der Lösungsmittelzusammensetzung auf diese Parameter wurde mathematisch beschrieben. Die Gradientenprofile wurden mathematisch sowohl als Funktion der Zeit wie auch als Funktion eines Parameter zur Beschreibung der Gradientenform dargestellt. Zur Untersuchung des Potentials nichtlinearer Lösungsmittelgradienten wurden vier Fälle betrachtet, die sich hinsichtlich der Anzahl der freien Parameter unterschieden. Das Gleichgewichtsstufenmodell von Craig

wurde zum Einen zur Vorhersage der Elutionsprofile und zum Anderen zur Quantifizierung und zum Vergleich verschiedener Betriebsweisen (isokratisch und verschiedene Varianten der Gradientenelution) verwendet. Für die Produktion von Cyclohexanon wurden theoretisch optimale Betriebsbedingungen identifiziert. Der starke Einfluss der Form der Gradienten auf die Prozessleistung wurde untersucht. Bei den durchgeführten Optimierungen konnte ein künstliches neuronales Netz erfolgreich eingesetzt werden. Abschließend wurden ausgewählte Vorhersagen bezüglich optimaler Fälle experimentell validiert.

Acknowledgments

First of all I would like to thank the Almighty God for giving me the patience and wisdom to successfully finish my study.

I am very grateful for the support, guidance and supervision of Prof. Andreas Seidel-Morgenstern, his assistance was so vital that without his support I could not have even managed to finish this work. I would also like to thank Prof. Franziska Scheffler for her time to review my Dissertation and give valuable comments. Thanks to Prof. Evangelos Tsotsas for chairing the examination commission.

My gratitude also goes to my colleagues in the CPG and CVT research groups of the Otto-von-Guericke University and Max-Planck Institute of Magdeburg, specially to Dr. Hamel, Mrs Chrobog, Marion, Ludmila, Duc, Tino and Samuel.

The financial support of the Otto-von-Guericke University Magdeburg and the Max-Planck institute of Magdeburg is greatly appreciated.

I like to extend my heartfelt thanks to my beloved friends and relatives: Red, Bizu, Woyeni, Wossity, Mimicho, Emu, Ato Ahunm, Solomon, Dr. Alebel, Dr. Taye, Emebet, Lili, Mrs. Ingrid and Mr. Rolf Nagel, Beamlak, Zerihun, and others for their love and being with me when I needed them.

I extend my deepest gratitude to my mum w/ro Tsehaynesh Mengesha for her love and support.

Finally I dedicate this work to my father Ato Damtew Hamza whom I lost him at the beginning of my study.

Contents

1. Introduction	1
1.1. History of chromatography.....	2
1.2. Motivation and goals.....	3
2. Chromatographic separation process	6
2.1. Classifications of chromatographic techniques	6
2.2. Basics of elution chromatography	11
2.2.1. Retention mechanism and column characteristics	12
2.2.2. Band broadening.....	14
2.3. Analytic vs. preparative chromatography	17
2.4. Batch vs. continuous chromatography	19
2.5. Isocratic vs. gradient elution chromatography.....	22
3. Mathematical models of chromatography	26
3.1. Equilibrium dispersion model	27
3.2. Craig's cell model.....	30
3.2.1. Numerical solution.....	32
3.3. Adsorption isotherm models.....	35
3.3.1. Single component isotherm models	36
3.3.2. Multi-component isotherm models	38
3.3.3. Effect of gradients on isotherms.....	39
4. Determination of adsorption isotherms	41
4.1. Single-component systems	41
4.1.1. Frontal analysis method	41
4.1.2. Elution by characteristics points (ECP) method	42
4.1.3. Perturbation method.....	43
4.1.4. Inverse method (peak fitting method).....	44
4.2. Multi-component systems.....	45
4.2.1. Inverse method (peak fitting method).....	46
5. Gradients	47
5.1. Solvent gradients.....	47
5.2. Gradient shapes	48
5.3. Instrumentation to form gradients	50

6. Optimization	52
6.1. Performance criteria	52
6.1.1. Objective functions	55
6.2. Collection strategies and determination of cut times	55
6.3. Optimization Methods	58
7. Experimental part	62
7.1 Materials and Equipment	62
7.1.1. Characterization of the system.....	62
7.1.2. Dead volumes	64
7.2. Characterization of the column and the detector.....	67
7.2.1. Column porosity	68
7.2.2. Number of theoretical plates	69
7.2.3. Detector calibration	69
7.3. Isotherms parameters of the model components	71
7.4. Realization of gradient profiles	72
8. Optimization problems formulated	75
8.1. Free parameters.....	75
8.2. Scenarios studied.....	76
8.2.1. Case 1 (isocratic, two degrees of freedom).....	76
8.2.2. Case 2 (pre-specified gradient shape, three degrees of freedom)	76
8.2.3. Case 3 (linear gradients, four degrees of freedom).....	77
8.2.4. Case 4 (five degrees of freedom).....	77
8.3. Optimization ranges and intervals.....	77
9. Results and discussion.....	80
9.1. System characterization	80
9.1.1. Dead volume measurement	80
9.1.2. Column porosity and efficiency	82
9.1.3. Calibration factors	83
9.2. Adsorption isotherms.....	84
9.3. Effect of modifier concentration on isotherms	89
9.4. Analysis of optimization scenarios.....	91
9.4.1. Theoretical analysis	91
9.4.1.1. Case 1	92
9.4.1.2. Case 2	93
9.4.1.3. Case 3	94
9.4.1.4. Case 4	96
9.4.2. Experimental validation	99
9.4.2.1. Case 1	99
9.4.2.2. Case 2	100
9.4.2.3. Case 4.....	102

10. Conclusions.....	104
Nomenclature	106
References	112
Appendix A (Matlab codes used for all the simulations)	117
Appendix B (Programming various forms of gradient profiles)	123
Appendix C (Calibration curves)	125
Appendix D (Theoretical plate numbers)	129
Appendix E (Overloaded peaks)	130
Curriculum vitae	

1. Introduction

Separation processes play a critical role in industry considering for example the separation of valuable pharmaceutical products, the removal of impurities from raw materials, the purification of products, the separation of recycle streams or the removal of contaminants from air and water pollutants. Overall separation processes account for 40-70 % of both capital and operating costs in industry and their proper application can significantly increase process performance and profits [Humph97].

Separation operations typically achieve their objectives by the creation of two or more special zones which differ in temperature, pressure, composition and / or phase state. Each molecular species in the mixture to be separated reacts in a unique way with the differing environments offered by these zones. As such a system moves towards equilibrium, the species establish different concentrations in each zone, and this results in separation between the species.

There are various separation techniques differing in the principles and simplicity of the process. Examples are distillation, chromatography, extraction, crystallization, membrane separation elutriation, etc. Among these separation techniques chromatography is widely applied in particular in pharmaceutical industry. The best use of this technique is currently a research topic of many scientists.

Depending on the primary aim, two main areas of chromatography are distinguished: analytic chromatography and preparative chromatography. In earlier times the use of chromatography has been limited only to analytic purposes aiming at identification of mixture components and deals with dilute solutions. However the necessity of separating very complex chemical mixtures having similar chemical and physical properties, and the difficulty of separating these mixtures with other separation techniques opens the door for further development and exploitation of preparative chromatography. Preparative chromatography can be used also as intermediate step for the collection of data.

In order to get the optimum productivity of a certain target component, different chromatographic techniques are used, ranging from batch separation to the state of

the art simulated moving bed (SMB) processes. Of course each of these processes has their own advantages and disadvantages.

1.1. History of chromatographic separation processes

The Russian botanist M. S. Tswett is generally credited with the discovery of chromatography around the turn of the last century [Guio06, Sakod72]. In his experiments, Tswett tamped a fine powder (e.g. sucrose, chalk) into a glass tube to produce a column of the desired height. Before starting the separation he extracted the pigments from the leaves and brought them into a petroleum ether solution. He then brought on top of the column a small volume of this solution. When the solution had percolated and a narrow initial zone beneath the top of the adsorbent had formed, fresh solvent (e.g. petroleum ether) was added and pressure applied to the top of the column. The solvent flowed through the column; the individual pigments moved at different rates and got separated from each other. He also coined the name chromatography (colour writing) from the Greek colour (*chroma*) and write (*graphien*) to describe the process. However, column liquid chromatography as described by Tswett was not an instant success, and it was not used until its rediscovery in the early 1930s that it became an established laboratory method.

With the progress made in the development of sensitive detection methods, an analytical and preparative chromatography parted in the late 1940s. The first major preparative chromatography projects were the purification of rare earth elements by the group of Speeding for the Manhattan project, and the isolation of pure hydrocarbons from crude oil by Mair et al for the American Petroleum Institute (API) project [Guio89]. Later followed the development of the simulated moving bed technology by Broughton for UOP [Brough84]. Finally in the 1980s, the pharmaceutical industry began to show interest in high performance preparative chromatography and this interest is still increasing currently.

Preparative chromatography as a separation process has been used for the first time in the early 1970th as Union Oil developed and patented a chromatographic system based on the principle of a simulated moving bed. Various corresponding plants have been built and are operated for the fractionation of various petroleum distillates.

In recent years, the use of semi-preparative and preparative chromatography has expanded considerably. Numerous applications have been reported, mostly in the pharmaceutical industry. The amounts of purified products required are compatible with the use of columns ranging from a few inches to a few feet in diameter. The purifications of enantiomers, peptides, and proteins are the most widely published applications [Guio06].

1.2. Motivation and goals of the work

Currently, in the chemical, pharmaceutical or bio processing industries the need to separate and purify a product from a complex mixture is a necessary and important step in the production line. Today, there exists a wide market of methods in which industries can accomplish these goals. In fact, chromatography can purify basically any soluble or volatile substance if the right adsorbent material, carrier fluid, and operating conditions are employed. Second, chromatography can be used to separate delicate products since the conditions under which the separations performed are typically not severe. For these reasons, chromatography is quite well suited to a variety of uses in the field of pharmaceutical and biotechnology.

To this end there are various techniques within chromatography to fulfil the demand of getting high precision separation of complex mixtures. Many liquid chromatography separations can be performed at constant operation conditions, but the desired resolution of complex samples containing compounds with great differences in the affinities to the stationary phase can often not be accomplished at a constant mobile phase composition (isocratic elution) or at a constant temperature (isothermal elution). This problem can often be solved by using programmed elution techniques, where the operation conditions change during the process to achieve adequate resolution for early eluting compounds while keeping acceptably short elution times for the later eluting compounds .

The aim of this work is to investigate and analyse the potential of solvent gradients focusing on nonlinear gradient profiles in preparative liquid chromatography for an optimized isolation of the second eluting component of a ternary mixture. Thus, optimum separation conditions of various gradient profiles were evaluated

theoretically and experimentally. Binary solvent mixtures were used to form gradients.

Earlier works have been devoted to the separation of binary mixtures using isocratic or linear gradient chromatography. However a recent theoretical study on the application of nonlinear gradients for an optimized separation of the middle component from a ternary mixture performed by Shan et al. [Shan05] has been the inspiration to further investigate the technique in this study.

Therefore in this work more emphasis has been given to the modelling, simulation and experimental verification of applying nonlinear gradients for the separation of ternary mixtures targeting the second eluting component. In case of binary mixtures the separation of either component may be treated only from one direction. In contrast, in case of multi component mixtures the separation of the intermediate component has to be treated from two directions when calculating the cut times during collection. Hereby the separation of the middle component of a ternary mixture resembles to the more general separation problem of multi component mixtures where the target component is affected by neighbouring components. Therefore we can say that ternary mixtures are model representatives of a multi component mixture. Thus, the results obtained by investigating such ternary system can easily be transformed to solve separation problems of multi-component mixtures.

An equilibrium stage model was used to quantify and compare different modes of operation (isocratic and various variants of gradient elution). In a first stage, optimal conditions were identified theoretically for the production of the second eluting component in a ternary mixture. The strong impact of the shape of gradients on process performance is elucidated. These predictions were validated experimentally using the separation of cyclopentanone, cyclohexanone and cycloheptanone on a RP-C18 stationary phase using mixtures of water and methanol with varying compositions as the mobile phase.

In Chapter 2 a summary of the general theory of chromatography is given. Then in Chapter 3, mathematical modelling of gradient chromatography and isotherm models are addressed. In Chapter 4, methods to determine isotherm parameters are presented. Chapter 5 focuses on describing mathematically linear and non linear gradient shapes. In Chapter 6 optimization techniques used for the separation of

ternary mixtures are presented. In Chapter 7 experimental analysis was performed followed by a short summary of the different case studies in Chapter 8. Finally In chapters 9 and 10, the results obtained are analysed and summarized followed by the conclusions this work.

2. Chromatographic separation processes

Due to the broad spectrum (interdisciplinary nature) of chromatography, various definitions are given by different authors [Poole03]. A concise definition of chromatography might be as follows: Chromatography is a sorptive separation process where a portion of mixture (feed) is introduced at the inlet of the column containing a selective adsorbent (stationary phase) and separated over the length of the column by the action of a carrier fluid (mobile phase) that is continuously supplied to the column following the introduction of the feed. In elution chromatography the mobile phase is generally free of the feed components, but may contain various other species introduced to modulate the chromatographic separation [Perry97].

This definition suggests that chromatographic separations have three distinct features: (a) they are physical methods of separation; (b) two distinct phases are involved, one of which is stationary while the other mobile; and (c) separation results from differences in the distribution constants of the individual sample components between the two phases. The definition could be broadened to allow for the fact that it is not essential that one phase is stationary, although this may be more experimentally convenient. What is important is either the rate of migration or the directions of migration of the two phases are different [Poole03].

Useful chromatographic separations require an adequate difference in the strength of physical interactions for the sample components in the two phases, combined with a favourable contribution from system transport properties that control the movement within and between phases. Several key factors are responsible, therefore, or act together, to produce an acceptable separation.

2.1. Classifications of chromatographic techniques

According to the state of aggregation of the fluid phase chromatographic systems can be divided into several categories. If the fluid phase is gaseous the process is called gas chromatography (GC).

If the fluid phase is a liquid the process is called liquid chromatography (LC). For a liquid kept at temperature and pressure conditions above its critical point the process

is called supercritical-fluid chromatography (SFC). Liquid chromatography can be further divided according to the geometrical orientation of the phases.

A widely used process for analytical purposes as well as rapid method development and, in some cases, even a preparative separation process is thin-layer chromatography (TLC). The adsorbent is fixed onto a support (glass, plastic or aluminium foil) in a thin layer. The feed mixture is placed onto the adsorbent in small circles or lines. In a closed chamber one end of the thin-layer plate is dipped into the mobile phase, which then progresses along the plate due to capillary forces [Miller05].

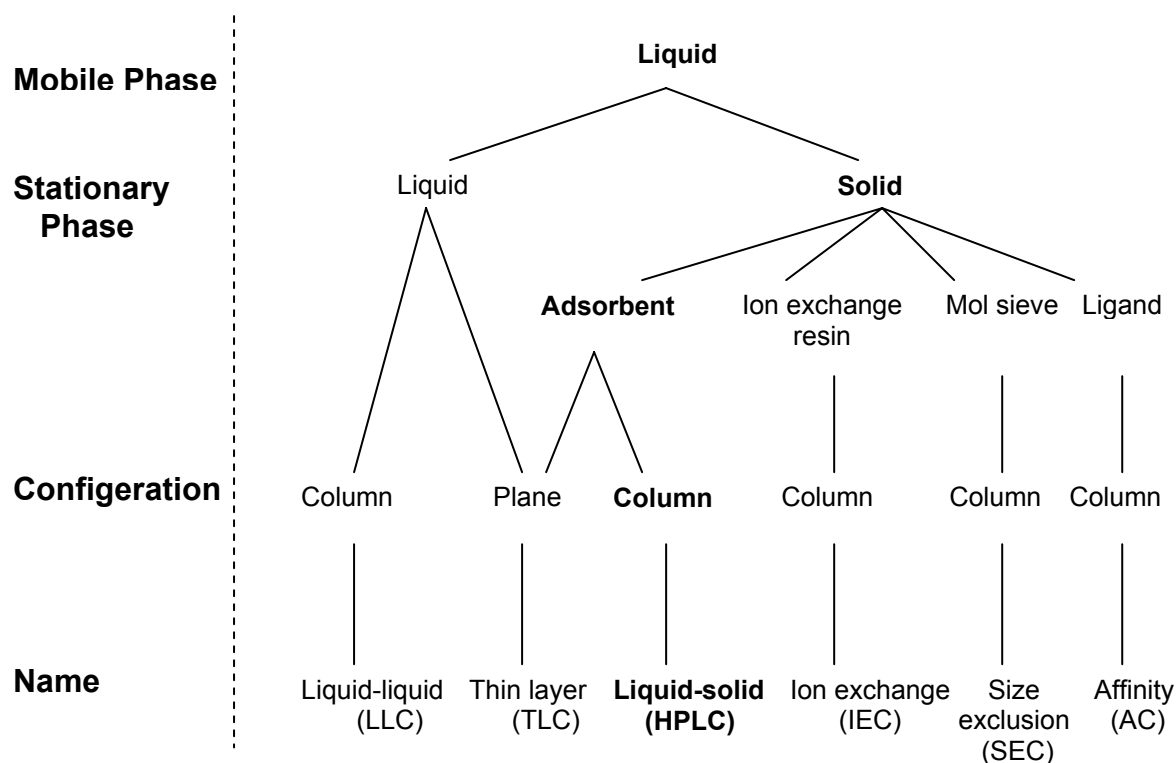


Figure 2.1. Classifications of chromatographic techniques for a liquid mobile phase.

(In bold: technique used in this work)

Figure 2.1 shows a complete classification scheme for Liquid –Solid and Liquid-Liquid chromatography listing the popular names and abbreviations.

Individual substances can be visualized by either fluorescence quenching or after chemical reaction with detection reagents.

In GC and LC the adsorbent is fixed into a cylinder (column) that is usually made of glass, polymer or stainless steel. In this column the adsorbent is present as a porous or non-porous randomly arranged packing or as a monolithic block. Because of the high separation efficiency of packed columns made of small particles this type of chromatography is called high-performance liquid chromatography.

Chromatographic behaviour is determined by the interaction of all single components in the mobile and stationary phases. The mixture of substances to be separated in LC (the solute), the solvent, which is used for their dissolution and transport (eluent), and the adsorbent (stationary phase) are summarized as the chromatographic system [Traub05].

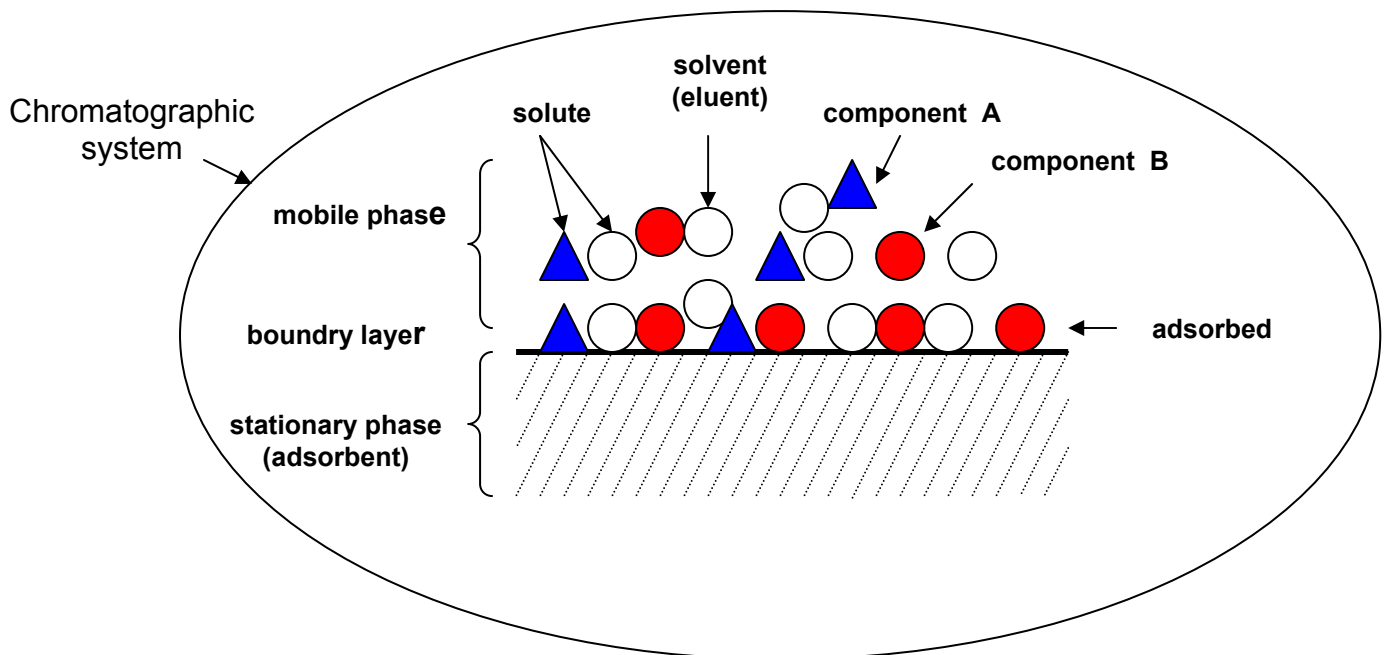


Figure 2.2. Definition of adsorption and chromatographic system

On a molecular level the adsorption process is the formation of binding forces between the surface of the adsorbents surface and the molecules of the fluid phase. The binding forces can be different in nature and, therefore, of different strength. Hence the energetic balance of the binding influences the adsorption equilibrium, which can also be very different in strength. Basically, two different types of binding forces can be distinguished [Atkins90].

a. Physisorption (physical adsorption): is a weak binding based typically on van der Waals forces, e.g. dipole, dispersion or induction forces. These forces are weaker than the intramolecular binding forces of molecular species. Therefore, physisorbed molecules maintain their chemical identity.

b. Chemisorption (chemical adsorption): is a stronger binding type caused by valence forces, equivalent to chemical, mainly covalent, bindings. The energy of the free adsorbent valences is strong enough to break the atomic forces between the adsorbed molecules and the adsorbent.

In chromatography, transport of solute zones occurs entirely in the mobile phase. Transport is an essential component of the chromatographic system since the common arrangement for the experiment employs a sample inlet and a detector at opposite ends of the column with sample introduction and detection occurring in the mobile phase. There are three basic approaches for achieving selective zone migration in column chromatography, (see, Figure 2.3).

In *frontal chromatography*, the sample is introduced continuously onto the column as a component of the mobile phase. Each solute is retained to a different extent as it reaches equilibrium with the stationary phase until eventually, the least retained solute exits the column followed by other zones in turn, each of which contains several components identical to the solutes in the zone eluting before it [Poole03]. Ideally the detector output will be comprised of a series of rectangular steps of increasing height. Frontal analysis is used to determine sorption isotherms for single component and to isolate a less strongly retained trace component from a major component. Quantification of each component in a mixture is difficult and at the end of the experiment, the column is contaminated by the sample. For these reasons frontal analysis is used only occasionally for separations.

In *displacement chromatography* the sample is applied to the column as a discrete band and a substance (or mobile phase component) with a higher affinity for the stationary phase than any of the sample components, called the displacer, is continuously passed through the column. The displacer pushes sample components down the column and, if the column is long enough, a steady state is reached and a succession of rectangular bands of pure components exit the column. Each component displaces the component ahead of it, with the last and most strongly retained component being forced along by the displacer. At the end of the separation

the displacer must be stripped from the column if the column is to be reused [Poole03].

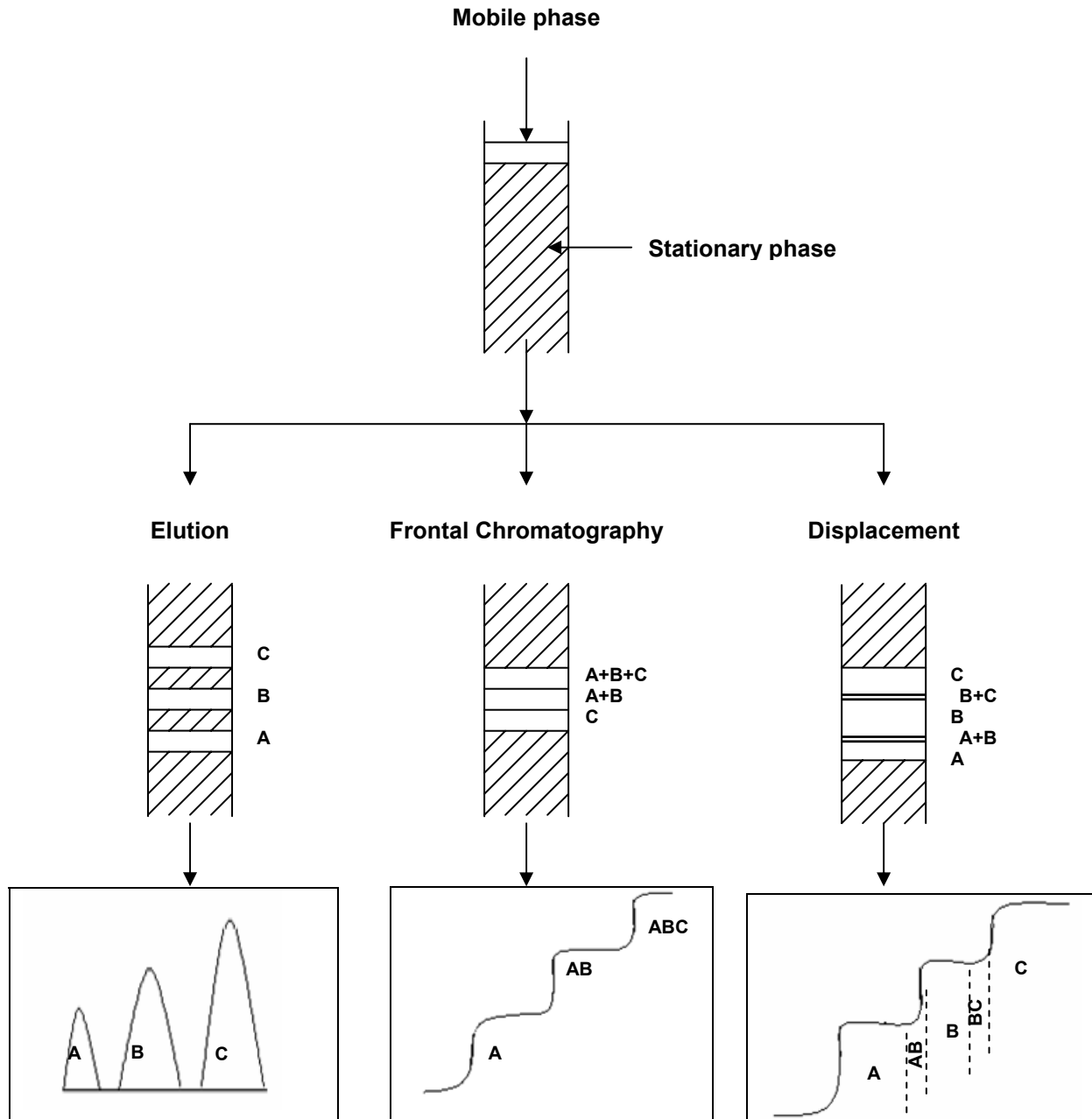


Figure 2.3. Mode of zone migration in column chromatography

In *elution chromatography*, the mobile and stationary phases are normally at equilibrium. The sample is applied to the column as a discrete band and sample components are successively eluted from the column diluted by mobile phase. The

mobile phase must compete with the stationary phase for the sample components and for a separation the distribution constants for the sample components resulting from the competition must be different. Elution chromatography is the most convenient method for analysis and is commonly used in preparative chromatography. As gradient elution chromatography is the focus of this study, it is discussed in more detail subsequent sections.

2.2. Basics of elution chromatography

As it is defined in previous sections, chromatography is a separation process based on the difference between the migration velocities of the different components of a mixture when they are carried by a stream of fluid percolating through a bed of solid particles. The fluid and the solid phases constitute the chromatography system. Between the two phases of this system, phase equilibrium is reached for all the components of the mixture. The separation may be successful if the equilibrium constants of all these components have 'reasonable different' values. If they are too small for some components, these compounds travel at a velocity too close to that of the mobile phase and their complete separation may not be possible. If these constants are too large, the corresponding components do not leave the column or leave it so late and in bands that are so diluted that no useful purpose can be achieved. Temperature, the nature of the solid surface, the nature and composition of the mobile phase and the nature of the components to be separated together control these equilibrium constants. All particles used in preparative chromatography are porous and penetrable by the molecules of the compounds investigated, in order to maximize the capacity of the corresponding column and to allow the handling and the separation of large samples. If phase equilibrium is reached rapidly, then best results are obtained. This requires the percolation of the mobile phase through a homogeneously packed bed of porous particles. Thus, the particles should be sufficiently small to ensure a rapid diffusion of the component molecules into these particles and back out to the bulk mobile phase which conveys along the column the batch of product separated. Then, elution chromatography is a procedure in which the mobile phase is continuously passed through or along the chromatographic bed and the sample is fed into the system in a definite slug. This chromatographic

process is also known as batch chromatography, since samples are applied periodically in narrow zones [Ettre93].

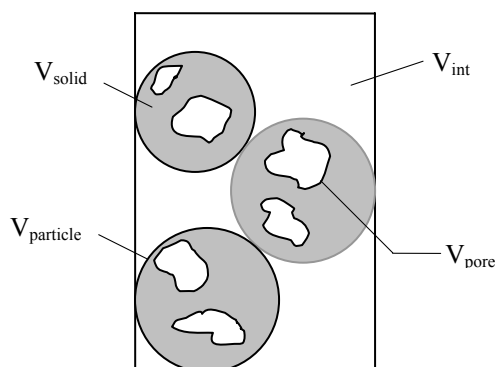
2.2.1. Retention mechanisms and column characteristics

In general, HPLC is a dynamic adsorption process. Analyte molecules, while moving through the porous packed column, tend to interact with the surface adsorption sites. Depending on the HPLC mode, different types of adsorption forces may be included in the retention process. Hydrophobic interactions are the main ones in a reversed phase system, dipole-dipole (polar) interactions are dominant in normal phase mode and ionic interactions are responsible for the retention in ion-exchange chromatography [Traub05].

All these interactions are competitive. Analyte molecules compete with the eluent molecules for the adsorption sites. So, the stronger the analyte molecules interact with the surface, the weaker the eluent interaction, and then the analyte will be retained for longer time (having higher retention time) on the surface. Whereas in size-exclusion chromatography (SEC) any positive surface interactions should be avoided (eluent molecules should have much stronger interaction with the surface than analyte molecules). Thus, the basic principle of SEC separation is that the bigger the molecule, the less possibility to penetrate into the adsorbent pore space, the bigger the molecule the less it will be retained.

a) Voidage and porosity

The total volume of a packed column (V_c) consists of the interstitial volume (V_{int}) between the particles and the volume of the stationary phase (V_{sta}). Beside that, the volume of the stationary phase contains the volume of the solid and the pore volume [Traub05].



Where :

V_{int} : interstitial volume

V_{pore} : pore volume

$V_{particle}$: particle volume

V_{solid} : solid volume

Figure 2.4. Cross section of packed column.

The volume of the column is the sum of the volume of particle and the interstitial volume:

$$V_c = \pi \frac{d_{col}^2}{4} L_{col} = V_{particle} + V_{int} \quad (2.1)$$

where d_{col} and L_{col} are diameter and length of the column respectively.

As mentioned above, the volume of the particle consists of the volume of the solid and volume of the pores:

$$V_{particle} = V_{solid} + V_{pore} \quad (2.2)$$

From these different volumes, corresponding porosities are calculated:

Void fraction:

$$\varepsilon_v = \frac{V_{int}}{V_{col}} \quad (2.3)$$

Porosity of the particle:

$$\varepsilon_p = \frac{V_{pore}}{V_{particle}} \quad (2.4)$$

Finally the total porosity:

$$\varepsilon = \frac{V_{int} + V_{pore}}{V_{col}} = \varepsilon_v + (1 - \varepsilon_v) * \varepsilon_p \quad (2.5)$$

Experimental estimation of the total porosity is discussed in Chapter 8.

b) Retention time

The time between sample injection and an analyte peak of component i reaching a detector at the end of the column is termed the retention time ($t_{R,i}$). It can be calculated with Eq. 2.6. Each analyte in a sample can have a different retention time. The time taken for non absorbable mobile phase to pass through the column is referred in this work as t_d :

$$t_{R,i} = t_d \left(1 + \left(\frac{1 - \varepsilon}{\varepsilon} \right) K_{H,i} \right) \quad (2.6)$$

Where $K_{H,i}$ is Henry's constant of component i which is discussed in section 3.3.1.

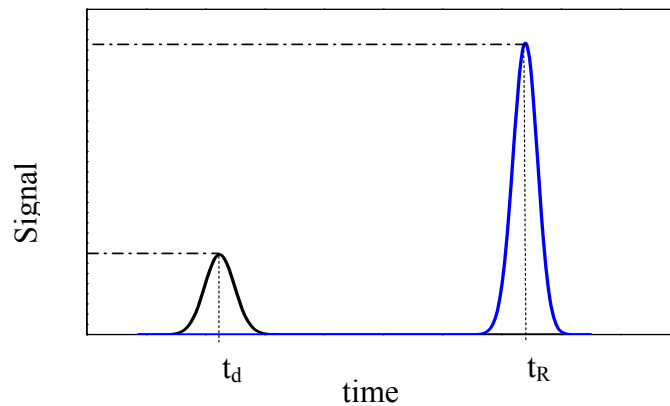


Figure 2.4. Retention time, t_R , and time taken for a non absorbable substance to pass through the column, t_d .

c) Capacity factor

A term called the capacity factor of component i , k'_i , is often used to describe the migration rate of an analyte on a column. You may also find it called the retention factor. The capacity or retention factor for component i is defined as:

$$k'_i = \left(\frac{t_{R,i} - t_d}{t_d} \right) \quad (2.7)$$

2.2.2. Band broadening

To obtain optimal separations, sharp, symmetrical chromatographic peaks must be obtained. This means that band broadening must be limited. It is also beneficial to quantify the efficiency of a column. The theoretical plate model supposes that the chromatographic column contains a large number of hypothetically separated layers, called *theoretical plates*. Separate equilibrations of the sample between the stationary and mobile phase occur in these "plates".

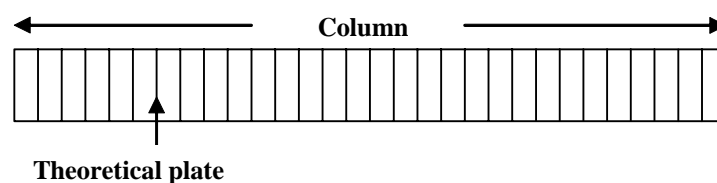


Figure 2.5. Column showing the hypothetical theoretical plates.

The analyte moves down the column by transfer of equilibrated mobile phase from one plate to the next.

They are a figment of the imagination that helps us to understand the processes at work in the column. They also serve as a way of measuring column efficiency, by stating a number of theoretical plates in a column, N (the more plates the better), or by stating the corresponding plate height H ; the Height Equivalent to a Theoretical Plate (the smaller the better).

If the length of the column is L , then H is:

$$H = \frac{L}{N} \quad (2.8)$$

The number of theoretical plates that a real column possesses can be found by examining a chromatographic peak after elution [Deem56];

$$N = \frac{5.55t_R^2}{w_{1/2}^2} \quad (2.9)$$

where $w_{1/2}$ is the peak width at half-height.

As can be seen from this equation, columns behave as if they have different numbers of plates for different solutes in a mixture. These numbers vary for different mobile phase compositions.

A more realistic description of the processes at work inside a column takes account of the time taken for the solute to equilibrate between the stationary and mobile phase (unlike the plate model, which assumes that equilibration is infinitely fast). The resulting band shape of a chromatographic peak is therefore affected by the rates of binding and elution. It is also affected by the different path lengths available to solute molecules as they travel between particles of stationary phase. If one considers the various mechanisms which contribute to band broadening, the famous Van Deemter equation can be derived describing the by plate height by [Deem56, Guio03, Traub05];

$$H = A + B/u + Cu \quad (2.10)$$

where u is the average velocity of the mobile phase. A , B , and C are factors which quantify different effects causing band broadening.

A-Eddy diffusion: - The mobile phase moves through the column which is packed with stationary phase. Solute molecules will take different path ways through the stationary phase randomly.

B- Longitudinal diffusion: - refers to the diffusion of individual analyte molecules in the mobile phase along the longitudinal direction of a column. Longitudinal diffusion contributes to peak broadening only at very low flow rates below the minimum (optimum) plate height.

C- Resistance to mass transfer: - The analyte takes a certain amount of time to equilibrate between the stationary and mobile phase. If the velocity of the mobile phase is high, and the analyte has a strong affinity for the stationary phase, then the analyte in the mobile phase will move ahead of the analyte in the stationary phase. The band of analyte is broadened. The higher the velocity of mobile phase, the worse the broadening becomes.

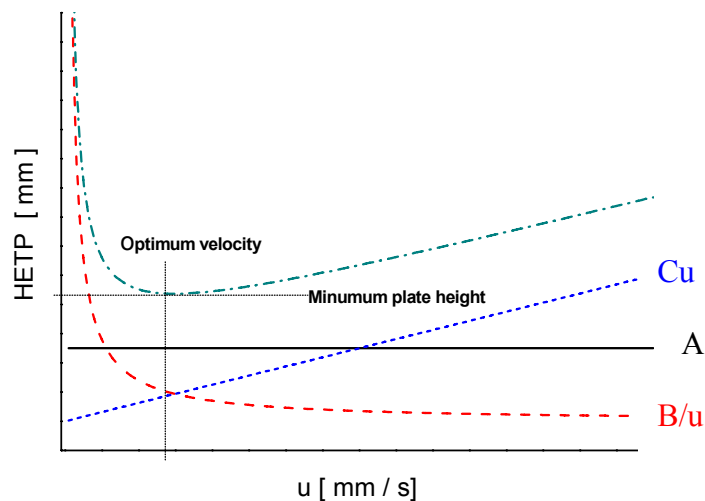


Figure 2.6. Van Deemter plot showing relationship between the column plate height and the mobile phase velocity for a packed column in liquid chromatography [Deem56, Guio03, Well06].

An important general contribution of the van Deemter equation was the illustration that an optimum mobile phase velocity existed for a column at which its highest efficiency could be realized. For less demanding separations columns may be operated at mobile phase velocities higher than the optimum value to obtain shorter separation times. This is in particular useful provided that the ascending portion of van Deemter's curve is fairly flat for higher velocities than the optimum velocity. Then the saving of time for a small loss of efficiency is often justified.

2.3. Analytic vs. preparative chromatography

Analytical chromatography is carried out with smaller quantities, (often as little as one microgram), in order to identify and quantify the concentrations of the components in a mixture. The technique was first used in the separation of coloured mixtures into their component pigments. In contrast preparative chromatography is carried out on a larger scale for the purification and collection of one or more of a mixture's constituents. That means in preparative chromatography, larger amounts of sample are usually injected and the usual goal is to recover as much purified product as possible in each run, i.e. in the shortest time and with the least costs and efforts. Figure 2.7 shows chromatograms for typical cases of analytic and preparative chromatography.

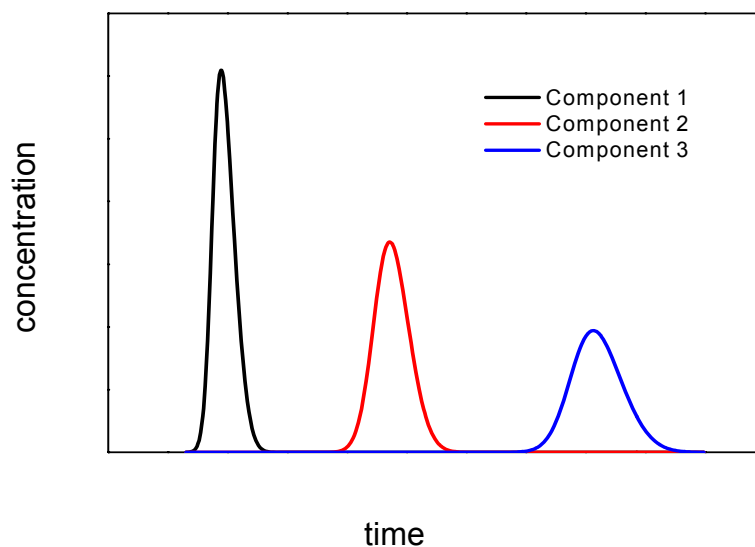
Therefore the main difference between analytical and preparative work is not defined by the size of either sample or equipment. It is exclusively determined by the „goal“ of the separation process. If “information” is the goal of the separation, it is analytical chromatography. If the “collection of products” is the intention, it is a preparative separation.

In an analytical mode, the sample can be processed, handled and modified in any way suitable to generate the required information, including degradation, labelling or otherwise changing the nature of the compounds under investigation, as long as a correct result can be documented. In the preparative mode, the sample has to be recovered in the exact condition that it was in before undergoing the separation, i.e. no degrading elution conditions, etc. This determines the whole separation strategy far more than any consideration of the size of the process or dimensions of columns ever would.

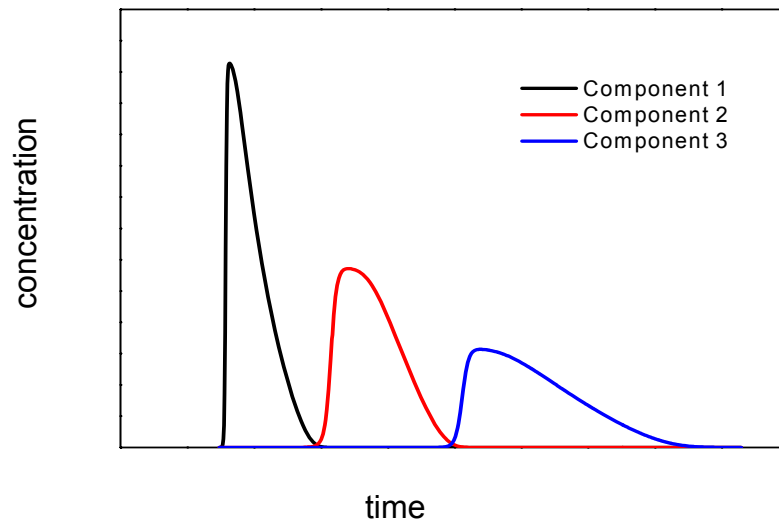
Based on the above definitions and as the purpose of the study is to investigate the separation of the middle component from a ternary mixture, this work entirely focuses on preparative chromatography.

Preparative chromatography could be done in linear or nonlinear mode. That is, in case of linear chromatography the equilibrium concentrations of a component in the stationary and mobile phases are proportional. The individual band shapes and retention times are independent of the amount and composition of the sample. The peak height is proportional to the amount of each component in the injected sample. Linear chromatography accounts well for most of the phenomena observed in analytical applications of chromatography, as long as the injected amounts of the sample are kept sufficiently low and if the goal is to get information [Traub05].

On the other hand, in case of nonlinear chromatography the concentration of a component in the stationary phase at equilibrium is no longer proportional to its concentration in the mobile phase. Thus, band shape, peak maximum and retention time depend on the amount and composition of the sample. This is the situation found in practically in all preparative applications.



a)



b)

Figure 2.7 Typical chromatograms simulated using Craig's model (Chapter 3) for ternary mixtures of a) injection of diluted feed which characterizes condition of analytic chromatography and b) overloaded injection of a preparative chromatography.

2.4. Batch vs. continuous chromatography

In traditional Chemical Process Industries (CPI), processes are developed typically in a batch-mode, but as these processes further emerge and are moved to the production phase, great emphasis is put on converting them from batch to repeated batch and then to continuous operation. The same is true in chromatographic separation process.

In batch chromatography, as shown in Fig. 2.8a, the feed mixture is injected at the column inlet periodically and the separated fractions are collected at the other end of the column. Examples of batch chromatography may include simple single column batch chromatography, flip-flop chromatography, closed loop recycling chromatography [Guio06]. These techniques could be performed under gradient or isocratic conditions. In continuous chromatography the feed is pumped incessantly in the system.

Chromatography which is normally a batch separation process could be turned into a continuous process if the stationary phase is forced to move along the column as

shown in Fig. 2.8b. Physically moving the stationary phase bed is impractical. However the moving bed operation can be simulated as in SMB (simulated moving bed) chromatography [Guio06, Antia03]. The easiest way of transforming a batch separation into a continuous one is the multi-column switching approach, which can be applied for relatively simple adsorption desorption processes. At a certain moment the injection is switched to a second column, while the first one is desorbed by introducing a desorption eluent by a second pump. In a preparative scale, modes for continuous operation have to consider productivity, product concentration and saving of fresh eluent. Batch operations are relatively easy to operate compared to continuous operations. Batch operations are capable to separate multi-component mixtures whereas the most widely used continuous chromatographic method the SMB technique is limited to separate binary mixtures, e.g. racemates [Antos02, Juza00, Traub05].

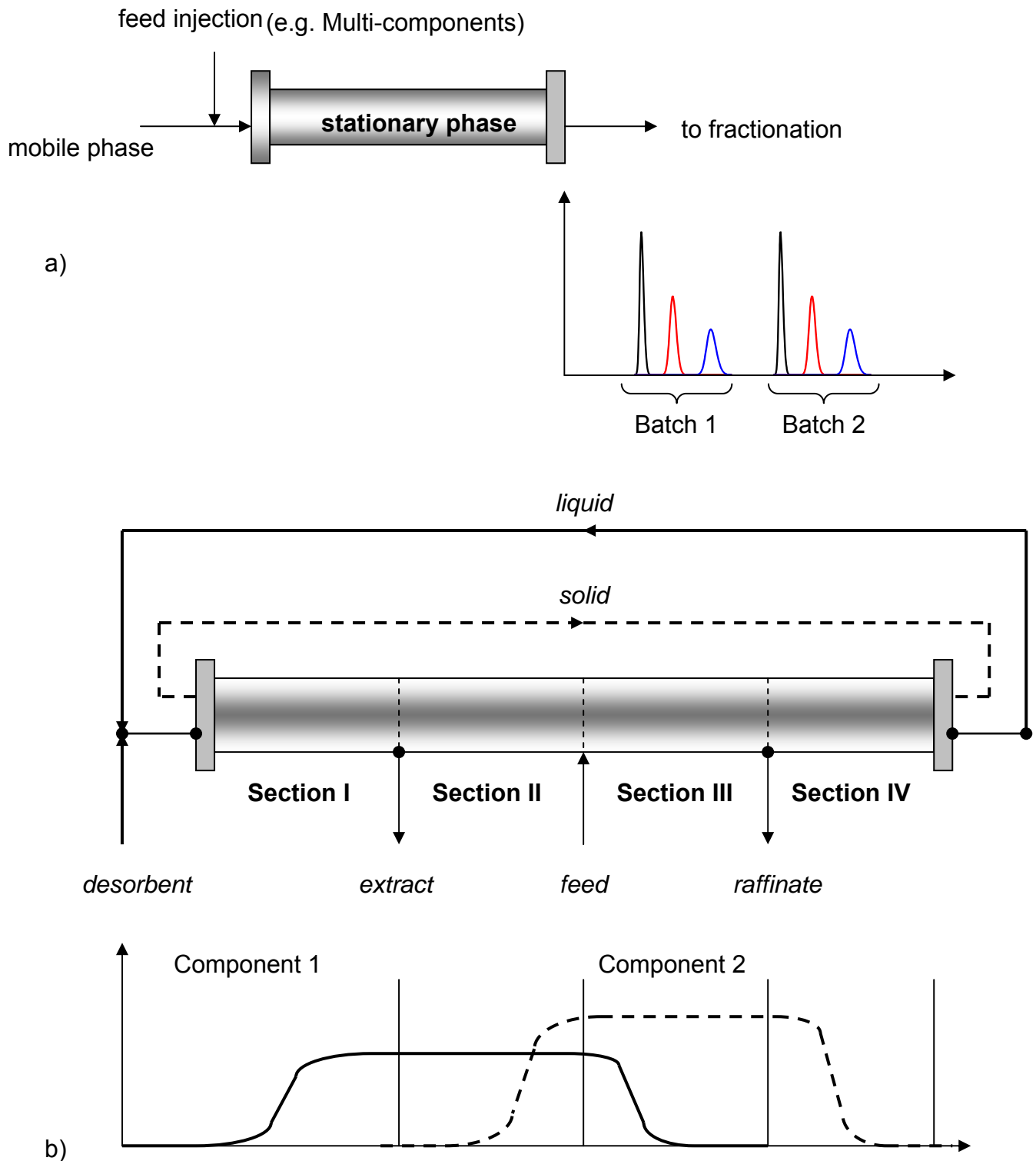


Figure 2.8. Column setup and corresponding profiles of typical, a) batch chromatography and b) moving bed continuous chromatography [Traub05].

2.5. Isocratic vs. gradient chromatography

In chromatography method development, after choosing the appropriate stationary phase and mobile phase, the next step will be choosing the type of elution mode, isocratic or gradient elution. The task is to provide an adequate separation within acceptable process time. In elution chromatography, an isocratic process is a procedure in which the composition of the mobile phase remains constant during the elution process. In contrast, gradient elution is based on forced changes in mobile phase composition, flow rate or column temperature during the resolution process. The most important mode in liquid chromatography is the change in mobile phase composition [Jand85, Poole85]. This Procedure was first introduced 40 years ago by Alan et al. [Alan52]. Solvent composition gradient elution is widely applied in analytical chromatography to reduce the separation time and/or to improve the selectivity of the separation.

The theory of gradient elution chromatography is based on quantifying the interrelationships between the composition of the mobile phase and retention behaviour in isocratic elution chromatography [Guio06, Traub05].

The potential of modulating the solvent strength during gradient operation is increasingly exploited in preparative liquid chromatography. In order to deal with the theory of gradient chromatography, it is necessary to understand the basic principles of the influence of the mobile phase composition on the chromatographic behaviour of sample compounds under isocratic conditions.

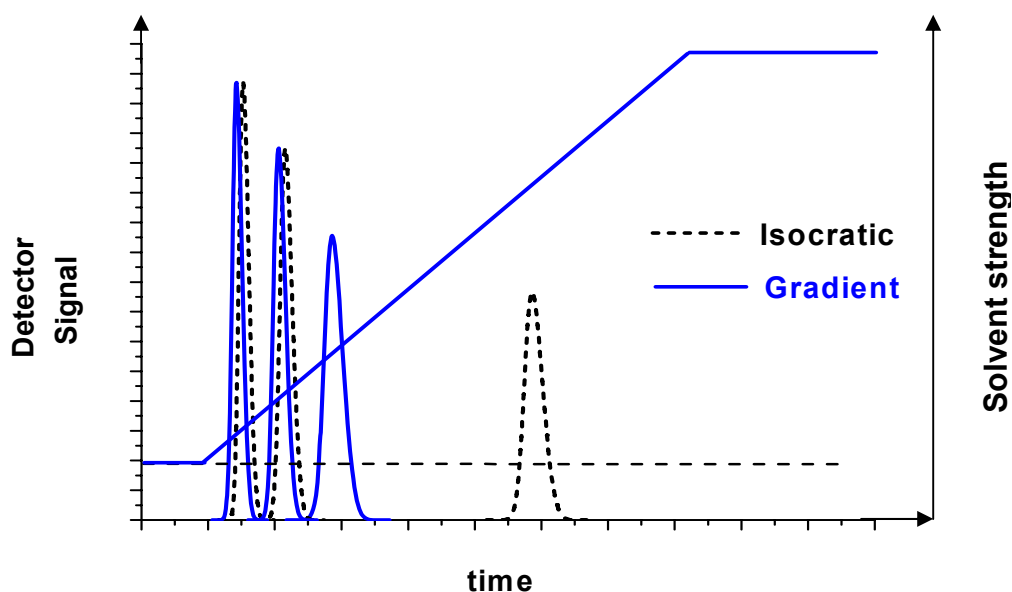


Figure 2.9. Chromatograms of isocratic vs. gradient operations.

The gradient technique makes it possible to elute in a single chromatographic run compounds that differ widely in retention on a given column and to overcome the so-called “general elution problem”. If such samples are chromatographed under isocratic conditions, relatively strong elution strength of the mobile phase is required to elute all sample components in a reasonable time. However, weakly retained sample components are eluted with retention times closer to t_d and are very poorly separated. In contrast, with the elution strength of the mobile phase adjusted so as to achieve the separation of weakly retained compounds, the elution of strongly retained sample components require a very long time and the respective peaks may be very broad [Adam06].

A linear gradient expands the chromatogram in its first part and compresses it for the late-eluting solutes. An example is given in Fig. 2.9. As shown in the figure, gradient operations results in shorter cycle time and better selectivity of the chromatograms compared to the isocratic mode.

In gradient elution chromatography, the elution strength of the mobile phase is altered with time. The number of sample components that can be analysed in a single chromatographic run is increased in gradient elution chromatography compared with isocratic operation.

After running a gradient one has to go back to the initial conditions, which means that the column has to be washed and reconditioned. This is a certain drawback of the method.

a) General schematic diagram of gradient elution chromatography

A typical gradient chromatographic process consists of a pumping system offering the option to adjust the solvent composition from at least two reservoirs, injection port, a column (which is the heart of the process), a detector, a computer (where data acquisition and control of the whole process takes place), fraction collector and flow rate measuring device (see Figure 2.10). First the column is equilibrated by the mobile phase, and then the sample mixture is injected at the injection port. The injected sample is transported by the mobile phase which is formed at the intersection point of the two pump outlets according to the programmed gradient profile.

During the process sample components are separated in the column and the respective band profiles are recorded at the detector. The chromatograms recorded at the detector will be analysed and the whole process is controlled by the computer. The separated components are collected at the column outlet by the fraction collector based on pre-calculated cut times.

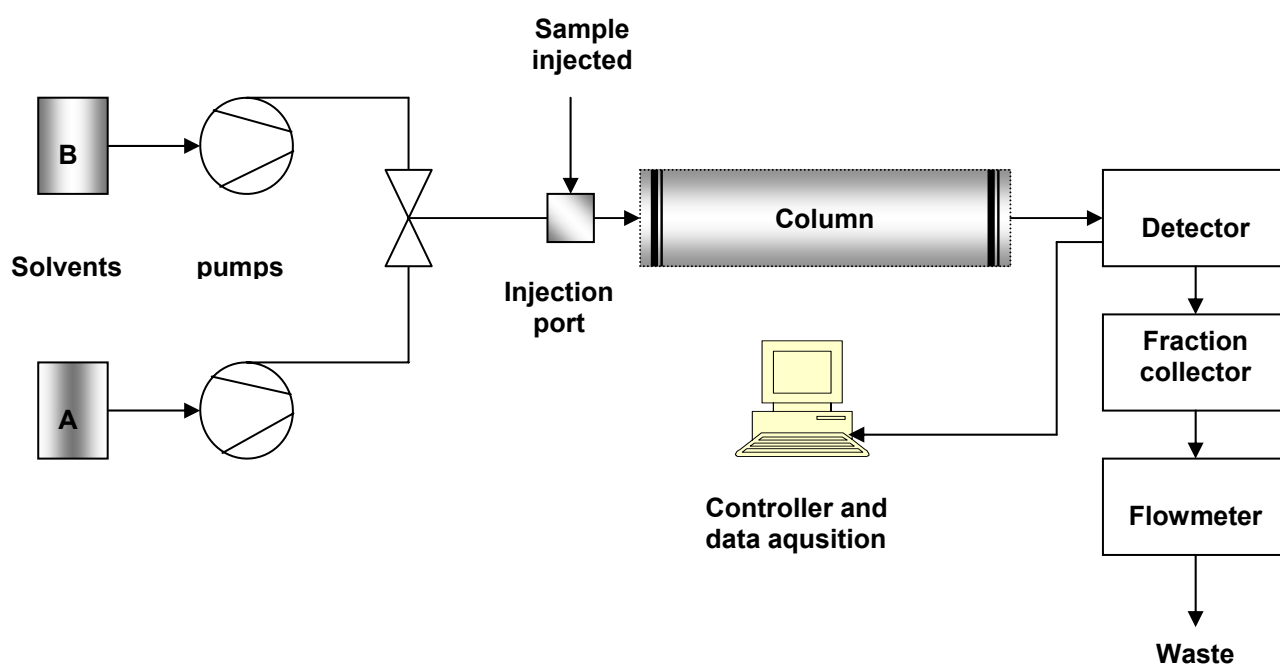


Figure 2.10. Schematic diagram of gradient elution chromatography

b) Classification of mobile phase gradients

Mobile phase gradients may be classified according to the number of components of the mobile phase or according to the form of the mobile phase concentration change with time (the latter will be discussed in chapter 5).

Binary gradients (as e.g. water-methanol mixture used in this study), are formed from two components of the mobile phase, i.e. from a mixture of a less efficient eluting component and a more efficient eluting component. The two solutions used for preparing a binary gradient are either pure or contain their mixtures in different proportions. Further compounds can be added at the same concentration to the two solutions.

If the concentrations of three components of the mobile phase are changed simultaneously during gradient elution, such gradients are termed ternary gradients.

Recently, the use of multi-solvent gradients has been proposed, in which the concentrations of four or more components in the mobile phase are changed at the same time [Jand85]. Such gradients may prove potentially useful for adjusting the separation selectivity and retention either simultaneously or independently of one another during the chromatographic run. Thus in a reversed phase system, a four – solvent gradient can be formed by mixing for example water, methanol, acetonitrile and tetrahydrofuran.

Because of the simplicity to understand and control, binary mobile phase gradients are at present much more frequently than ternary gradients.

3. Mathematical models of chromatography

Preparative chromatography is playing a major role as a purification process in the pharmaceutical and fine chemical industries. It is important to calculate and evaluate the performance of a separation unit for the isolation and purification of a given target component from a certain feedstock. It is also important to optimize the design and operating conditions, which offer minimum cost and maximum production rate. This requires the availability of a model of the chromatographic process which gives an accurate description of the band profiles, so that the production rate of the target component for specified degrees of purity and recovery yield can be calculated.

Chromatography is a complex phenomenon, which results from the superimposition of a number of different effects. A mobile phase percolates through a bed of porous particles: It carries the components of a mixture which interact to different degrees with the stationary phase. Each physical model of chromatography can be translated into a system of equations and conditions that expresses its different features. This set of equations is the mathematical model of chromatography. The degree of correctness of the translation of the physical model into a mathematical model is important. Neglecting or simplifying certain features of the physical model is often necessary. But this must be clearly acknowledged, so that it is possible to understand the limits of the validity of the solutions obtained by the corresponding mathematical model. The equations in a mathematical model typically include algebraic equations and partial differential equations stating the mass conservation of each feed or mobile phase components involved, and expressing further the mass transfer kinetics of these compounds. The models also include the boundary conditions of the equations, translating the physical condition of the process actually performed into mathematical terms.

There are several models available which are capable to quantify the development of concentration profiles in chromatographic columns [Guio06]. In this study, two important mathematical models of chromatography are discussed. These are the equilibrium dispersion model and the Craig's model. The latter model is used in this work to quantify band profiles of various gradient elution processes. Reasons for this choice are a) that this model was often already to be found successful in describing chromatographic separation processes, b) the simplicity of its implementation and c)

the fact that it can be easily extended to describe gradient elution chromatography, which requires taking into account changing isotherm parameters [Shan05].

3.1. Equilibrium-dispersive model

In this model, the column is assumed to be one-dimensional and homogeneous. All the column properties are constant in a given cross-section and so are the concentrations of the individual components [Guio06].

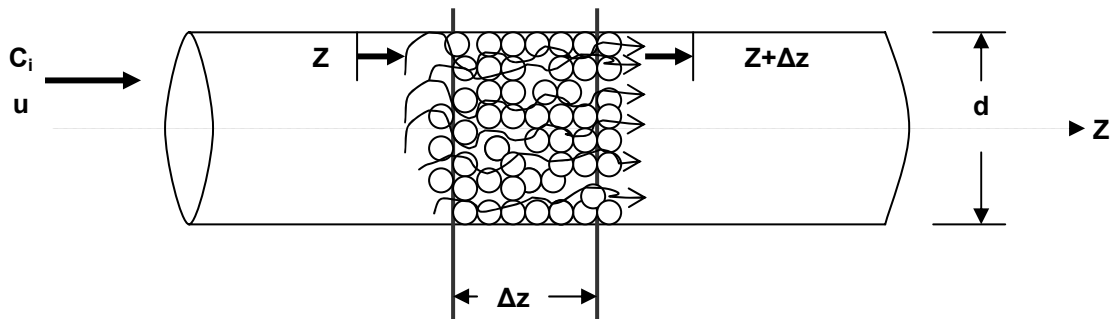


Figure 3.1. Differential mass balance in a column slice

The differential mass balance in the bulk mobile phase states that the difference between the amount of component i , which enters a slice of column of thickness Δz during time Δt and the amount of the same component which exits that slice at the same time is equal to the amount accumulated in the slice (Figure 3.1).

The flux of component, $N_{i,z}$, which enters the slice is:

$$N_{i,z} = \varepsilon A_c \left(u C_i - D_{a,i} \frac{\partial C_i}{\partial z} \right) \Big|_{z,t} \quad (3.1)$$

Where ε is the total porosity of the column, A_c the column geometric cross sectional area, u the local average mobile phase velocity, C_i the local solute concentration in the mobile phase, $D_{a,i}$ the axial dispersion coefficient of the component in the mobile phase and z the distance along the column.

The flux of solute which exits from the slice is:

$$N_{i,z+\Delta z} = \varepsilon A_c \left(u C_i - D_{a,i} \frac{\partial C_i}{\partial z} \right) \Big|_{z+\Delta z,t} \quad (3.2)$$

The rate of accumulation in the slice of volume $A_c \Delta z$ is:

$$A_c \Delta z \left(\varepsilon \frac{\partial C_i}{\partial t} + (1-\varepsilon) \frac{\partial q_i}{\partial t} \right) \Big|_{\bar{z},t} \quad (3.3)$$

where q_i is the local solute concentration in the stationary phase, \bar{z} the average value of z for the slice.

Hence the differential mass balance for component i in the mobile phase is:

$$\varepsilon A_c \left(u C_i - D_{a,i} \frac{\partial C_i}{\partial z} \right) \Big|_{z,t} - \varepsilon A_c \left(u C_i - D_{a,i} \frac{\partial C_i}{\partial z} \right) \Big|_{z+\Delta z,t} = A_c \Delta z \left(\varepsilon \frac{\partial C_i}{\partial t} + (1-\varepsilon) \frac{\partial q_i}{\partial t} \right) \Big|_{\bar{z},t} \quad (3.4)$$

Assuming u and $D_{a,i}$ are constant along the column, and making Δz tend toward zero, after some rearrangement gives:

$$\frac{\partial C_i}{\partial t} + F \frac{\partial q_i}{\partial t} + u \frac{\partial C_i}{\partial z} = D_{a,i} \frac{\partial^2 C_i}{\partial z^2} \quad (3.5)$$

Where F_R is the phase ratio, V_s and V_m are volumes of the stationary and mobile phases respectively

$$F_R = \frac{V_s}{V_m} = \frac{1-\varepsilon}{\varepsilon} \quad (3.6)$$

The equilibrium-dispersive model (Eq. 3.5) assumes that all contributions due to the nonequilibrium can be lumped into one apparent axial dispersion term.

Where the equation relating the apparent dispersion term to the apparent column efficiency as:

$$Da = \frac{Hu}{2} = \frac{Lu}{2P} \quad (3.7)$$

In this model, the important assumptions are that:

- ✓ the mobile and the stationary phase are always in equilibrium
- ✓ the contributions of all the nonequilibrium effects can be lumped into an apparent axial dispersion coefficient.
- ✓ the HETP is independent of the solute concentration and remains the same in overloaded elution as the one valid for linear chromatography.

The equilibrium-dispersive model is the simplest model which takes axial dispersion and mass transfer kinetics into account. This model permits, with good approximation, the accurate prediction of the important self-sharpening and dispersive phenomena caused by thermodynamics of phase equilibria and kinetics. This in turn, results in correct prediction of the band profiles and often excellent agreement with experimental data.

Thus, the equilibrium dispersive model of chromatography does account well for band profiles under almost all experimental conditions used in preparative chromatography. In nonlinear chromatography, there are no known solutions to the equilibrium-dispersive model in closed form. Numerical solutions are easily obtained, using computation methods such as finite differences, finite elements or collocation [Guio06].

The Initial condition is the state of the column when the experiment begins. Mostly it holds that the column is free from the sample mixture, and equilibrated only with a non retained mobile phase, i.e.

$$C_i(z, t = 0) = 0 \text{ for } 0 \leq z \leq L \quad (3.8)$$

The most common boundary condition in elution chromatography assumes a pulse injection of height corresponding to the feed concentration and width to injection time:

$$C_i(z = 0, t) = \begin{cases} C_{i,\text{feed}} & 0 \leq t \leq t_{\text{inj}} \\ 0 & t > t_{\text{inj}} \end{cases} \quad (3.9)$$

$$C_i(z = L, t) = 0 \quad (3.10)$$

t_{inj} is the ratio of the injection volume, V_{inj} , and the volumetric flow rate, F :

$$t_{\text{inj}} = \frac{V_{\text{inj}}}{F} \quad (3.11)$$

The second boundary condition is:

$$\left. \frac{\partial C_i}{\partial z} \right|_{z=L, t} = 0 \quad (3.12)$$

3.2. Craig's cell model

The Craig model [Craig44] is a classical tool to describe the development of concentration profiles in chromatographic columns. In the model, the column is divided into N stages of equal size consisting out of a fraction filled with the stationary phase and a fraction filled with the mobile phase (see Figure 3.2). In a first step, the components are equilibrated in each stage between the two phases in accordance with the adsorption isotherms. Then, in a second step, the liquid phase is withdrawn from the last stage. The liquid fractions in the other stages are transferred in the next stage in the direction of the mobile phase flow. Sample or fresh mobile phase is introduced in the first stage. This process is repeated several times, typically until the whole amount injected has left the last stage.

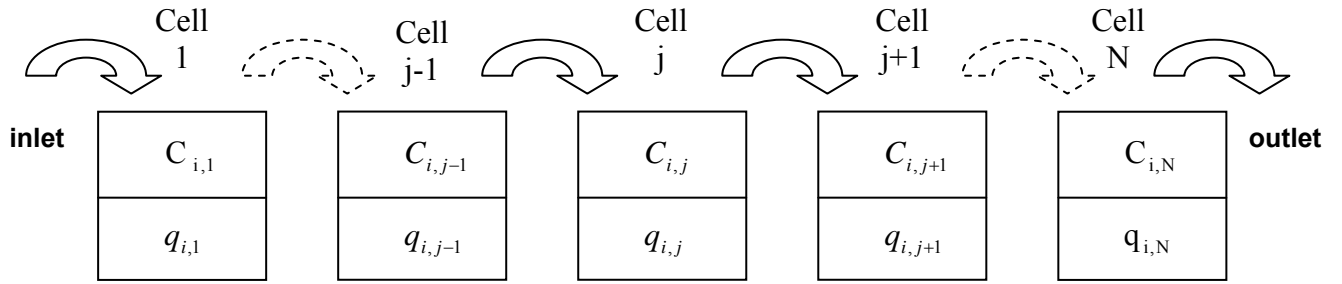


Figure 3.2. Schematic description of the Craig cell model

The mass balance in cell j , with the volume fraction of the mobile phase εV_j and the volume fraction of the stationary phase $(1-\varepsilon)V_j$ is for a k^{th} time step:

$$m_{\text{total},j}^k = m_{\text{mob},j}^k + m_{\text{sta},j}^k = \varepsilon V_j C_j^k + (1-\varepsilon)V_j q_j^k(\bar{C}_j^k) \quad (3.13)$$

where the volume of cell j is, $V_j = V_c/N$, with V_c being the volume of column.

After the transfer of the mobile phase to the next cell, at time $k+1$, the total mass balance in the same cell j will be,

$$m_{\text{total},j}^{k+1} = m_{\text{total},j}^k + \varepsilon V_j C_{j-1}^k - \varepsilon V_j C_j^k \quad (3.14)$$

The total mass at the $k+1$ time step could be written as:

$$m_{\text{total},j}^{k+1} = \varepsilon V_j C_j^{k+1} + (1 - \varepsilon) V_j q_j^{k+1} (\bar{C}_j^{k+1}) \quad (3.15)$$

Combining Eqs.12-14, the mass balance equation of the Craig process can be expressed for a component i , a stage j and an exchange step k as follows

$$C_{i,j}^{k+1} - C_{i,j-1}^k + \frac{1 - \varepsilon}{\varepsilon} (q_{i,j}^{k+1} (\bar{C}_j^{k+1}) - q_{i,j}^k (\bar{C}_j^k)) = 0 \quad i = 1, n; \quad j = 1, N; \quad k = 1, K \quad (3.16)$$

where C , is again the liquid phase concentration, ε the column porosity and q the concentration in the stationary phase in equilibrium with the local liquid phase concentrations. The time difference between two exchange steps, designated by k and $k+1$, corresponds to the characteristic mobile phase residence time in a stage, Δt . It is related to the dead time of the column, t_0 , divided by the total number of stages, N :

$$\Delta t = \frac{t_0}{N} \quad (3.17)$$

with

$$t_0 = \frac{A_c L_c \varepsilon}{F} = \frac{V_c \varepsilon}{F} \quad (3.18)$$

In Eq. 3.18 A_c , L_c and V_c are the cross section area, the length and the volume of the column. F is the volumetric flow rate of the mobile phase. Similar to Eq. 3.8, considering initially ($k=0$) not preloaded columns as initial condition holds:

$$C_{i,j}^0 = 0 \text{ and } q_{i,j}^0 = 0 \quad i=1, n; \quad j=1, N. \quad (3.19)$$

In elution chromatography, typically, rectangular injection profiles are imposed at the inlet of stage 1 ($j=0$). They can be described as follows which is similar to Eq. 3.9:

$$C_{i,0}^k = \begin{cases} C_{i,\text{Feed}} & \text{for } k \times \Delta t \leq t_{\text{inj}} \\ 0 & \text{for } k \times \Delta t > t_{\text{inj}} \end{cases} \quad i = 1, n; \quad k = 1, K. \quad (3.20)$$

In Eq. (3.20), $C_{i,\text{Feed}}$ is again the injection feed concentration

For nonlinear and coupled isotherms $q(C_1, C_2, \dots, C_N)$, the nonlinear algebraic system of Equation 3.16 has to be solved iteratively in order to determine the unknown concentration profile at the column exit for the new step $k+1$. In order to solve this

model equation, we need to have a model which can describe the equilibrium relationship of the components with the mobile and stationary phases as discussed in Section 3.3.

Initially the classical iteration method was used to solve this model equation. Later in this work, the Craig model (Eq. 3.16) has been solved for isocratic and gradient conditions by a Matlab programme [Matlab], which uses the classical Newton-Raphson iteration method [Press92]. Due to the slow calculation speed of the classical iteration method, Newton-Raphson method was implemented to solve the equations, which was found to be fast and reliable to predict the band profiles.

3.2.1. Numerical solution

For nonlinear and coupled isotherms $q(C_1, C_2, \dots, C_N)$, Eq. 3.16 has to be solved iteratively in order to determine the unknown concentration profile at the column exit for the new step $k+1$. In order to solve Craig's model equation, we need to have a model which can describe the equilibrium relationship of the components with the mobile and stationary phases which has been discussed in section 3.3. The first step to solve the Craig model was to create a grid as shown in Fig. 3.3 dividing the column hypothetically into N number of cells and K number of time intervals.

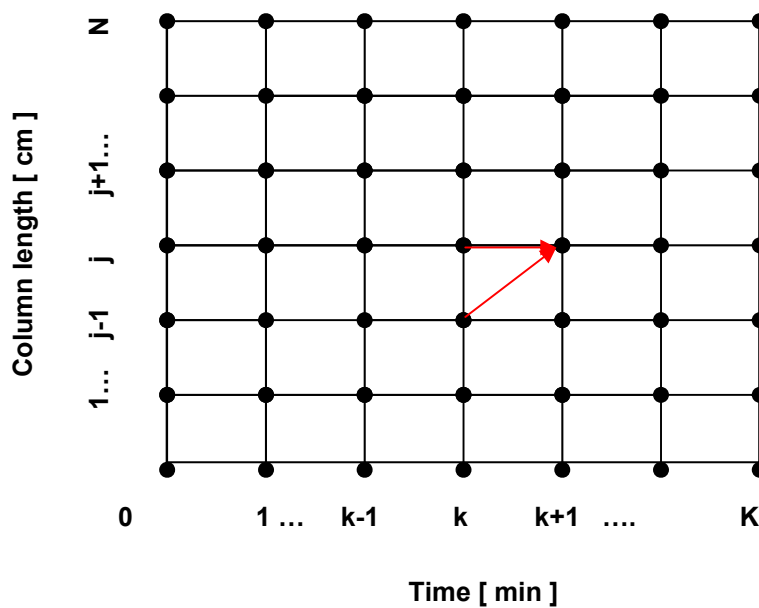


Figure 3.3. Grid used in solving the Craig model.

Thus, computation of the concentration of each of the components at each point on the grid follows (see the Algorithms below).

i) Algorithm using the classical iterative method

The concentration of component i , at the next time stage $j+1$ and at cell k will be written in the form of:

$$C_{i,j}^{k+1} = f(C_{i,j-1}^k, q_{i,j}^{k+1}, q_{i,j}^k) \quad (3.21)$$

where

$$q_{i,j}^{k+1} = f(C_{i,j}^{k+1}) \text{ and } q_{i,j}^k = f(C_{i,j}^k) \text{ for } i=1,n \quad (3.22)$$

- a) initial value of $C_{i,j}^{k+1}$ was assumed arbitrarily (normally some percentage of the feed concentration)
- b) new value of $C_{i,j}^{k+1}$ was generated using the assumed value in step a and Eq. 3.16.
- c) if the difference between the newly calculated and assumed values of $C_{i,j}^{k+1}$ drops below a certain threshold value, then the newly calculated $C_{i,j}^{k+1}$ is the final solution, therefore the calculation continues to the next time step at the same cell. If not, then
- d) the newly calculated value of $C_{i,j}^{k+1}$ will be used to generate another value, and the steps a-c will be repeated until the difference between the new and old calculated concentrations drops below a certain predefined threshold limit.

The above steps were done for each point in time and column point so that the development of the concentration profile determined.

ii) Algorithm for the Newton-Raphson iterative method

First, Eq. 3.16 was written in the form of $f(C_{i,j}^{k+1}) = 0$:

$$f(C_{i,j}^{k+1}) = f(C_{i,j-1}^k, q_{i,j}^{k+1}, q_{i,j}^k, C_{i,j}^{k+1}) = 0 \quad (3.23)$$

Again, the concentrations of each component in the stationary phase are described in Eq. 3.22.

Then the derivative of this equation with respect to $C_{i,j}^{k+1}$ was generated as $f'(C_{i,j}^{k+1})$:

- a) initial value of $C_{i,j}^{k+1}$ was assumed arbitrarily (normally some percentage of the feed concentration) similar to the step a of the classical iteration method.
- b) the values of $f(C_{i,j}^{k+1})$ and $f'(C_{i,j}^{k+1})$ were calculated using the assumed value of $C_{i,j}^{k+1}$ in step a.
- c) the new estimate of $(C_{i,j}^{k+1})_{n+1}^{\text{th}}$ will be calculated as :

$$(C_{i,j}^{k+1})_{n+1}^{\text{th}} = (C_{i,j}^{k+1})_{n}^{\text{th}} - \frac{f((C_{i,j}^{k+1})_{n}^{\text{th}})}{f'((C_{i,j}^{k+1})_{n}^{\text{th}})} \quad (3.24)$$

where the subscript n^{th} refers to the iteration step.

- d) if the difference between the newly calculated and assumed values of $C_{i,j}^{k+1}$'s drops below a certain threshold value, then the newly calculated $C_{i,j}^{k+1}$ is the final solution, therefore the calculation continues to the next time step at the same cell. If not, the iteration continues to the next step.
- e) the newly calculated value of $C_{i,j}^{k+1}$ will be used as initial estimate and steps a-d continues until the difference between two consecutive calculated concentration values drops below a certain threshold limit.

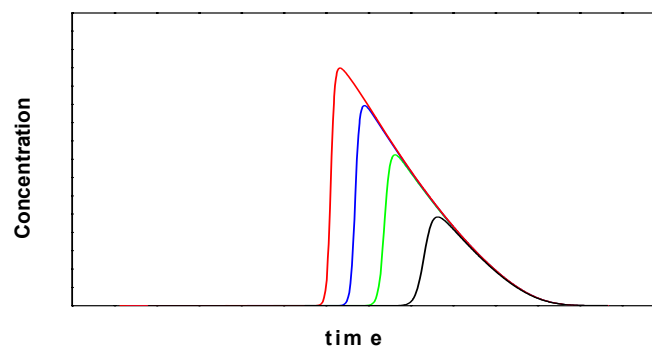


Figure 3.4. Illustration of concentration overloading of a single component system simulated using the Craig model for four different feed concentrations and the same injection volume.

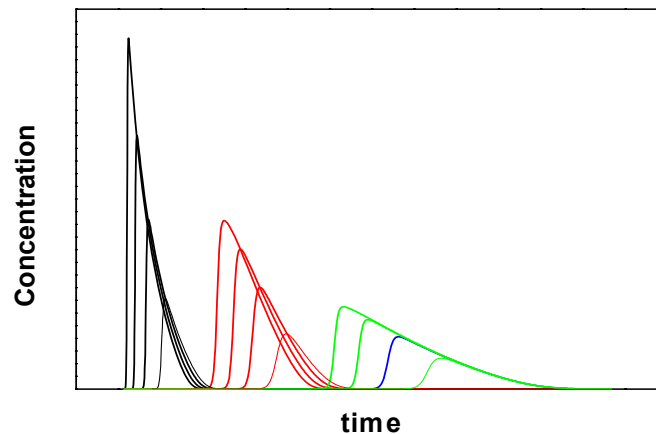


Figure 3.5. Illustration of concentration overloading of a ternary component system simulated using the Craig model for four different feed concentrations and the same injection volume.

Figures 3.4 and 3.5 are generated by solving the Craig model using the above algorithms for different feed concentrations and the same injection volume, for single and ternary component systems respectively.

3.3. Adsorption Isotherm models

In order to solve the above chromatographic models, an equilibrium relationship of the concentration of components in the stationary phase as a function of the concentration in the mobile phase is required. The equilibrium isotherm is a plot of the adsorbed amount of a component on the stationary phase versus its concentration in the mobile phase at equilibrium and at constant temperature. Typical single component isotherm shapes are shown in Fig. 3.6. [Traub05].

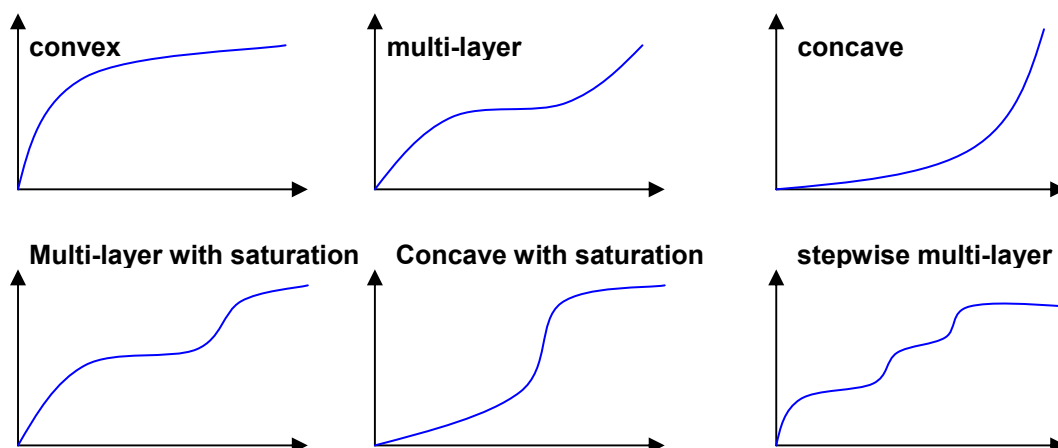


Figure 3.6. Different types of adsorption isotherms

Isotherm models are divided into single-component and multi-component models, where estimation of these thermodynamic parameters will be discussed in chapter 5.

3.3.1. Single component isotherm models

Among the various single component isotherm models, two of most important ones, the Henry isotherm and single component Langmuir and Toth isotherm models are discussed.

Henry's isotherm model is the simplest model applicable in the linear range of a chromatographic separation process. In this case the relationship between the mobile phase and the stationary phase concentrations C_i and q_i is expressed as:

$$q_i = K_{H,i} C_i \quad (3.25)$$

where $K_{H,i}$ is Henry's constant.

For the determination of Henry's constant from a chromatographic experiment, the total porosity and retention time of the respective component are needed.

$$K_{H,i} = \left(\frac{t_{r,i} - t_0}{t_0} \right) \left(\frac{1 - \varepsilon}{\varepsilon} \right) \quad (3.26)$$

The higher the Henry coefficient for a substance the stronger is its adsorption and thus the longer its retention time. This definition shows that for two components to be separated their Henry coefficients have to differ. Accordingly Separation factors $\alpha_{i,j}$, can be defined as the ratio between two Henry constants.

$$\alpha_{i,m} = \frac{K_{H,i}}{K_{H,j}} \quad \text{where } K_{H,i} > K_{H,m} \quad (3.27)$$

Single component Langmuir isotherm model is the most common type of isotherm model used in preparative chromatography.

$$q_i = q_{\text{sat},i} \frac{b_i C_i}{1 + b_i C_i} = \frac{a_i C_i}{1 + b_i C_i} \quad (3.28)$$

with

$$b_i = \frac{a_i}{q_{\text{sat},i}} \quad (3.29)$$

where $a_i = K_{H,i}$, b_i are Langmuir isotherm parameters and $q_{\text{sat},i}$ is the saturation capacity of component i .

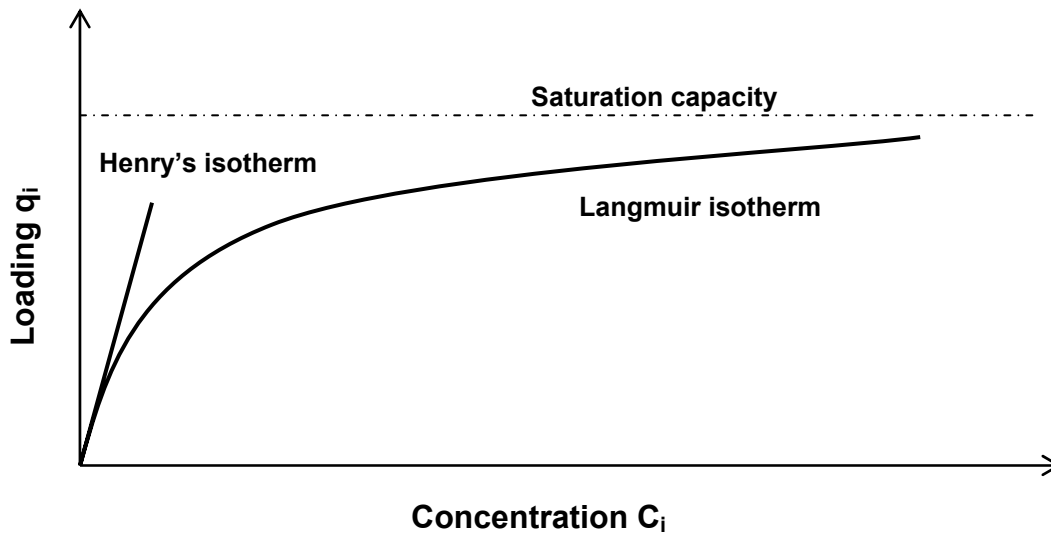


Figure 3.7. Single component Langmuir and Henry isotherms

The following assumptions are the theoretical background of the Langmuir type isotherms.

- all adsorption sites are considered energetically equal (homogeneous surface)
- each adsorption site can only adsorb one solute molecule
- only a single layer of adsorbed solute molecules is formed
- there are no lateral interferences between the adsorbed molecules

As shown in Fig. 3.7., for a Langmuirian system, when increasing the concentration of the solute in the mobile phase the amount adsorbed onto the stationary phase no longer increases linearly. Only the first region, with very low mobile phase concentrations, shows a linear relationship. In this region Henry's model is applicable. This diluted region is used for quantitative analysis in analytical chromatography because only this region ensures that no retention time shifts take place if different amounts are injected.

The *single component Bi-Langmuir isotherm* is an extension of the single component Langmuir model but with more number of parameters.

$$q_i(C_1, C_2, \dots, C_n) = \frac{a_{1,i} C_i}{1 + b_{1,i} C_i} + \frac{a_{2,i} C_i}{1 + b_{2,i} C_i} \quad i = 1, n. \quad (3.30)$$

With $a_{1,i}$, $a_{2,i}$, $b_{1,m}$ and $b_{2,m}$ as the single component Bi-Langmuir isotherm parameters.

One drawback of Langmuir-type adsorption isotherms is the conjunction between the initial slope of the isotherm and its curvature. This can be overcome by the Toth isotherm model [Toth71].

The *Toth isotherm model* has three independent free parameters, $q_{\text{sat},i}$, e and b_i , which allows independent control of slope and curvature.

$$q_i = q_{\text{sat},i} \frac{C_i}{\left(\frac{1}{b_i} + C_i^e \right)} \quad (3.31)$$

For $e=1$ the Toth isotherm approaches the Langmuir isotherm.

3.3.2. Multi-component isotherm models

In case of multi-component mixtures, an additional complexity results from the competition between the different components for interaction with the stationary phase. That means when mixtures of solutes are injected into a chromatographic system, not only interferences between the amount of each component and the adsorbent but also between the molecules of different solutes occur. The resulting displacement effects cannot be appropriately described with independent single-component isotherms. Therefore, an extension of single-component isotherms that also takes into account the interference is necessary.

Frequently, and also in this work, the following equation of the *competitive Langmuir* model is used:

$$q_i(C_1, C_2, \dots, C_n) = \frac{a_i C_i}{1 + \sum_{m=1}^n b_m C_m} \quad i = 1, n. \quad (3.32)$$

where the a_i and b_m are the competitive isotherm parameters.

The *Bi-Langmuir isotherm* can be extended in the same way to give the multi-component Bi-Langmuir isotherm.

$$q_i(C_1, C_2, \dots, C_n) = \frac{a_{1,i} C_i}{1 + \sum_{m=1}^n b_{1,m} C_m} + \frac{a_{2,i} C_i}{1 + \sum_{m=1}^n b_{2,m} C_m} \quad i = 1, n. \quad (3.33)$$

Again $a_{1,i}$, $a_{2,i}$, $b_{1,m}$ and $b_{2,m}$ are the Bi-Langmuir isotherm parameters.

Different experimental techniques are available in order to determine these isotherm parameters. Some of these techniques are discussed in Chapter 4.

3.3.3. Effect of gradients on isotherms

During isocratic processes, the mobile phase composition does not change with time or along the column. Thus also the corresponding isotherm parameters are constant. As it is mentioned in the previous sections, gradient processes are the focus of this work. Isotherm parameters will no more be constant in gradient chromatography. The parameters will rather vary according to the gradient applied. Therefore in order to model the elution profiles under gradient conditions the dependence of the parameters of the adsorption isotherm equation (Eq. 3.32), a_i and b_m , on the mobile phase composition (the concentration of the modifier, C_{mod} ,) must be known.

Several models have been suggested that describe relations $a_i(C_{\text{mod}})$ required in analytical chromatography. Hereby the suggested correlations differ for reversed phase and normal phase systems [Shan05]. Often the same correlations as for a_i are used to describe the additional isotherm parameters required in nonlinear models, e.g. b_i .

a) For reversed phase systems

The effect of the concentration of a modifier, present in the mobile phase and applied to generate the gradients, C_{mod} , on the isotherm parameters a and b of each component i , in aqueous-organic mobile phases in reversed-phase chromatography can be correlated e.g. by the following equations [Jand99].

$$a_i(C_{\text{mod}}) = \exp(P_{1,i} + P_{2,i} \cdot C_{\text{mod}}) \quad (3.34a)$$

$$b_i(C_{\text{mod}}) = \exp(P_{3,i} + P_{4,i} \cdot C_{\text{mod}}) \quad (3.34b)$$

where $P_{1,i}$ and $P_{2,i}$, $P_{3,i}$ and $P_{4,i}$ are constants which need to be known for each component i .

In this study, a reversed phase system has been used to separate the middle component from a ternary mixture of cycloketones. For this reason Eqs. 3.34a and 3.34b have been used to generate the required band profiles which are finally compared with those measured experimentally.

b) For normal phase systems

In normal-phase systems the dependence of isotherm parameters a_i and b_i for component i on C_{mod} the concentration of a more polar solvent in a less polar one, usually has the following form [Snyd68, Socz69]:

$$a_i(C_{\text{mod}}) = (\beta_{1,i} C_{\text{mod}})^{\beta_{2,i}} \quad (3.35a)$$

$$b_i(C_{\text{mod}}) = (\beta_{3,i} C_{\text{mod}})^{\beta_{4,i}} \quad (3.35b)$$

Consequently, the equilibrium model possesses four free parameters for each component i , i.e. $\beta_{1,i}$, $\beta_{2,i}$, $\beta_{3,i}$ and $\beta_{4,i}$. (Eqs. 3.35a and 3.35b) are based on the well-known Snyder-Soczewinski model of normal-phase adsorption chromatography.

4. Determination of adsorption isotherms

Estimation of adsorption isotherm parameters is the most important prerequisite for a prediction and optimization of chromatographic separation of mixtures. The adsorption isotherms have a very big influence on the chromatogram shapes and positions. Consequently single and multi-component isotherms have to be known with high accuracy. Since a theoretical prediction of these thermodynamic functions is in general not possible, experimental methods are required.

4.1. Single-component system

In order to determine single-component isotherm parameters, one can use the conventional static methods which are slow, use only the information of equilibrium states and less accurate than dynamic methods [Guio06, Morg04].

Dynamic methods are based on the mathematical analysis of the response curves corresponding to different well defined changes of the column inlet concentrations. Such methods are discussed in this work.

4.1.1. Frontal analysis method

In this method, successive abrupt step changes of increasing concentration are performed at the column inlet and the breakthrough curves are determined [Guio06, Morg04]. Figure 4.1 shows schematically a typical concentration profile applicable for the determination of adsorption isotherms by frontal analysis.

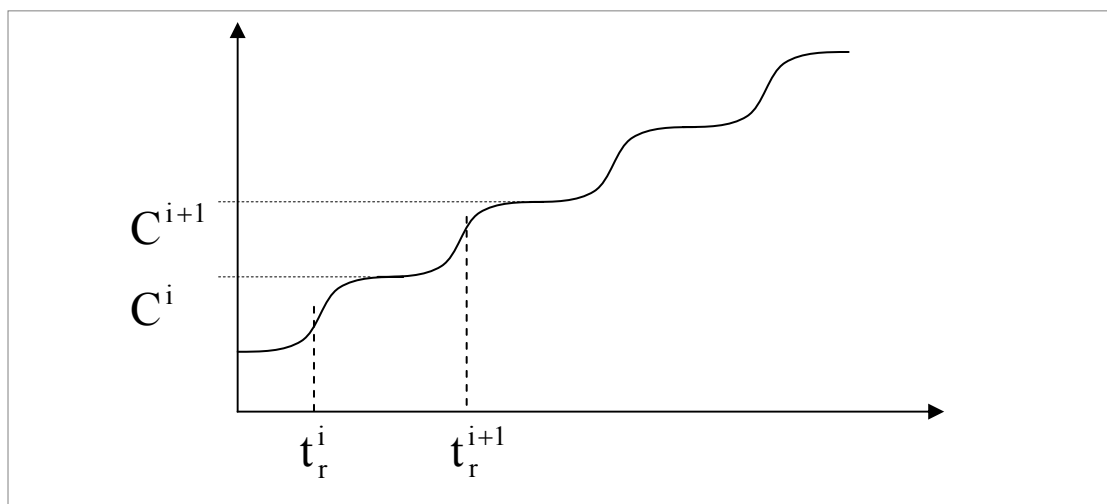


Figure 4.1. Demonstration of frontal analysis, stair case feed concentration profile and respective breakthrough curves.

Provided the i^{th} loading q^i , which is in equilibrium with C^i , the phase ratio F and the linear velocity u or the dead time $t_0 = \frac{L}{u}$ are known, an unknown loadings at the $(i+1)^{\text{th}}$ step, q^{i+1} , in equilibrium with the concentrations C^{i+1} , can be determined using following the rearranged mass balance equation (e.g. [Guio06] and [Morg04]):

$$q^{i+1}(C^{i+1}) = q^i + \left(\frac{(t_r^{i+1} - t_0)(C^{i+1} - C^i)}{Ft_0} \right) \quad (4.1)$$

Hereby t_r^{i+1} is the retention time of the inflection point of the $(i+1)^{\text{th}}$ breakthrough curve.

Frontal analysis is a very popular method of isotherm determination. It has been applied to the determination of a great number of equilibrium isotherms, in many modes of chromatography. Major drawbacks of frontal analysis method are the considerable amount of time needed for the determination of isotherm and the large amount of sample required to saturate the column.

Details of applying this method to determine competitive isotherm parameters could be found in the works of Guichon et. al for binary mixtures, by Seidel-Morgenstern [Morg04] and Lisec et. al [Lisec01] for ternary mixtures.

4.1.2. Elution by characteristic points (ECP) method

In the ECP method, isotherms are derived from the dispersed parts of overloaded elution profiles. When a large sample size is injected into a chromatographic column, often an unsymmetrical band is eluting with a steep front and a diffuse rear. The evaluation method uses the ideal model of chromatography assuming that the column efficiency is infinite [Guio06, Craig44, Morg04]. Therefore the ECP method should be used only with highly efficient columns, where the contribution to band broadening is negligible. The data points close to the top of the profile, which are more affected by of band broadening, should not be used in the determination of the isotherm.

Fig.4.2 shows as an illustration for the ECP method a typical series of concentration overloading where a significant branch of the single component isotherm can be determined from the largest injection.

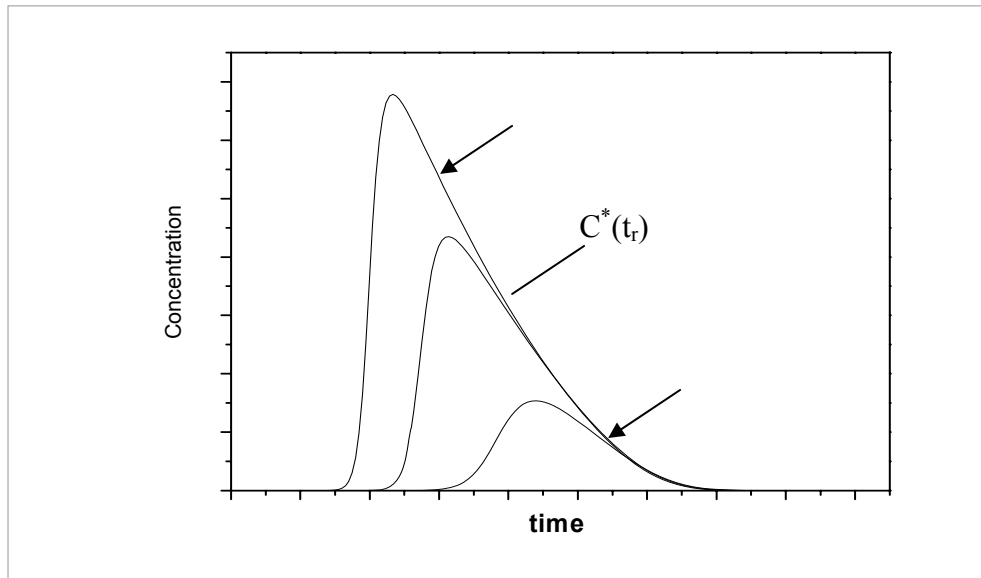


Figure 4.2. Illustration of the ECP method. Elution bands of concentration overloading showing dispersed bands. The largest peak can be used to estimate isotherm parameters.

The knowledge of the course of the retention times of the dispersed rear parts, $t_r(C^*)$, allows for Langmuirian systems (characterized by dispersed tails of the peaks) determining the course of the slope of the single solute adsorption isotherm, $\frac{dq}{dC}$, as follows:

$$\left. \frac{dq}{dC} \right|_{C^*} = \frac{t_r(C^*) - t_{inj} - t_0}{t_0 \left(\frac{1-\varepsilon}{\varepsilon} \right)} \quad (4.2)$$

with the injection time, $t_{inj} = \frac{V_{inj}}{F}$ as shown in Eq. 3.11.

4.1.3. Perturbation method

In this method [Guio06, Morg04], a solution of the studied component in the mobile phase is pumped through the column until equilibrium is reached, i.e. until the

breakthrough of the constant concentration plateau is accomplished. Then a small pulse with different concentrations is injected.

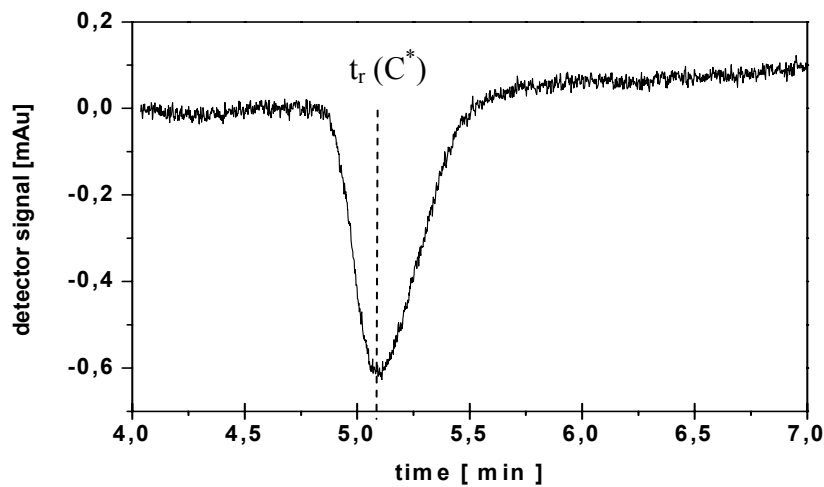


Figure 4.3. Illustration of perturbation method, retention time at single isotherm point of 3 μ l cyclohexanone injected in a column equilibrated by a concentration of 1 vol. %

The retention time, t_r , of this small pulse will be related to the slope of the isotherm,

$\frac{dq}{dC}$ as shown in Eq. 4.2. The injection performed should be as small as possible to

leave the column in equilibrium. If larger perturbations are required due to detection limits, the retention times of injections for higher and smaller concentrations than the plateau values can be averaged. Figure 4.3 shows an illustration of perturbation method, where 3 μ l cyclohexanone was injected in HyPurity C₁₈ reversed phase column equilibrated by 1 vol. % Cyclohexanone using a 40:60 methanol: water mobile phase.

4.1.4. Inverse method (peak fitting method)

The inverse method (IM) estimates adsorption isotherm parameters by fitting simulated elution profiles to experimental ones [Feli03, Morg04, Arne05]. This is a numerical method of parameter estimation which requires a reliable column model and the provision of respective isotherm equations.

The following steps are needed to determine isotherm parameters using this method.

- a) an isotherm model was selected (e.g. the competitive Langmuir isotherm model)
- b) initial estimates can be determined for its numerical parameters (initial estimates can be computed by, e.g. the ECP method).
- c) band profiles of the feed mixture can be calculated with the Craig model using isotherm equation of step a and the parameters of step b.
- d) the measured and calculated band profiles are compared by evaluating the following objective function:

$$\min \sum_i r_i^2 = \min \sum_i (C_i^{\text{sim}} - C_i^{\text{meas}})^2 \quad (4.3)$$

where C_i^{sim} and C_i^{meas} are the calculated and the measured concentrations at point i and r_i is their difference.

- e) the isotherm parameters are changed to minimize the objective function, using e.g. the Levenberg–Marquardt algorithm of Matlab [Matlab].

4.2. Multi-component system

In the case of multi-component mixtures, an additional complexity results from the competition between the different components for sites on the stationary phase. Also in this case the adsorption isotherms of the different components which are simultaneously present in the feed mixture are not linear. In addition they are no longer independent when the feed is not very dilute. For single-component, the amount of component adsorbed at equilibrium is a function of the concentration of this component in the mobile phase, but in case of multi-component mixtures the amount of component adsorbed by the stationary phase is also a function of the concentration of all other components present in the solution which are adsorbed by the stationary phase. This competitive behaviour of the feed components for access to the retention mechanism constitutes a fundamental problem of nonlinear chromatography.

4.2.1. Inverse method (peak fitting method)

The inverse method can also be applied to determine competitive adsorption isotherm parameters. This method was used for the determination of competitive isotherm parameters of three model substances in this work. Hereby single component isotherm parameters of each component determined by the ECP method, was used as initial estimates in this method.

For the calculation of the individual profiles, Craig's cell model (Eq.3.16) and the competitive Langmuir isotherm (Eq. 3.32) were used.

5. Gradients

In gradient chromatography, there are various gradient types used to optimize selectivity, improve resolution and increase productivity. These include temperature gradients, flow-rate gradients, stationary phase gradients and mobile phase (solvent) gradients. In this work, mobile phase gradients are the focus.

By gradient profile is meant the mathematical description of how the mobile phase composition changes with time. In this section, different gradient profiles which are useful for separating multi-component mixtures are discussed. Much of the focus is on the design and implementation of the mobile phase compositions as a function of time with time for the separation of the middle component of a ternary mixture using chromatographic batch processes. Mobile phase gradients may be classified according to the number of components of the mobile phase or according to the form of the mobile phase composition change with time.

5.1.Solvent gradients

Binary gradients are formed from two components of the mobile phase, a less efficient eluting component and a more efficient eluting component. The two solutions A and B used for preparing a binary gradient are either pure components, or contain their mixtures in different proportions. Further compounds can be added at same concentration to the two solutions. If the concentrations of three components of the mobile phase are changed simultaneously during gradient elution, such gradients are termed ternary gradients.

Recently, the use of multi-solvent gradients have been proposed, in which the concentrations of four more components in the mobile phase are changed at the same time. Such gradients may prove potentially useful for programming the separation selectivity and retention either simultaneously or independently of one another during the chromatographic run. Typically in reversed-phase liquid chromatography, water, methanol, acetonitrile and tetrahydrofuran can be used to form four-component mobile phase gradients. Most of the time it is preferred to use two solvents with relatively small differences in polarities (elution strengths) to form binary gradients in chromatography on polar adsorbents to suppress the so called

demixing effect, which may adversely affect the separation under certain circumstances [Jand85, Snyder07].

Instruments where three, four or more liquids (components of the multi-solvent gradient) are mixed in pre-programmed proportions changing with time have recently become commercially available. In this work however, only binary mixtures of water and methanol are used to form gradients.

5.2. Gradient shapes

Before the introduction of gradient processes, liquid chromatographic separation was carried out with mobile phases of fixed composition that is isocratic elution. Isocratic separation works well for many samples and it represents the simplest and most convenient form of liquid chromatography. However in order to increase the productivity of chromatographic separation processes gradient chromatography becomes one of the most preferred and widely used technique in recent days.

To exploit the potential of gradient chromatography, the respective gradient profiles should be properly designed. These gradients are typically formed by altering the composition of the mobile phase at the column inlet. Various approaches can be applied to realize such gradient profiles experimentally. In this work, two solvent reservoirs having different solvent compositions and two pumps will be used [Jand85]. A second solvent or a solvent mixture is added to the initial mobile phase according to a specified time program to form the gradients. Thus, positive (increasing elution strength with time, “step up”) or “negative” (“step down”) gradients can be realized.

Mobile phase gradients are usually characterized as a time function of the modifier concentration at the outlet from the gradient –generating device, $C_{\text{mod}}=f(t)$.

Besides the common types of gradients, i.e. the step gradients and multi-linear gradients shown in Fig. 5.1., irrespective of the type, a gradient can be described by the following parameters: initial composition of the solvent (characterized by an initial concentration of a modifier, C_{mod}^0), time for starting the gradient (t_g^0), final composition

of the solvent (characterized by final concentration of a modifier, C_{mod}^f) and time for reaching the final solvent composition (t_g^f). Further, the shape of the gradient between t_g^0 and t_g^f needs to be defined. Typical gradient shapes are illustrated in Figs. 5.1 and 5.2.

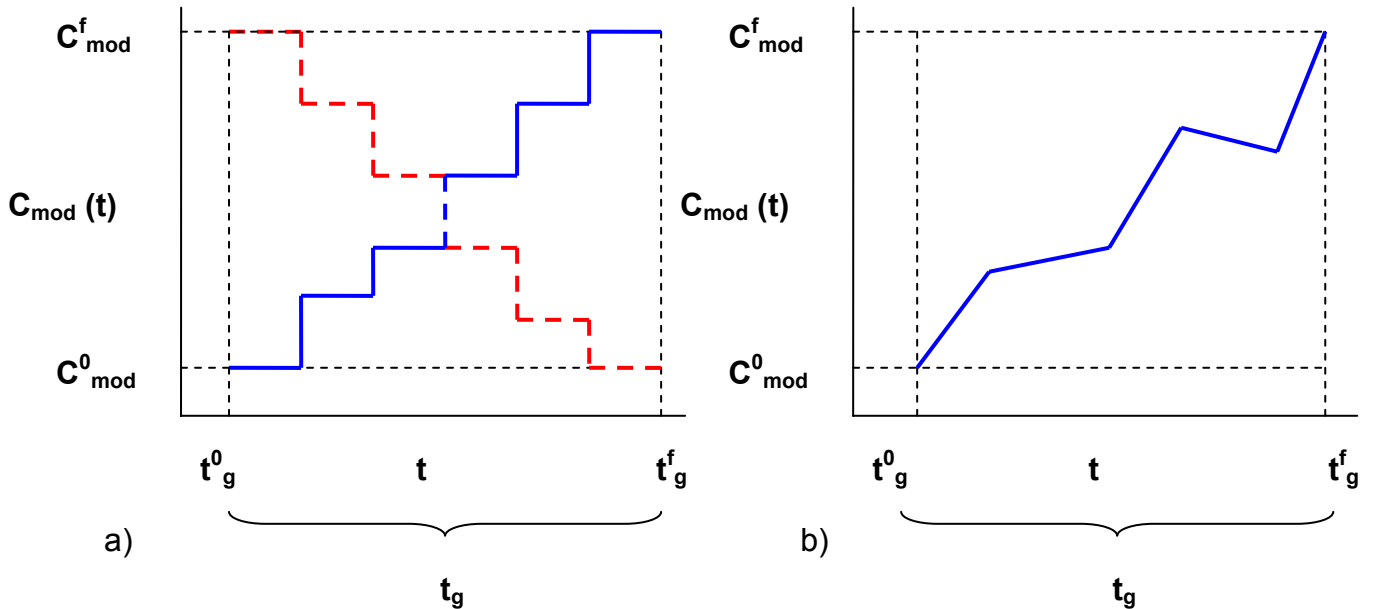


Figure 5.1. a) Step gradients of “step-up” (solid line) and “step-down” (dashed line) and b) multi-segmented linear gradient modes.

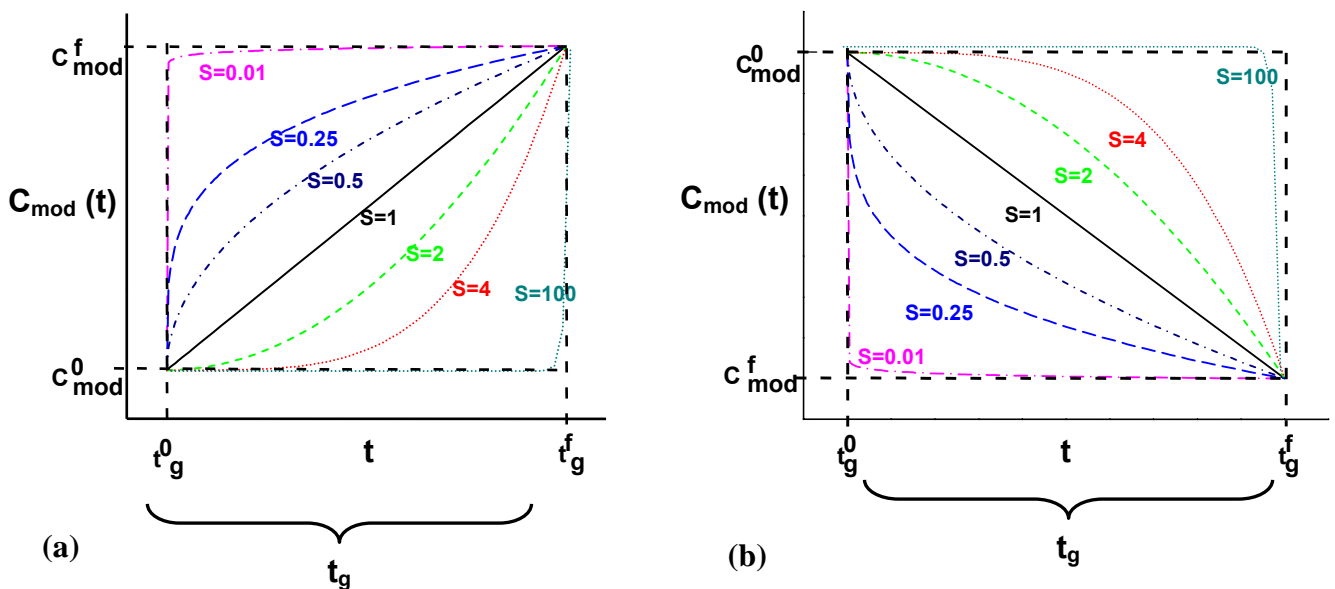


Figure 5.2. Linear and nonlinear gradients and effect of shape parameter S for a) “step up” gradient mode ($C_{\text{mod}}^0 < C_{\text{mod}}^f$) and b) “step down” gradient modes, ($C_{\text{mod}}^0 > C_{\text{mod}}^f$), (Eq. 5.1).

The courses shown were generated using the following flexible continuous function possessing the gradient shape parameter S:

$$C_{\text{mod}}(t) = C_{\text{mod}}^0 + (C_{\text{mod}}^f - C_{\text{mod}}^0) \cdot \left[\frac{t - t_g^0}{t_g} \right]^S \quad \text{with,} \quad t_g^0 \leq t \leq t_g^f \quad (5.1)$$

In Eq. 5.1, t_g is the gradient duration which corresponds to $(t_g^f - t_g^0)$. Useful alternative functions to describe gradient shapes were suggested in [Jand99].

Instead of the gradient duration time, t_g , alternatively an overall gradient slope, G can be used.

$$G = \frac{C_{\text{mod}}^f - C_{\text{mod}}^0}{t_g} \quad (5.2)$$

Using Eq. (5.2), Eq. (5.1) can be expressed also in the following way:

$$C_{\text{mod}}(t) = C_{\text{mod}}^0 + (C_{\text{mod}}^f - C_{\text{mod}}^0)^{1-S} \cdot (t - t_g^0)^S G^S \quad (5.3)$$

When the shape factor is unity ($S=1$), the change in the mobile phase composition is proportional to time (linear gradient). Otherwise, the changes in mobile phase composition become nonlinear. To distinguish, gradients might be called concave for $S>1$ and convex for $S<1$. Gradients often start immediately after the end of the sample injection (and the unavoidable dead time from the pump exit to the column inlet), i.e. $t_g^0 = t_{\text{inj}}$.

Linear gradients can be easily realized practically. However, using modern HPLC equipment, also nonlinear gradients of arbitrary shape could be approximated, e.g. by using a larger number of adjusted multi-linear or multi-step segments.

5.3. Instrumentation to form gradient profiles

The success of gradient elution chromatography is determined above all by the instrumentation used. The reproducibility and retention characteristics depend on the performance of the equipment generating gradients of the mobile phase. In modern gradient elution chromatographs the concentration of the gradient is controlled by the

electronic part of the system, which is usually located in a separate module. These instruments can be classified according to the hydraulic system into two groups as shown in Figures 5.3 a and 5.3b [Jand85].

a) *Low-pressure mixing (Two tank method)*: In this case the devices in which the solvent which form gradients are mixed in a low pressure part at the inlet of a single high pressure pump. This method is less accurate and cheaper because of requiring only a single pump.

b) *High-pressure mixing (Two pump method)*: in this case the apparatus in which the components of the mobile phase are mixed in the high pressure part by means of two high pressure pumps. This method results in relatively accurate gradient profiles but is expensive because of the two pumps needed.

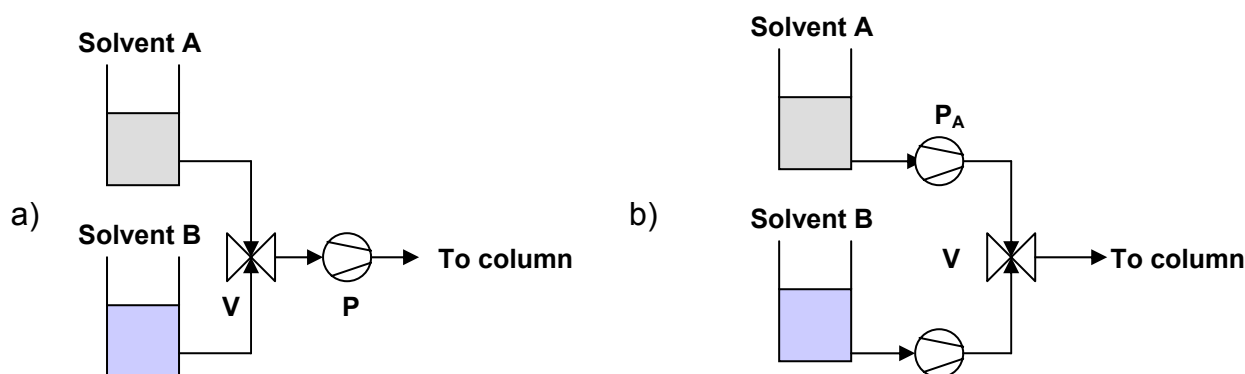


Figure 5.3. Illustration of a) low-pressure b) high-pressure mixing methods to form gradients.

6. Optimization of gradient chromatography

In this section are discussed, the optimization techniques applied to optimize gradient elution chromatography. This optimization is based on a through understanding of the whole process. As a matter of fact, economic production is the best justification for the optimization of the experimental conditions and the detailed study of the fundamentals of nonlinear chromatography in general.

The optimization of chromatographic elution process will be based on the shape of the corresponding peak profiles of the individual components. These profiles determine the cut points for fractionation and thus the purities, the amounts produced and the cycle times. These factors further determine the yields, productivities and ultimately the costs of the separation [Guio06]. These and other quantities are introduced below.

6.1. Performance criteria

In preparative chromatography the choice of an appropriate objective function typically depends on the concrete separation problem. Usually productivity, Pr , and/or yield, Y , of a certain target component are used to evaluate the performance of a preparative chromatographic separation process [Guio06].

a) Productivity

The rate of producing, for example the target component 2 of a ternary mixture, Pr_2 , can be defined as amount of this compound collected per injection, $m_{2, coll}$, divided by the cycle time, Δt_c , and the column cross-section area [Guio06]:

$$Pr_2 = \frac{m_{2, coll}}{\Delta t_c \varepsilon A_{col}} \quad (6.1)$$

To determine the productivity, the corresponding amounts of purified component and the cycle time must be determined. This requires the specification of a desired purity,

$Pur_{2, des}$, and a threshold concentration, $C_{threshold}$, to fix the cut times. A suitable mathematical procedure capable to calculate Pr_2 based on integrating the individual band profiles was described e.g. in [Shan04].

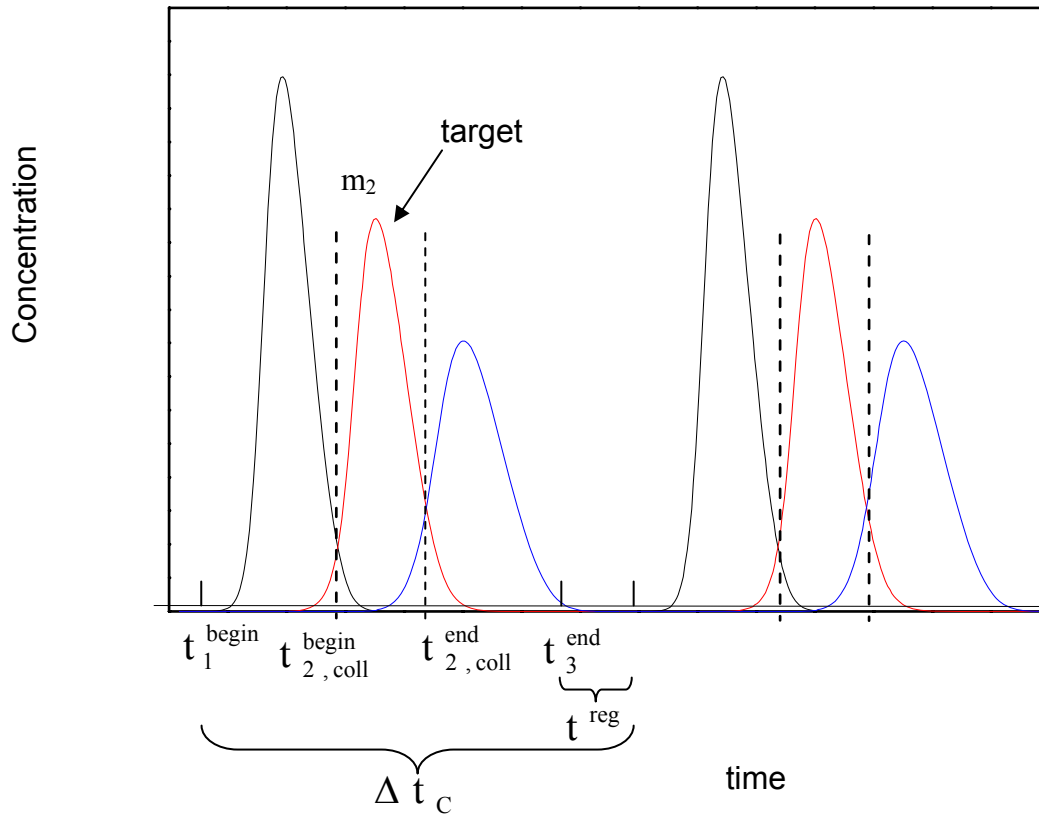


Figure 6.1. Schematic plot showing the cut times, the regeneration time, the cycle time and the threshold concentration of an elution profile of a ternary mixture, targeting the middle component.

The cycle time, Δt_c , must evaluate the retention time of the injected sample and also the time needed for regenerating the column after the end of the gradient. Thus, a suitable cycle time can be estimated from the time when the outlet concentration of the most retained component N drops below the threshold concentration (t_n^{end}), the time when the concentration of the first eluting component exceeds the threshold concentration (t_1^{begin}) and the time needed for the regeneration of the column (t^{reg}):

$$\Delta t_c = (t_n^{end} - t_1^{begin}) + t^{reg} \quad (6.2)$$

The determination of the cycle time Δt_c Eq. 6.2 requires simply the determination of t_1^{begin} and t_n^{end} using a specified value for $C_{\text{threshold}}$ (Fig. 6.1).

More complicated is the determination of the collection times, $t_{i,\text{coll}}^{\text{begin}}$ and $t_{i,\text{coll}}^{\text{end}}$, and the corresponding amount of purified sample, m_i , for a certain target component i travelling somewhere in the elution train.

The specification of the beginning and the end times for collecting a component i between $t_{i,\text{coll}}^{\text{begin}}$ and $t_{i,\text{coll}}^{\text{end}}$ is related to the desired purity in the target fraction. This integral purity can be calculated according to:

$$\text{Pur}_{i,\text{int}} = \frac{m_{i,\text{coll}}}{\sum_{m=1}^N m_{m,\text{coll}}} = \frac{A_i}{\sum_{m=1}^N A_m} \quad i = 1, n. \quad (6.3)$$

with the corresponding partial peak areas of all components:

$$A_m = \sum_{k=\frac{t_{i,\text{coll}}^{\text{begin}}}{\Delta t}}^{\frac{t_{i,\text{coll}}^{\text{end}}}{\Delta t}} C_{m,j=P}^k \Delta t \quad m = 1, n. \quad (6.4)$$

Due to the discrete character of the Craig model the time axis is expressed as a function of the number of exchange steps k . For larger time steps (in case of smaller stage numbers) round off error might occur performing these discrete calculations. These round-off errors are negligible if the efficiency is high as a typical case.

b) Yield

The yield of a target component i , Y_i , is defined as the ratio of the amount recovered with a given purity in the fraction collected over the amount of the same component injected in the corresponding sample [Guio01]:

$$Y_i = \frac{m_{i,\text{coll}}}{V_{\text{inj}} C_{i,\text{Feed}}} 100\%, \quad i=1, n \quad (6.5)$$

6.1.1. Objective function

The nonlinear nature of preparative chromatography complicates the separation process so much that the derivation of general conclusions regarding these optimum conditions is a rather difficult task. Furthermore, the very choice of the objective function of preparative chromatography is not simple.

When using just the productivity as an objective function, the optimization can not take into account the fact that a productivity increase causes often a yield decrease.

In this work, following Felinger and Guiochon [Feli96], as a good compromise the product of the production rate and the yield was considered. The following objective function OF was maximized for the second eluting target component:

$$OF = Pr_2 \cdot Y_2 \quad (6.6)$$

6.2. Collection strategies and determination of cut times

There are various ways of calculating the amount of target component collected at certain purity from the respective elution profile. This matter was discussed by Shan and et al. [Shan04]. The cut times might vary depending on the collection strategy. It is not trivial to specify suitable collection times for a component i eluting at an arbitrary intermediate position ($1 < i < n$). To identify such times it is useful to investigate possible courses of the “local” (differential) purity in the whole elution profile. In Fig. 6.2, is shown for a ternary mixture the course of the local purity of component 2 at the column outlet.

As the 2^{nd} component is considered here as the target of separation, the collection of this component can be only collected if there exist a time interval in which the local purity of this component is equal or larger than the desired integral purity ($Pur_{2,\text{local}}^k \geq Pur_{2,\text{des}}$). Then it is reasonable to identify at first the interval of the elution profile in which the local purity of the target component exceeds the desired purity $Pur_{2,\text{des}}$, i.e.

$$[t_{2,\text{pur}}^{\text{begin}}, t_{2,\text{pur}}^{\text{begin}}].$$

As illustrated in Fig. 6.2 there exist essentially three simple strategies to frame the size of this interval in order to match integral and desired purity. Two strategies consist in expanding the initial interval just in one direction, i.e. in the direction of lower or in the direction of higher retention times. The third strategy, which has been implemented in this work, is based on expanding the interval simultaneously into both directions. The mathematical description of these three strategies is summarized below.

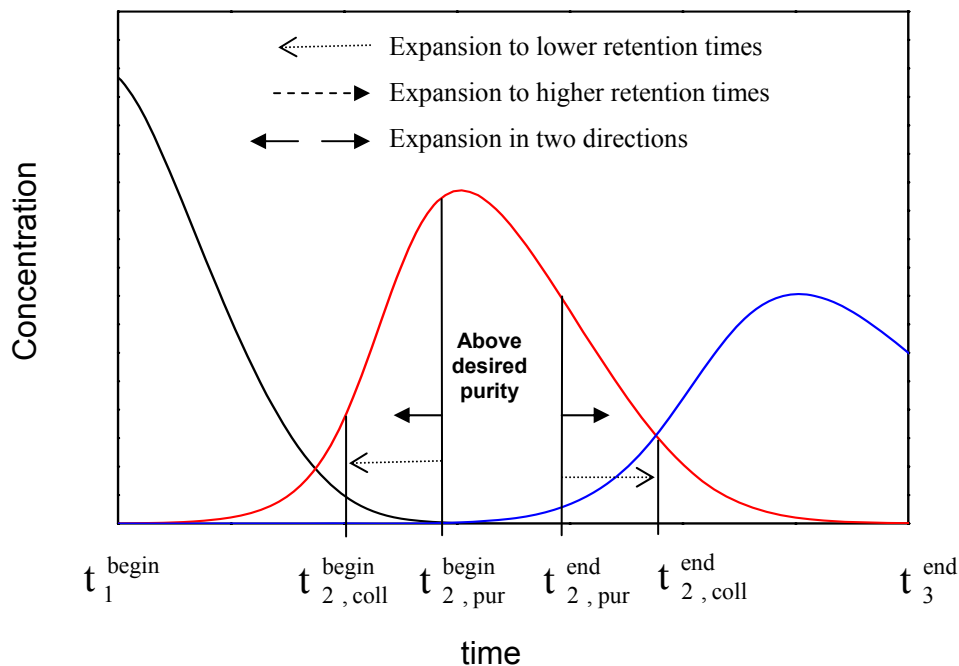


Figure 6.2. Chromatogram illustrating the different collection strategies of the second eluting component from a ternary mixture.

(a) Expansion to higher retention times

In this method, the concentration of component 2 in the fraction is determined by integrating between $t_{2,coll}^{begin} = t_{2,pur}^{begin}$ and a time $t_{2,coll}^{end}$. The latter time will be longer than $t_{2,pur}^{end}$. It has to be determined in a way that the integral purity of the fraction matches the specified desired value.

(b) Expansion to lower retention times

This method is based on keeping the last time at which the local purity of the target component is larger than the desired purity, $t_{2,pur}^{end}$. The method consists in integrating the concentrations of the components in the direction of lower retention times until

the integral purity reaches the set value. Thus, a $t_{2,\text{coll}}^{\text{begin}}$ can be found which is smaller than $t_{2,\text{pur}}^{\text{begin}}$.

(c) Expansion in two directions

The following algorithm was implemented in this work to calculate the local productivities and integral purities so as to determine the final objective function of a given chromatogram of ternary mixtures.

This more sophisticated expansion is based on enlarging the initial time interval $[t_{2,\text{pur}}^{\text{begin}}, t_{2,\text{pur}}^{\text{end}}]$ step by step in one of the two directions. This strategy is applied in this work for all cases of optimization. The interval is initially characterized by the following two discrete grid points:

$$k^{\text{begin}} = \frac{t_{2,\text{pur}}^{\text{begin}}}{\Delta t} \quad \text{and} \quad k^{\text{end}} = \frac{t_{2,\text{pur}}^{\text{end}}}{\Delta t} \quad (6.7)$$

The specific partial peak areas corresponding to this interval can be obtained by integration as follows:

$$A_{2,\text{pur}} = \sum_{k^{\text{begin}}}^{k^{\text{end}}} C_{2,N} \Delta t \quad (6.8)$$

In order to decide in which direction the stepwise enlargement of the interval should be performed the following scheme was used:

$$\begin{aligned} \text{if } \text{Pur}_i^{k^{\text{begin}-1}} = \text{Pur}_i^{k^{\text{end}+1}} \text{ then } A_{i,\text{pur}} &= A_{i,\text{pur}} + \max[C_{i,N}^{k_1-1}, C_{i,N}^{k_2+1}] \Delta t \\ \text{if } C_{i,N}^{k,\text{begin}-1} \geq C_{i,N}^{k,\text{begin}+1} \text{ then } k^{\text{begin}} &= k^{\text{begin}-1} \end{aligned} \quad (6.9)$$

$$\text{if } C_{i,N}^{k,\text{begin}-1} < C_{i,N}^{k,\text{begin}+1} \text{ then } k^{\text{end}} = k^{\text{end}+1}$$

$$\text{if } \text{Pur}_i^{k^{\text{begin}-1}} > \text{Pur}_i^{k^{\text{end}+1}} \text{ then } A_{i,\text{pur}} = A_{i,\text{pur}} + C_{i,N}^{k^{\text{begin}-1}} \Delta t \text{ and } k^{\text{begin}} = k^{\text{begin}} - 1 \quad (6.10)$$

$$\text{if } \text{Pur}_i^{k^{\text{begin}-1}} < \text{Pur}_i^{k^{\text{end}+1}} \text{ then } A_{i,\text{pur}} = A_{i,\text{pur}} + C_{i,N}^{k^{\text{end}+1}} \Delta t \text{ and } k^{\text{end}} = k^{\text{end}} + 1 \quad (6.11)$$

This enlarging of the interval can be repeated as long as the ratio of the collected amount of component i over the collected amount of the total sample is equal to or larger than $Pur_{2,des}$.

The termination of this procedure yields the required collection times:

$$t_{2, coll}^{begin} = k^{begin} \Delta t \quad \text{and} \quad t_{2, coll}^{end} = k^{end} \Delta t \quad (6.12)$$

6.3. Optimization methods

Optimization focuses on minimizing or maximizing a mathematical function, e.g. the objective function OF given in Eq. 6.6, by changing one or more decision variables influencing OF. The values of these free variables can be restricted by including lower and upper bounds. Further constraints can also be added as linear or nonlinear functions. When using one or two decision variables the objective function surface is easy to plot and the optimum can easily be identified. If there are more decision variables, the objective function surface is difficult to visualize. There are several powerful methods and algorithms available which are capable to solve various types of optimization problems occurring in chromatography. Examples are the simplex method [Feli98], genetic algorithms [Zhan04, Niki07, Cela03] and the use of artificial neural network (ANN).

a) Simplex method

The simplex procedure is a hill-climbing method whose direction of advance is dependent solely on the ranking of responses [Borg87]. The calculations and decisions that guide the procedure are rigorously specified, yet almost trivially simple. The great advantages of the simplex procedure in the optimization of liquid chromatographic separations are that it is able to optimize many interdependent variables with no prior knowledge about the mode of separation or the complexity of the sample. Nor does it require any pre-conceived model of the retention behaviour of solutes and so does not require that the solutes be identified or recognized in individual separations. The method has the further advantages of permitting the introduction of new variables during the optimization process for the price of just one

additional experiment per variable and one can also assess the progress of the optimization during rather than at the end of the experimental sequence. The procedure is therefore relatively efficient and has an empirical feedback which should permit rapid attainment.

A simplex is defined as a geometric figure having one more point (vertex) than the number of variables being optimized. Thus, for two variables a simplex is a triangle and for three variables the simplex is a tetrahedron. Although it is difficult to visualize a simplex for more than three variables, the mathematics do not become more complex and the procedure is easily handled by manual or digital computation.

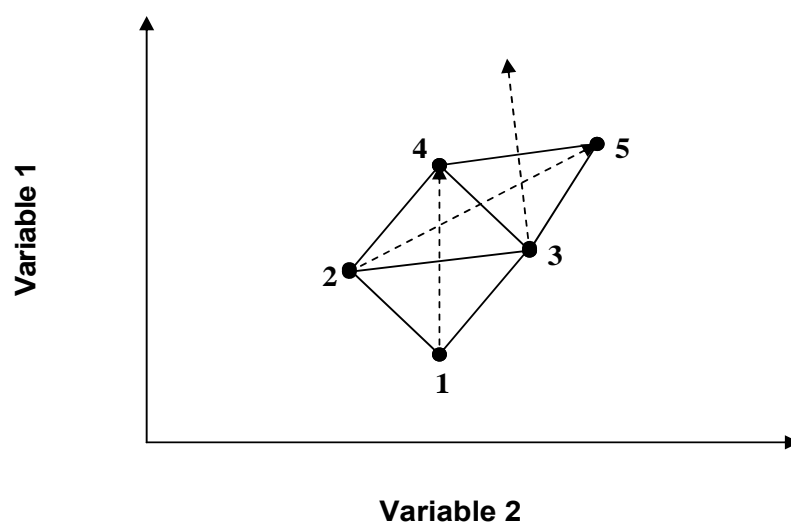


Figure 6.3. Illustration of the simplex optimization algorithm for two variables.

Fig. 6.3. shows a two-variable (dimension) simplex as it moves with fixed step sizes across the range of the two parameters. The optimization proceeds by rejection of the vertex which has the worst experimental response and reflecting its coordinates through the mid point of the hyperline.

The simplex algorithm has been successfully used in optimizations of chromatographic separations [Wrig88, Berr89, Crow90, Mats94].

b) Genetic algorithms (GAs)

Genetic algorithms have been proposed by Holland in the 1960s. It was possible to apply them with reasonable computing times only since the 1990s, when computers became much faster. Genetic algorithms (GAs) are recent technique of optimization, whose basic concept is mimicking the evolution of a species, according to the

Darwinian theory of the “survival of the fittest.” The application of genetic algorithms to complex problems usually produces much better results [Mich94].

The basic idea is to perform a computer simulation of what occurs in nature, and the first problem to be solved is how to code the information in such a way that the computer can treat it. It can therefore be said that the fitness to the environment is a function of the genetic material, in the same way as the result of an experiment is function of the experimental conditions. Therefore, a correspondence genetic material-experimental condition can be established. At a lower level, we can say that the genetic material is defined by the genes, in the same way as an experimental condition is defined by the values of the variables involved in the experiment. Therefore, correspondence genes-variables can be established. According to the evolution theory, the improvement of a species occurs because, through a very high number of generations, the genetic material of its individuals is constantly improving. The reason of this is that the “bad” individuals do not survive and the best ones have a greater probability of spreading their genetic material to the following generation. Beyond this “logical” development, mutations allow the exploration of new “experimental conditions”; usually mutations produce bad results (e.g., severe pathologies).

A genetic algorithm for a particular problem must have the following five components:

- a genetic representation for potential solutions to the problem,
- a way to create an initial population of potential solutions,
- an evaluation function that plays the role of the environment, rating solutions in terms of their “fitness”.
- genetic operators that alter the composition of next generation,
- values for various parameters that the genetic algorithm uses (population size, probabilities of applying genetic operators, etc.)

GAs have been successfully applied in optimization of nonlinear chromatographic separations e.g. in [Lear07, Zhan03, Niki02].

c) Artificial Neural Network (ANN)

In this work, the ANN method was used for optimizing different free parameters to evaluate different gradient separation conditions. In HPLC optimization, ANNs have been already used successfully for peak tracking, in response surface modelling [Mett96] and mobile phase optimization. This method is based on approximating initially the relationships between the free parameters and the objective function using an artificial neural network, and subsequently using this information to find the optimum [Fiss04]. Thus, at first a suitable architecture and parameters for the ANN must be specified. The size of the input layer is determined by the number of parameters that are to be optimized. In this study, the maximum number of optimized parameters was 5, therefore the maximum size of the input layer was set to 5. The output layer, for the cases considered, contains just one node representing the value of the objective function OF (Eq. 6.6). The size of the hidden layer (number of hidden neurons) is a free parameter of the method that should be optimized to obtain best results. The structure of the ANN used below had, equal number of neurons as the number of free parameters to be optimized at the input layer, six neurons at the hidden layer and one output neuron at the third layer. The linear ($f(x) = x$) and tansig ($f(x) = 2 / (1 + \exp(-x)) - 1$) transfer functions, [Matlab], were used for the hidden and output layers. To model the response surface accurately and to train the ANN, a set of data covering the whole region of interest must be provided. This set of training data was obtained by simulating the chromatographic process for different operating conditions using the Craig model. An experimental design method based on orthogonal array (OA), was applied to plan the simulations [Heda]. An orthogonal array of strength r and index x over an alphabet A is a rectangular array with elements from A having the property that, given any r columns of the array, and given any r elements of A (equal or not), there are exactly x rows of the array, where those elements appear in those columns. The idea behind is to have an evenly distributed matrix of optimization parameters. The results obtained are used to train the ANN. The bigger the size of the OA matrix the better the accuracy of the results, but the higher the computation time.

7. Experimental part

In this section the samples, solvent, equipment used in the experimental study and the procedures applied to conduct chromatographic separations using isocratic, linear or nonlinear gradient mode are discussed. As an experimental example, a separation problem was studied which could be solved by reversed phase chromatography using water and methanol mixtures as the mobile phase. The composition of these two solvents was altered with time during the gradients to separate efficiently a ternary mixture of three cycloketones serving as a model system.

7.1. Materials and equipment

Below are described the model substances, the mobile and stationary phases and the equipment used.

7.1.1. Characterization of the system

a) Model components

The three cycloketones used were cyclopentanone (C₅H₈O, synthesis grade from Merck, Schuchardt Hohenbrunn, Germany, purity > 99 %), cyclohexanone (C₆H₁₀O, from Ferak laborat GmbH, Berlin, Germany, 99% purity) and synthesis grade cycloheptanone (C₇H₁₂O from Merck, Schuchardt Hohenbrunn, Germany, 98%

Component	Purity	Molecular weight	Density [g/l]	Melting point [°C]	Boiling point [°C]
Cyclopentanone	> 99 %	84.11	948	-58.2	129
Cyclohexanone	99%	98.14	947	-45	155
Cycloheptanone	98%	112.72	950	n.a	179

Table 7.1. Summary of the properties of the three cycloketones used as model substances.

purity). Some of the basic properties of these model substances are tabulated in Table 7.1 [Perry97].

b) Mobile phase

The water applied as the basic mobile phase was distilled and filtered with a 0.2 μm pore size filter paper. HPLC grade methanol (Merck Darmstadt, Germany) was used as the modifier. Gradients were limited above 30 vol. % methanol and below 50 vol. %, i.e. $C_{\text{mod}} = [30, 50]$. The reason to set the lower limit was to maintain a sufficient life time of the column. The upper limit of 50 vol. % was set based on preliminary experiments in which the retention times did not change anymore when using modifier concentrations above this limit since they reached already the dead time of the column.

c) Stationary phase

Chromatographic separation was studied using a commercially available reversed phase column (HyPURITY C₁₈, 5 μm particle size; 100 mm \times 4.6 mm i.d.) from Thermoelectron corporation (Mainz, Germany).

d) Equipment

The chromatographic analyses were carried out with a Shimadzu high-performance liquid chromatograph equipped with a LC-8A double pump, a SCL-10AP automatic injector, a 500 μL sample loop, a SPD-M10A VP diode array UV detector, and a SCL-10A VP system controller (see Figures 7.1-7.3). A computer with a 1.0 GB RAM and 3.41 GHz frequency has been used for data acquisition.

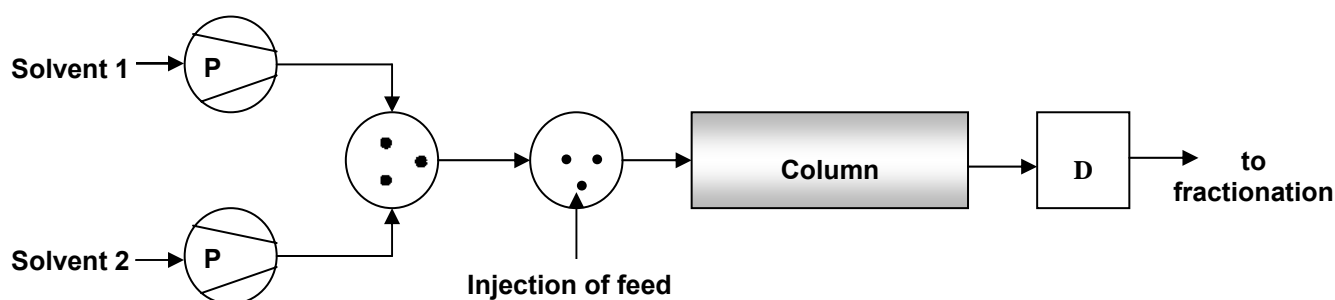


Figure 7.1. Illustration of the experimental setup applied to realize various forms of gradients.



Figure 7.2. Experimental setup of Shimadzu system used.

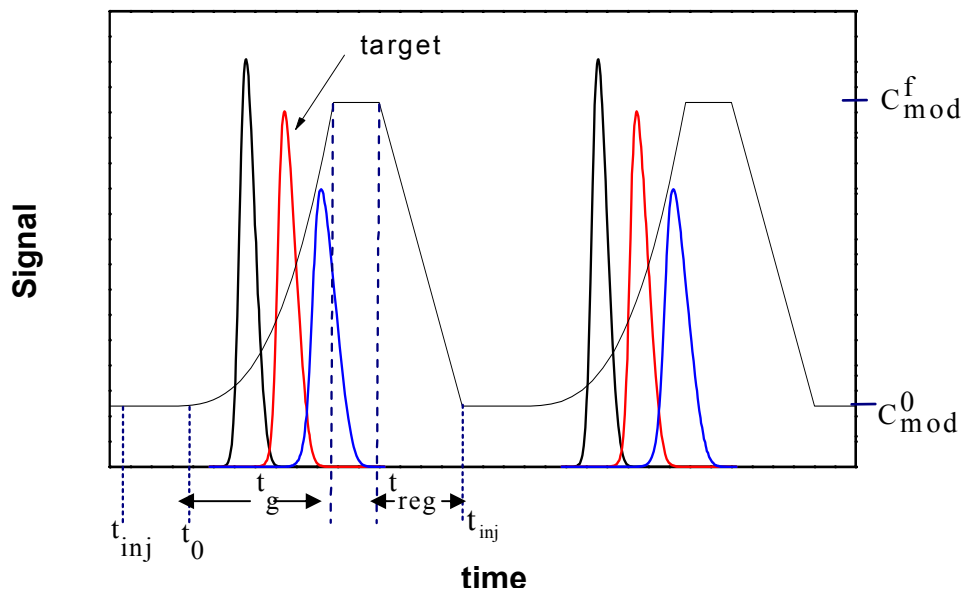


Figure 7.3. Typical chromatograms belonging to two subsequent injections indicating characteristic times.

7.1.2. Dead volumes

The system dead volume includes the void volumes of the column and the voids existing in the connecting tubes. The experimental techniques applied to quantify such undesired volumes are mainly based on the injection of small or large pulses

and an analysis of the obtained elution profile, thereby pure methanol was used as a tracer while equilibrating the system with pure water.

The dead volume of the column includes the sum of the voids between each particle and the pore volume inside each particle. Thus, the dead volume of the column consists of the entire space that small molecules can reach in the stationary phase.

Procedures to measure the different dead volumes, like the dead volume from the buffer selection valve to the detector, the dead volume from injection port to the detector and the dead volume of the column are discussed below.

a) Dead volume from buffer selection valve to detector ($V_{\text{dead}}^{\text{VD}}$)

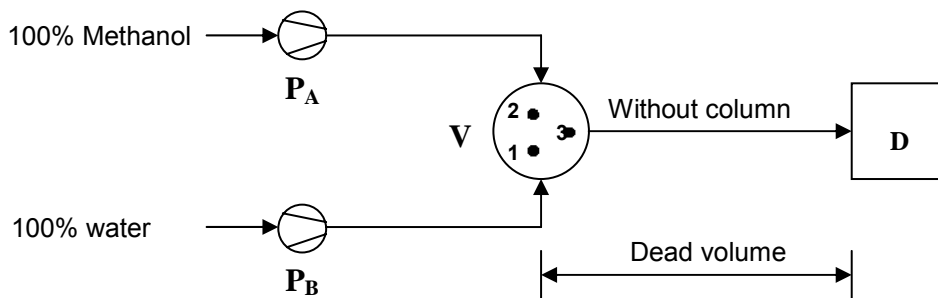


Figure 7.4. Experimental setup used to measure the dead volume from the buffer selection valve to the detector.

To measure the dead volume from buffer selection valve to detector ($V_{\text{dead}}^{\text{VD}}$), first both methanol and water were pumped to fill the tube from each pump till the buffer selection valve. Then the system was equilibrated with pure water using only pump B, while opening the valves 1 and 3 and closing valve 2. After equilibrium is reached, valves 2 and 3 were opened and valve 1 was closed. Finally methanol was pumped and detection started at the same time.

When the tracer reaches the detector, a breakthrough curve is recorded. The retention time for this process can be estimated at half height of the breakthrough curve.

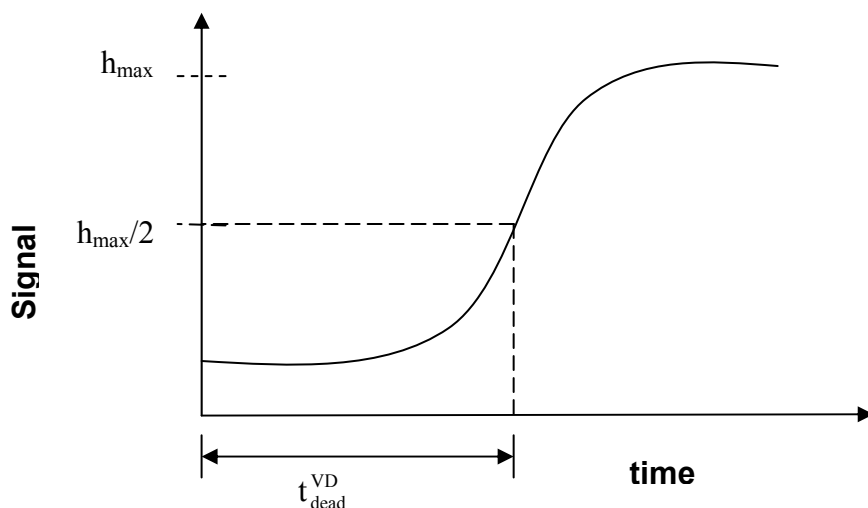


Figure 7.5. Breakthrough curve to estimate the dead volume from the buffer selection valve to detector.

The dead volume from the buffer selection valve to the detector was finally calculated as the product of the retention time (as shown in Fig. 7.5) and the flow rate.

$$V_{\text{dead}}^{\text{VD}} = t_{\text{dead}}^{\text{VD}} \cdot F \quad (7.1)$$

b) Dead volume from the injection port to the detector ($V_{\text{dead}}^{\text{ID}}$)

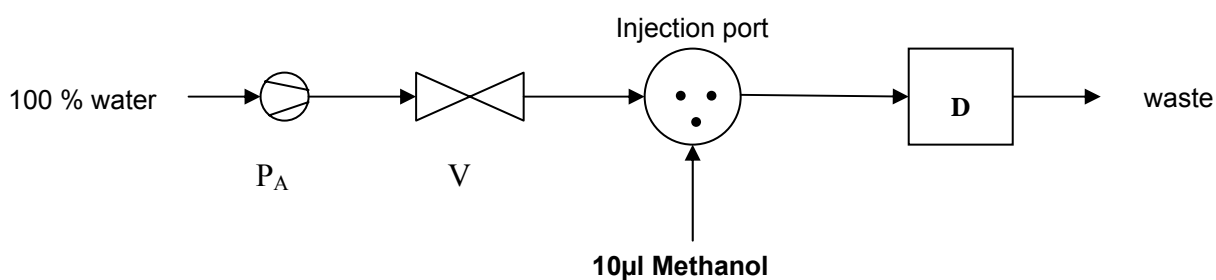


Figure 7.6. Experimental setup used to measure the dead volume from the injector to the detector.

Initially the system was equilibrated using pure water provided by pump A before 10µl methanol was injected to the system. The detector recorded the resulting peak.

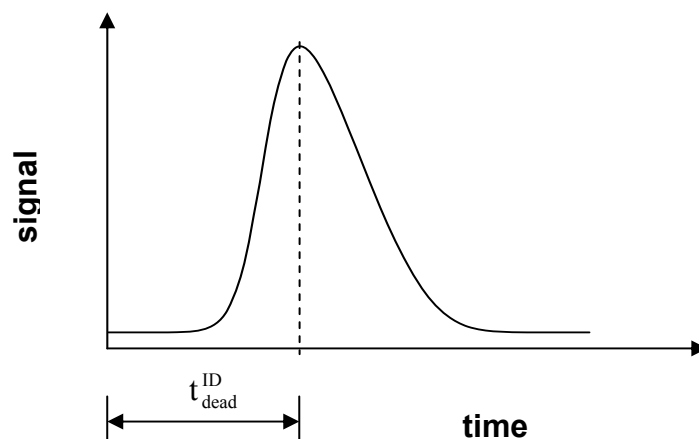


Figure 7.7. Chromatogram for the determination of the dead volume between the injector and the detector (injection of a small amount of tracer).

This experiment was repeated three times to assure reproducibility. The retention time at the maximum peak was taken to estimate the dead volume from the injection port to the detector as:

$$V_{\text{dead}}^{\text{ID}} = t_{\text{dead}}^{\text{ID}} \cdot F \quad (7.2)$$

The determination of the dead volume of the column (or porosity) will be discussed in the next section.

7.2. Characterization of the column and the detector

In order to characterize the column and to determine the parameters required to apply the Craig model (Eq. 3.16), the dead volume of the column, the porosity of the column (ϵ) and the number of theoretical plate (N) must be known.

7.2.1. Column porosity

The total porosity (ϵ), which is realized to the column dead volume, was determined by injecting 10 μ l of 100% modifier (methanol, which was assumed to be non-retained) and measuring the corresponding retention time t_0 in a mobile phase with 30 vol. % modifier concentration. The setup is illustrated in Figure 7.8.

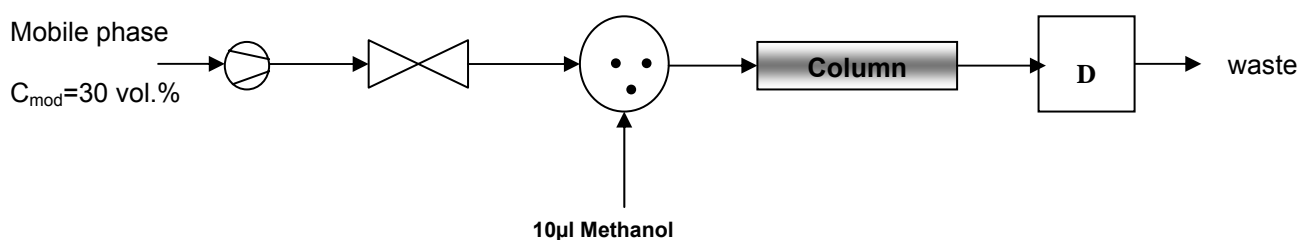


Figure 7.8. Experimental setup applied to measure column dead volume.

A typical peak measured by the detector is illustrated in Fig. 7.9.

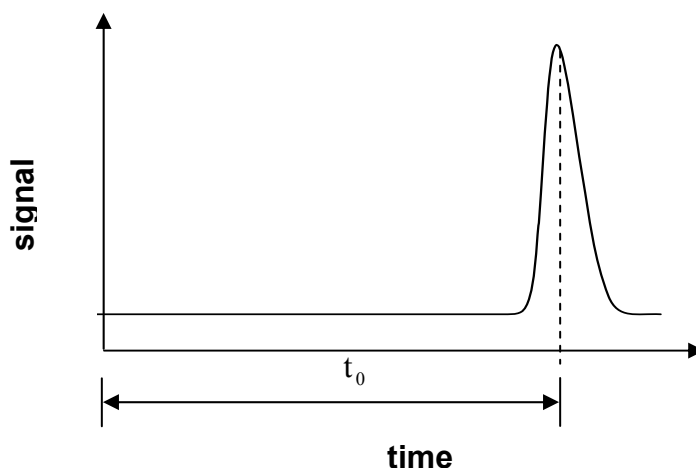


Figure 7.9. Chromatogram for the estimation of the dead volume (porosity) of the column.

From the dead time of the column measured above in Fig 7.9, the total porosity of the column was estimated to be:

$$\epsilon = \frac{t_0 F}{V_c} \quad (7.3)$$

where F is again the flow rate and V_c is the volume of the column.

7.2.2. Number of theoretical plates

The theoretical plate numbers (N), (Eq. 2.9), were estimated based on the widths and heights of analytical peaks. For this, 20 μ l of each of the individual three components were injected separately and the resulting peaks were analysed. Three different isocratic conditions have been considered in each case (C_{mod} =30, 40 and 50 vol. %). Finally an average plate number was determined and used for the simulations.

7.2.3. Detector calibration

Detector calibration is an important step in nearly all investigations involving nonlinear chromatography. The aim of detector calibration is to determine a relationship between the response or signal of a detector and the concentration of the studied compound in the detector cell. The relationship between the output signal and the analyte concentration is characterized by a response function. This function can be e.g. linear, logarithmic or any other form.

a) The Beer-Lambert law

Compounds absorb light when they are exposed to it. For each wavelength of light passing through the spectrometer, the intensity of the light passing through the reference cell is measured. If a beam of monochromic radiation of intensity I_0 , directed at a sample solution, absorption takes place. The beam leaving the sample has intensity I . Typically I is less than I_0 .

According to the Beer-Lambert law, the absorbance, A , of a beam of radiation in a homogeneous isotropic medium is proportional to the absorption path length, d , and to the concentration, c [Ingl88, Clar93,]:

$$A = \log\left(\frac{I_0}{I}\right) = \lambda cd \quad (7.4)$$

Where λ is the molar absorptivity.

b) Calibration of detectors for linear responses

In this work we verified that the detector operated in the linear range. The parameter which characterizes the calibration process is called the calibration factor (k_f), which is the slope of the calibration curve.

Considering a signal-time chromatogram, $Sg(t)$, as the output of the detector, the relationship between the signal and concentration in order to get a concentration time curve, $C(t)$, could be derived using the area method. The fundamental of determining the calibration factor is that the peak area under the curve of signal vs. time, $A^{\text{peak*}}$, will be proportional to the amount of component injected, M^{inj} , so that the calibration factor, k_f , will then be the proportionality constant as derived below.

$$A^{\text{peak*}} = \int_0^{\infty} Sg(t)dt \quad (7.5)$$

Multiplying this area by the volumetric flow rate gives $A^{\text{peak*}}$:

$$A^{\text{peak}} = A^{\text{peak*}}F \quad (7.6)$$

This should be proportional to the amount of injected sample m_{inj} :

$$M^{\text{inj}} = C_{\text{inj}} \cdot V_{\text{inj}} = k_f A^{\text{peak}} \quad (7.7)$$

Finally the calibration factor k_f , is:

$$k_f = \frac{M^{\text{inj}}}{A^{\text{peak}}} \quad (7.8)$$

This can be used to generate, $C(t)$, according to:

$$C(t) = k_f Sg(t) \quad (7.9)$$

7.3. Isotherm parameters of the model components

There are various methods available to determine adsorption isotherms and the parameters of Eq. 3.34. These methods were discussed in chapter 4. The main ones are frontal analysis (FA), frontal analysis by characteristics point (FACP), elution by characteristics (ECP), pulse methods and the inverse method [Guio06, Morg04].

a) Isotherm parameters

In this work, the ECP method has been used for the generation of first estimates of the three single component isotherm parameters at four different constant modifier concentrations ($C_{\text{mod}}=30, 35, 40$ and 45 vol. %). As it is discussed in section 4.1.2, in the ECP method, isotherms are derived from the rear part of an overloaded elution profile. When a large sample size is injected into a chromatographic column, often an unsymmetrical band is eluting with a steep front and a diffuse rear. The evaluation method uses the ideal model of chromatography assuming that the column efficiency is infinite [Guio06, Craig44]. The knowledge of the course of the retention times of the dispersed rear parts, $t_r(C)$, allows for Langmuirian systems (characterized by dispersed tails of the peaks) determining the course of the slope of the single solute adsorption isotherm, $\frac{dq}{dC}$, as follows [Morg04]:

$$\left. \frac{dq}{dC} \right|_c = \frac{t_r(C) - t_{\text{inj}} - t_0}{t_0 \left(\frac{1 - \varepsilon}{\varepsilon} \right)} \quad (7.10)$$

And from the Langmuir isotherm (Eq.3.28) $\frac{dq}{dC}$ is:

$$\frac{dq}{dc} = \frac{a}{(1 + bC)^2} \quad (7.11)$$

All experimental data were measured at room temperature, with a flow rate of $F= 1$ ml/min and using a UV detector at a wavelength of 290 nm. Initial estimates for the

isotherm parameters were determined from the $\frac{dq}{dC}$ belonging to the peak of the largest sample size injected and Eqs. 7.10 and 7.11. After this first rough parameter estimation, a refinement was performed based on analyzing overloaded elution profiles for mixtures of all the three cycloketones at the four constant modifier concentrations. Applying the inverse method [Feli03], numerical values of the parameters of the isotherm model were estimated from the best match between measured peaks and peaks generated numerically by the Crag model (Eq. 3.16), in combination with a least-square Marquardt algorithm provided by Matlab [Matlab].

b) Effect of modifier concentration on isotherms

Since reversed phase chromatography was used to separate the model components in this study, Eqs. 3.31 and 3.32 were used to determine the respective parameters which describe the effect of modifier concentration on the isotherm parameters ($a_i = f(C_{\text{mod}}, P_{1,i}, P_{2,i})$ and $b_i = f(C_{\text{mod}}, P_{3,i}, P_{4,i})$).

All isotherm parameters of various isocratic conditions together with the parameters which define the effect of mobile phase composition on isotherms are tabulated in chapter 9.

7.4. Realization of gradient profiles

The various setups which could be used to form gradient profiles were discussed in section 5.1. In this study, the two-tank method was implemented to form gradient profiles. Using this setup there are several options to realize an arbitrary gradient shape. One can use e.g. several successive step gradients to approximate a certain nonlinear gradient shape as shown in Figs.7.10, Fig.11 and Table 7.2.

One can also use a number of successive linear gradients to approximate the required nonlinear shape. Typically, the latter technique approximates more accurately continuous nonlinear gradients. Because of this reason, this approach was applied in this study.

To realize gradient shapes precisely, the gradient delay volume, which in this case is the dead volume between the intersection point of the flows from the two pump outlets (where the gradient is formed) and the column inlet should be kept as small as possible (see Figure 7.1). Instrumental dwell volumes and the dead volumes between the actual pump exits and the flow intersection point were neglected in the model.

The minimum possible flow rate increment of the pump also plays a major role for the precision of realizing nonlinear gradient shapes. In this work, the value was 0.1 ml/min for the vp LC-8A Shimadzu HPLC pump, which was found to be sufficiently adequate for the purpose of this work.

Pump programmes and procedures which are used to form the required linear or nonlinear gradient profiles are found in Appendix A.

With the setup described selected isocratic and gradient runs were carried out. Of particular interest were the final runs performed to realize the optimal gradients predicted theoretically (see Section 9.4.2).

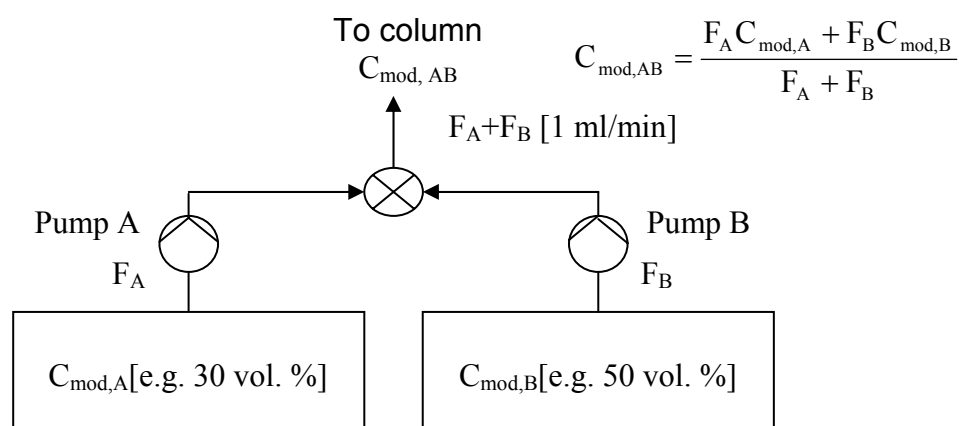


Figure 7.10. Pump setup for the formation of nonlinear gradient profile shown in Fig. 7.11.

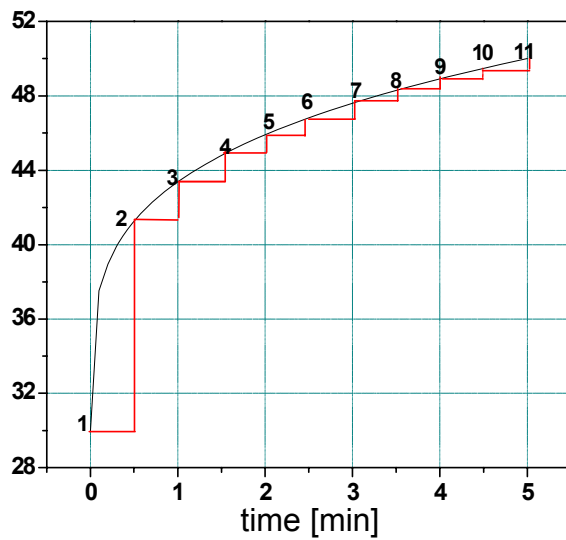


Figure 7.11. Gradient profile to be realized with the multi-step gradient approximations. (Shape factor $S=0.25$, gradient time $t_g=5$ min, initial and final modifier concentrations, $C_{\text{mod,A}}=30$ vol. % and $C_{\text{mod,B}}=30$ vol. %).

Point	C_{mod} [vol.%]	F_A (ml/min)	F_B (ml/min)
1	30	1	0
2	41,2	0,44	0,56
3	43,37	0,33	0,67
4	44,8	0,26	0,74
5	45,9	0,2	0,8
6	46,81	0,16	0,84
7	47,6	0,12	0,88
8	48,29	0,09	0,91
9	48,91	0,05	0,95
10	49,48	0,03	0,97
11	50	0	1

Table 7.2. Pump flow rates and corresponding modifier concentrations of Figure 7.11.

8. Optimization problems formulated

In order to study the potential of applying nonlinear gradients for the separation of the middle component of a ternary mixture, different approaches can be used. In this study, various gradient operations having different shapes as discussed in Section 5.2 are investigated thereby ternary mixtures are considered as a subset of more general multi-component mixtures. The investigation of the separation of ternary mixtures described below could easily be extended to solve multi-component separation problems.

As it was mentioned in Section 3.2, Craig's cell model has been used to describe the chromatographic separation process quantitatively. Competitive isotherm parameters of the model components which were determined using the ECP and inverse methods were used in this model to compute elution profiles. As it has been discussed in Section 6.4, the ANN method was used to determine optimum operating conditions and the corresponding yield and productivity values. These optimum operating conditions which resulted from the optimization have been finally used to generate elution profiles experimentally. Thus, the simulated and measured peaks were compared in order to verify the capability of the models and approaches used in this study.

8.1. Free parameters

The essential free parameters which can be specified in order to optimize a chromatographic separation in an available column are the volumetric flow rate ($F=1$ ml/min), the injection volume (V_{inj}), the feed concentrations ($C_{i, Feed}=3$ vol. %, 1:1:1 $C_5:C_6:C_7$), and the gradient profile parameters, i.e. the shape factor (S), the gradient time (t_g) and the initial and final modifier concentrations (C_{mod}^0 , C_{mod}^f). Other fixed constant parameters are shown in Fig. 8.1.

Primary goal of this work is to demonstrate the potential of nonlinear gradients. Thus emphasis was given to optimize the gradient shape factor S . The feed concentrations were held constant. The gradient shape factor, the gradient time, the initial and final modifier concentrations and the injection volume were taken as the free parameters to be optimized.

The range of optimization for each of the free parameters, other related issues and different scenarios investigated are discussed in the following sections.

8.2. Scenarios studied

The four scenarios considered evaluating nonlinear gradients and comparing linear gradients and isocratic operation are presented as follows:

8.2.1. Case 1 (isocratic, two degrees of freedom)

This case focuses on optimization of the conditions for isocratic operation as a base or reference state. Optimized were two important free operating parameters: the injection volume, V_{inj} , and the (constant) modifier concentration, C_{mod} . This case was used as reference to evaluate the gain available by optimizing more free parameters.

8.2.2. Case 2 (three degrees of freedom)

In this case three parameters were optimized: V_{inj} , and the initial and final modifier concentrations, C_{mod}^0 and C_{mod}^f . These calculations were carried out for three different predefined gradient shape factors (linear, concave and convex) and a given gradient duration t_g . That is, three typical gradient shapes which represent the three modes of gradients have been selected based on pre-optimization investigations. For each of these three gradient shapes, the respective three parameters have been optimized.

8.2.3. Case 3 (linear gradients, four degrees of freedom)

Case 3 focuses entirely on linear gradients (i.e. on gradient shape factors $S=1$). Four free parameters were considered. These are again V_{inj} , C_{mod}^0 and C_{mod}^f . In addition the gradient time t_g was optimized. In this case the maximum potential of optimizing a linear gradient profile was computed.

8.2.4. Case 4 (five degrees of freedom)

The last case focuses on the overall optimization of the five free parameters, V_{inj} , C_{mod}^0 , C_{mod}^f , t_g and S . The gradient shape is initially unknown, i.e. it is not specified whether the best operation is optimum is isocratic, a linear or a nonlinear gradient.

A summary of the four cases with the corresponding ranges of optimized parameters is shown in Table 8.2.

8.3. Optimization ranges and intervals

As discussed in Chapter 6, an artificial neural network (ANN) technique has been used to optimize the separation processes considered. Thus, the first step was to specify a suitable architecture and the parameters of the ANN. The input layer of the network varies with the number of free parameters of the cases introduced in Section 8.2. Thereby, the ANN has only one output layer that represents the objective function (OF), which is the product of purity and yield, (Eq.6.6). Therefore for the above four cases, based on the number of decision variables, four different ANN architectures were used. An example is shown in Figure 8.1 for case 4.

During all optimizations the required purity of cyclohexanone was set to $Pur_{2,des}=98\%$, the column regeneration time to $t_{reg}=4$ min, i.e. four times the column hold-up time

and the threshold concentration to $C_{\text{threshold}}=0.00001$ vol.%, see Table 8.1. The feed concentration was kept constant: $C_{5, \text{Feed}}=C_{6, \text{Feed}}=C_{7, \text{Feed}}=1$ vol. %. The optimization range of each of the parameters was set based on the results of preliminary explorative experimental investigations. The optimization range for the initial and / or final modifier concentration was within 30-50 vol. % and for the injection volume 100-500 μl . The range for gradient time was set to 1-6 min and for the gradient shape factors to 0.10-4.00.

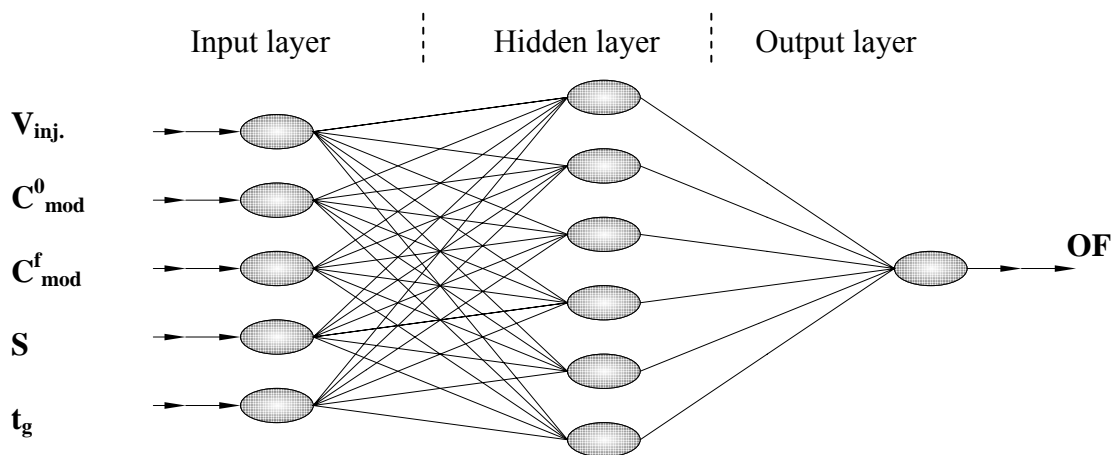


Figure 8.1. Architecture of the ANN used for the optimization steps, with tansig and linear transfer functions used before and after the hidden layer respectively, for case 4 with five input parameters.

In all cases, for the free parameters specific realistic intervals were provided to generate the orthogonal array matrix. The step changes used were: 5 vol. % for the modifier concentration, 15 μl for the injection volume, 0.5 min for the gradient time and 0.25 for the gradient shape factor. The resulting optimum operating conditions and the corresponding optimum yield and productivities are presented in Section 8.4.

Fixed constant values	
------------------------------	--

$C_{\text{threshold}}$ [vol.%] (threshold concentration)	0.00001
$\text{Pur}_{2, \text{des}}$ [%] (desired purity)	98
t_{reg} [min] (regeneration time)	4

Table 8.1. Parameters fixed in the optimizations.

Table 8.2. Summary of the different cases considered for optimizing productivities, yields and the corresponding operating conditions. In all cases constant parameters: see Table 8.1 and $C_{1, \text{Feed}}=C_{2, \text{Feed}}=C_{3, \text{Feed}}=1$ vol. %, $F=1$ ml/min, $t_g^0=V_{\text{inj}}/F$, $P=500$.

Cases	Additional constant parameters	Number of Free Parameters	Free parameters*	Optimization range
Case 1	Isocratic	2	V_{inj} $C_{\text{mod}}=C_{\text{mod}}^0$	[100,500 μl] [30-50 vol.%]
Case 2	a) $S=0.25$, $t_g=4$ b) $S=1.0$, $t_g=4$ c) $S=1.2$, $t_g=4$	3	V_{inj} C_{mod}^0 C_{mod}^f	[100,500 μl] [30-50 vol.%] [30-50 vol.%]
Case 3	$S=1$	4	V_{inj} C_{mod}^0 C_{mod}^f t_g	[100,500 μl] [30,50 vol.%] [30,50 vol.%] [1.0 , 6.0 min]
Case 4	None	5	V_{inj} C_{mod}^0 C_{mod}^f t_g S	[100,500 μl] [30,50 vol.%] [30,50 vol.%] [1.0,6.0 min] [0.10,4.0]

9. Results and discussion

In this section, main results of the study are discussed. In the Section 9.1, the results of the characterization of the system used for experimental analysis are given followed by a presentation of the adsorption isotherm parameters of the three model components (Section 9.2). The effect of modifier concentration on these isotherm parameters is presented in Section 9.3. In section 9.4, the results of the analysis of applying isocratic, linear and nonlinear gradients for the optimized separation of the middle component out of a ternary mixture are discussed. In this section different scenarios are compared. These scenarios are divided based on the number of free parameters to be optimized. Finally the calculated and measured elution profiles were compared in order to verify the mathematical models used to predict the development of concentration profiles along the column.

9.1. System characterization

The system characterization included measurement of various dead volumes of the capillaries and calibration of the detector cell at different modifier compositions as well as measurement of column porosity and theoretical plate numbers for each of the three model components.

9.1.1. Dead volume measurement

In reference to Figures 7.1-7.3, the whole system has different sections where each section fulfils a certain task (e.g. injector, column, detector etc.). In between these devices there are capillaries connecting the parts of the whole system. Thus it was

necessary to measure the dead volume of each section as shown in Section 7, to know the real values of retention times.

a) Dead volume from buffer selection valve to detector

With reference to Figure 7.4, the dead volume between buffer selection valve (intersection point of the two pump outlets) and the detector was measured as shown in Fig. 9.1.

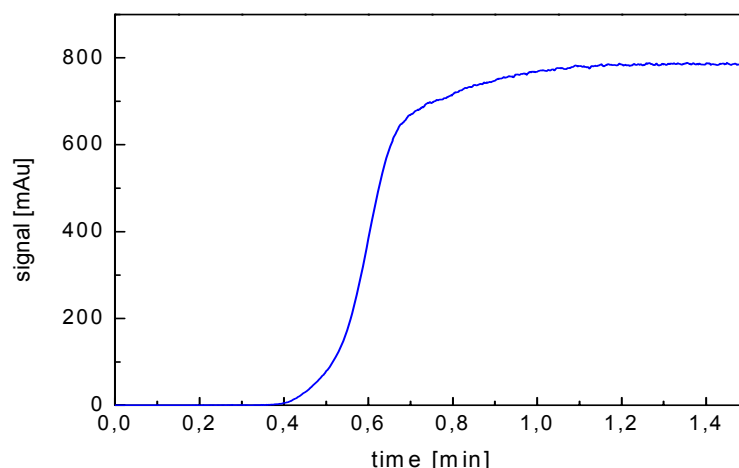


Figure 9.1. Breakthrough curve recorded to measure the dead volume between buffer selection valve and detector ($V_{\text{dead}}^{\text{VD}}$) using mobile phase with $C_{\text{mod}}=50$ vol. % and a flow rate $F=1$ ml/min at wave length of 290nm.

b) Dead volume from injector to detector

Based on the experimental set up of Figure 7.6, the dead volume between the injection port and the detector was measured as shown in Fig. 9.2.

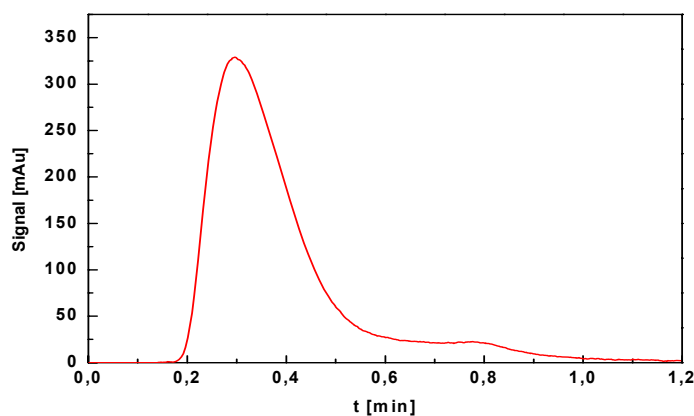


Figure 9.2. Chromatogram obtained at wave length of 190nm after injecting $5\mu\text{l}$ of methanol to measure dead volume between the injection port and detector ($V_{\text{dead}}^{\text{ID}}$) using pure water as mobile phase and flow rate $F=1$ ml/min.

The values of dead volumes determined from the respective Figures 9.1 and 9.2 which are shown in Table 9.1, were average values taken after repeating each measurement three times.

Dead volumes	Average measured value [ml]
Between valve and detector ($V_{\text{dead}}^{\text{VD}}$)	0.5450
Between valve and injector ($V_{\text{dead}}^{\text{VI}}$)	0.2256
Between injector and detector ($V_{\text{dead}}^{\text{ID}}$)	0.3194

Table 9.1. Dead volumes of the system.

These dead volumes are used to get the real concentration profiles and respective experimental gradient shapes at the column exit depicted in Section 9.4.2 and else where.

9.1.2. Column porosity and efficiency

Porosity of the column and efficiency (theoretical plate number) were determined based on the experimental procedures presented in Chapter 7.

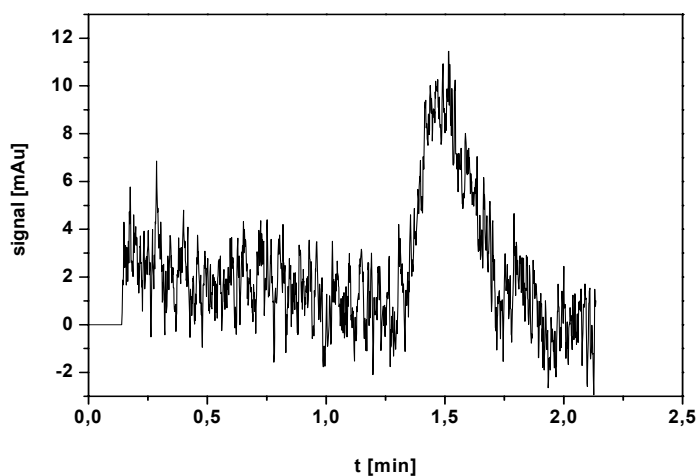


Figure 9.3. Signal-time curve to determine the retention time of the presumed non retained component so as to measure column porosity. (10 μ l Methanol, in $C_{\text{mod}} = 30$ vol. % at wavelength of 190nm).

The overall porosity of the column was calculated, from the retention time of a small methanol pulse recorded at 190 nm, as $\varepsilon=0.65$ (Fig. 9.3).

The plate numbers were measured by injecting a feed concentration of $C_{\text{feed}}=1$ vol. % and injection volume of $V_{\text{inj}}=5\mu\text{l}$ for each of the three cycloketones at three different isocratic conditions ($C_{\text{mod}}=30, 40$ and 50 vol. %) each of cycloketones. The analytic peaks used to estimate plate number for each of the three cycloketones at four different isocratic conditions are attached in appendix D.

Summary of the plate number values are shown in the same appendix. The differences between the plate number values of the three cycloketones for the different mobile phase compositions considered were less than 10%. An average theoretical plate number of $N\approx 500$ was estimated and used in the simulations. These parameters estimated along with the column dimensions are given in Table 9.2.

Column dimensions and properties	
L_{col} [cm]	10
d_{col} [cm]	0.46
ε	0.65
N (average value)	500

Table 9.2. Parameters of the chromatographic system.

9.1.3. Calibration factors

Calibration factors of the UV-detector used to record concentration profiles in this work are estimated according to the procedure discussed in Section 7.2.3.

In Table 9.3 are shown, the calibration factors estimated using Eq. 7.9. The corresponding plots are attached in Appendix C.

Components	Calibration factor k_f (Eq. 7.9) for modifier concentration, C_{mod} [vol.%]		
	30	40	50
Cyclopentanone (C_5)	6.5E-6	6.9E-6	9.2E-6
Cyclopentanone (C_6)	9.3E-6	10.0E-6	9.9E-6
Cyclopentanone (C_7)	8.6E-6	9.7E-6	8.9E-6

Table 9.3. Calibration factors estimated for the three cycloketones using the area method at 290nm of a UV-detector cell.

9.2. Adsorption isotherms

Before analyzing the optimum operating conditions of a given chromatographic separation process, the respective adsorption isotherm parameters of the mixture components should be determined. In this section, adsorption isotherm parameters of the three cycloketones are presented.

At first single component adsorption isotherms were estimated from the rear parts of chromatograms recorded for four isocratic conditions (30, 35, 40 and 45 vol. %) with feed concentrations of $C_{Feed}=10$ vol. % and injection volumes of $V_{inj}=10$ μ l applying Eq. 7.9 for each of the three model components. As an example, a series of concentration overloading are shown in Figs. 9.4 - 9.12, for all the three components (cyclohexanone) at 30 vol. % methanol. See Appendix E for additional overloaded peaks of the three cycloketones measured at different isocratic conditions.

Using these initial parameters peaks for different overloaded injections of the ternary mixture were evaluated using the inverse method as discussed in Section 4.2.1, to get the final isotherm parameters for isocratic conditions.

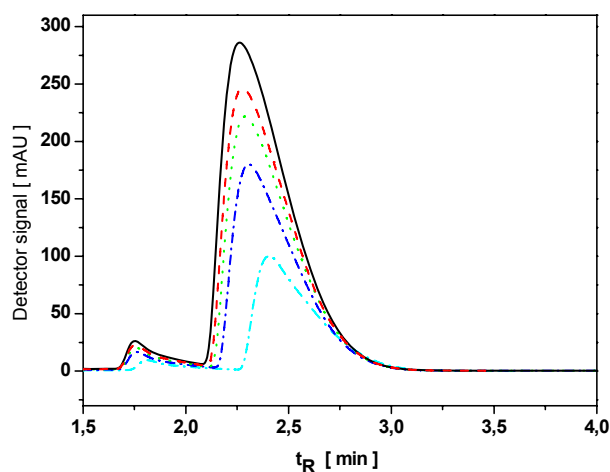


Figure 9.4. Illustration of the ECP method. Elution Profiles for a series of concentration overloading of cyclopentanone (C_5) at a modifier concentration of 30 vol. % ($V_F=1$ ml/min, $V_{inj}=10$ μ l, $C_{Feed} = 2, 4, 6, 8$ and 10 vol. %).

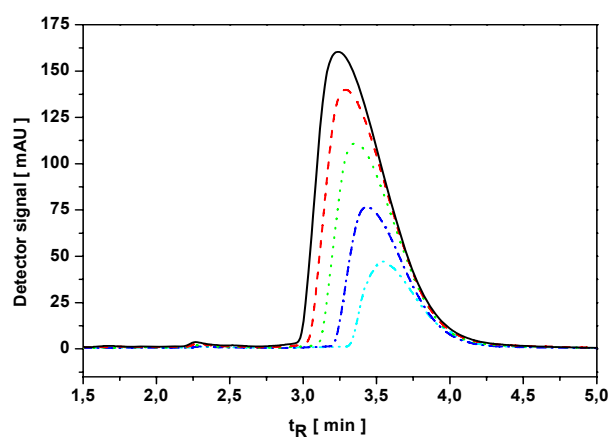


Figure 9.5. Elution Profiles for a series of concentration overloading of cyclohexanone (C_6) at a modifier concentration of 30 vol. % ($V_F=1$ ml/min, $V_{inj}=10$ μ l, $C_{Feed} = 2, 4, 6, 8$ and 10 vol. %).

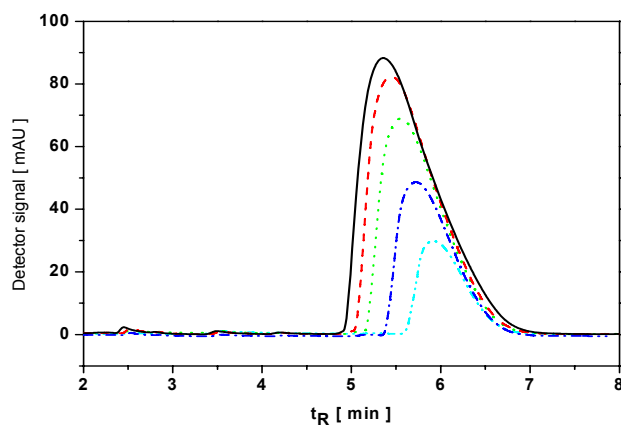


Figure 9.6. Elution Profiles for a series of concentration overloading of cycloheptanone (C_7) at a modifier concentration of 30 vol. % ($V_F=1$ ml/min, $V_{inj}=10$ μ l, $C_{Feed} = 2, 4, 6, 8$ and 10 vol. %).

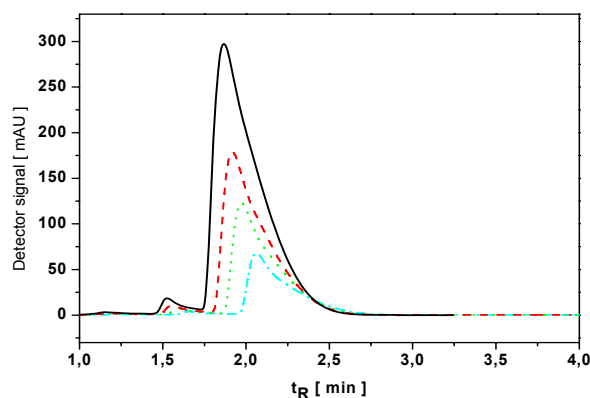


Figure 9.7. Elution Profiles for a series of concentration overloading of cyclopentanone (C_5) at a modifier concentration of 40 vol. % ($V_F=1$ ml/min, $V_{inj}=10$ μ l, $C_{Feed} = 2, 4, 6$ and 10 vol. %).

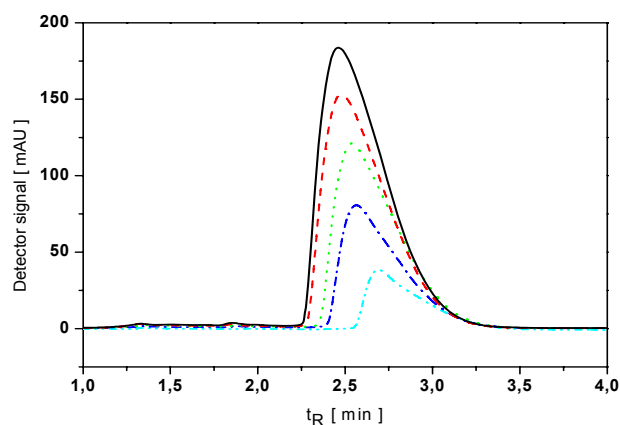


Figure 9.8. Elution Profiles for a series of concentration overloading of cyclohexanone (C_6) at a modifier concentration of 40 vol. % ($V_F=1$ ml/min, $V_{inj}=10$ μ l, $C_{Feed} = 2, 4, 6, 8$ and 10 vol. %).

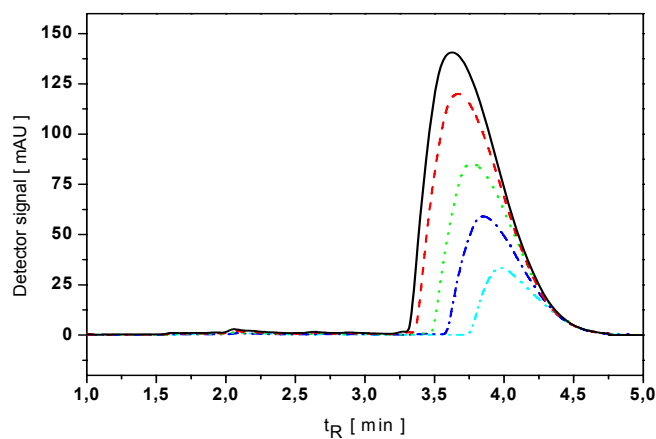


Figure 9.9. Elution Profiles for a series of concentration overloading of cycloheptanone (C_7) at a modifier concentration of 40 vol. % ($V_F=1$ ml/min, $V_{inj}=10$ μ l, $C_{Feed} = 2, 4, 6, 8$ and 10 vol. %).

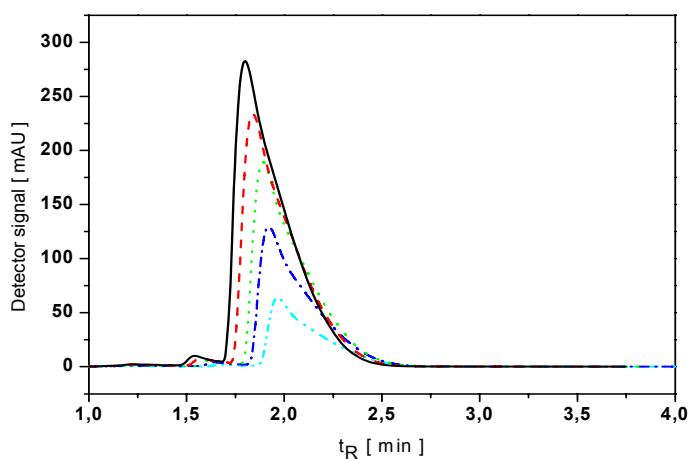


Figure 9.10. Elution Profiles for a series of concentration overloading of cyclopentanone (C_5) at a modifier concentration of 50 vol. % ($V_F=1$ ml/min, $V_{inj}=10$ μ l, $C_{Feed} = 2, 4, 6, 8$ and 10 vol. %).

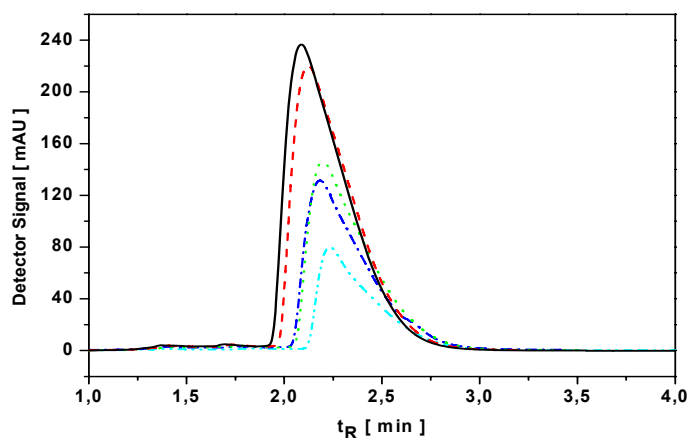


Figure 9.11. Elution Profiles for a series of concentration overloading of cyclohexanone (C_6) at a modifier concentration of 50 vol. % ($V_F=1$ ml/min, $V_{inj}=10$ μ l, $C_{Feed} = 2, 4, 6, 8$ and 10 vol. %).

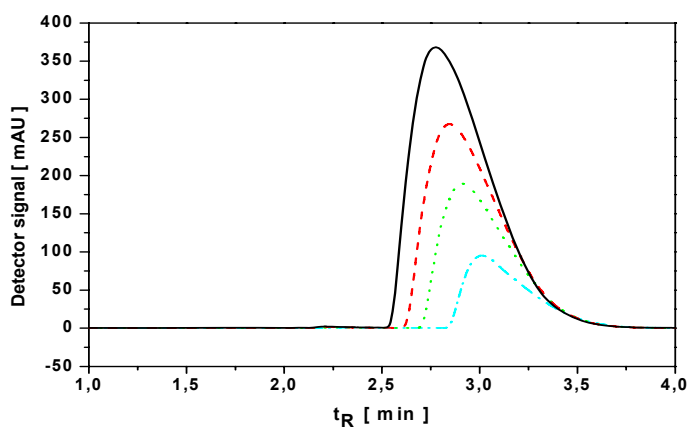


Figure 9.12. Elution Profiles for a series of concentration overloading of cycloheptanone (C_7) at a modifier concentration of 50 vol. % ($V_F=1$ ml/min, $V_{inj}=10$ μ l, $C_{Feed} = 2, 4, 8$ and 10 vol. %).

The above concentration overloading profiles show that the higher solute concentrations in the peak moving through the column more rapidly than the lower concentrations, thus a sharp front and a sloping tail for all the three cycloketones, is observed. This is typical case of Langmurian systems. Again as the modifier concentration increases the retention times of the corresponding components increases.

The respective competitive isotherm parameters of the three cycloketones at the four selected isocratic conditions are depicted in Table 9.4.

C_{mod} [vol. %]	Cyclopentanone (C₅)		Cyclohexanone (C₆)		Cycloheptanone (C₇)	
	a_i [-]	b_i [vol. %⁻¹]	a_i [-]	b_i [vol. %⁻¹]	a_i [-]	b_i [vol. %⁻¹]
30	1.95	0.350	4.11	0.450	8.4	1.00
35	1.59	0.300	3.29	0.380	6.2	0.87
40	0.95	0.275	2.50	0.340	4.5	0.58
45	0.80	0.270	2.28	0.300	3.8	0.42

Table 9.4. Competitive adsorption isotherm parameters of cyclopentanone, cyclohexanone and cycloheptanone according to Eq. 3.32.

In Table 9.4 can be seen that the Langmuir parameter *a* increases as the carbon number increases from cyclopentanone to cycloheptanone. This is because of the nature of interaction between the stationary phase and the mixture components. In reversed phase columns, for hydrophobic solutes the retention time increases with the hydrophobicity. Generally, the hydrophobic character of a solute is proportional to its carbon content, its number of methylene groups in the case of a homologue series, its number of methyl groups in the case of alkanes, or its number of aryl groups in the case of aromatic compounds [Traub05]. Thus, the elution order of the three cycloketones in the implemented reversed phase system resulted from these interactions.

9.3. Effect of modifier concentration on isotherms

In gradient chromatography, the isotherm parameters change as the modifier concentration changes with time. In order to estimate the development of concentration of a gradient process, the dependency of these isotherm parameters on the modifier concentration was evaluated. Using the four discrete values obtained for each component (see Table 9.4), the parameters ($P_{1,i}$, $P_{2,i}$, $P_{3,i}$ and $P_{4,i}$) which correlate the competitive isotherm parameters (a_i and b_i) of any of the model components to the change of modifier concentration with time ($C_{\text{mod}}(t)$) are generated by fitting with Eq.3.34a and 3.34b. The resulting parameters are given in Table 9.5 and the corresponding plots shown in Figures 9.13 and 9.14. The courses of the selectivities are shown in Fig. 9.15.

Parameters acc. to Eq. 3.34	1 st Component (Cyclopentanone)	2 nd Component (Cyclohexanone)	3 rd Component (Cycloheptanone)
$P_{1,i}$ [-]	2.2480	3.2210	4.2920
$P_{2,i}$ [vol. % ⁻¹]	-0.0544	-0.0603	-0.0689
$P_{3,i}$ [-]	3.6420	4.5380	6.2940
$P_{4,i}$ [vol. % ⁻¹]	-0.0069	-0.0252	-0.0557

Table 9.5. Coefficients P_1 , P_2 , P_3 and P_4 of the isotherm model for the three cycloketones, (Eqs. 3.34a and 3.34b).

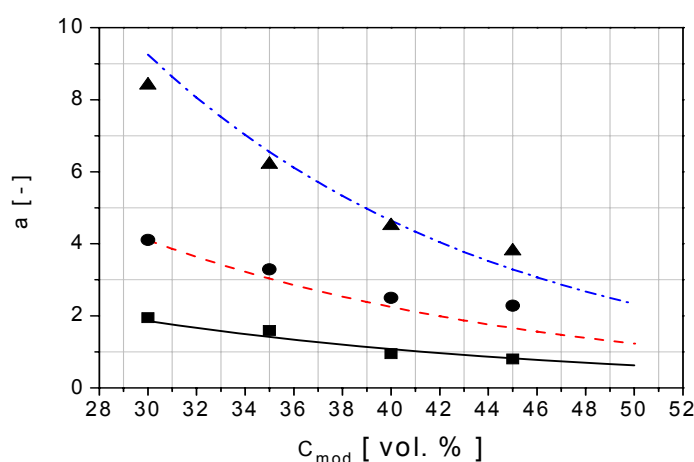


Figure 9.13. Effect of modifier concentration on the adsorption isotherm parameter “a”, according to Eq. 3.34a. The solid, dashed and dash dotted lines refer to cyclopentanone, cyclohexanone and cycloheptanone, respectively.

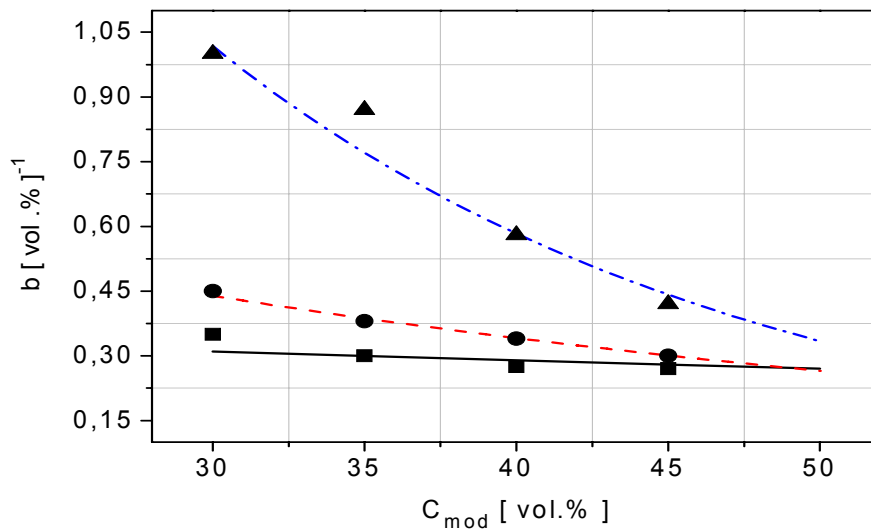


Figure 9.14. Effect of modifier concentration on Langmuir's adsorption isotherm parameter "b" according to Eq 3.34b. The solid, dashed and dash dotted lines refer to cyclopentanone, cyclohexanone and cycloheptanone respectively.

From Figures 9.13 and 9.14, the isotherm parameters decrease with increasing modifier concentration. The course of selectivities (Eq. 3.27) show similar trend as shown in Fig. 9.15.

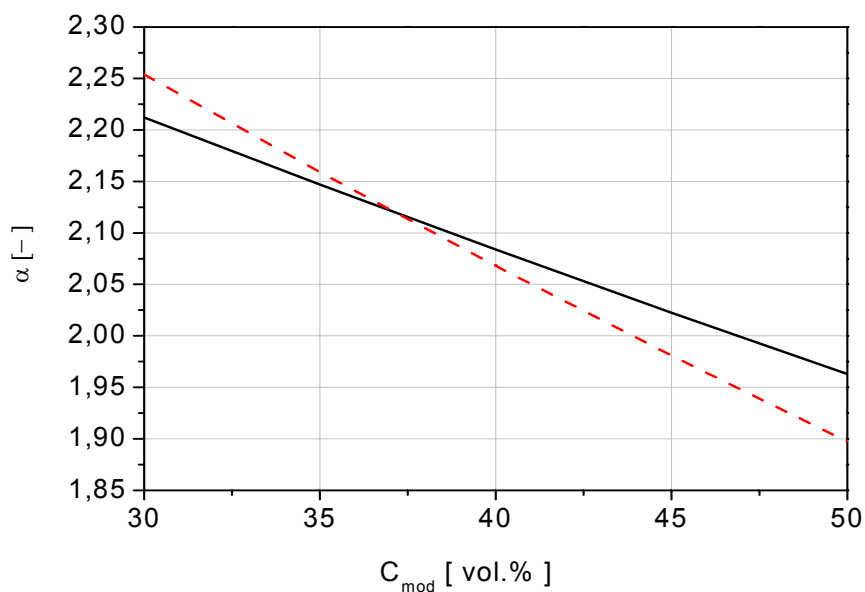


Figure 9.15. Separation factors $\alpha_{C5,C6}$ (solid line) and $\alpha_{C6,C7}$ (dashed line) vs. C_{mod} modifier concentration.

9.4. Analysis of optimization scenarios

As discussed in Section 7.5, four different scenarios of increasing flexibility were considered in order to study the potential of various solvent gradients for the separation of the middle component from a ternary mixture. These four cases have been chosen based on the number of free parameters to be optimized. Particular emphasis was given to the parameters characterizing the gradient profiles including the shape factors S , (Eq. 5.1). The upper and lower limits of the free parameters were set based on preliminary experimental investigations.

The features of the four cases are summarized in Table 8.2. In this section, the potential of applying various nonlinear gradient shapes compared to conventional isocratic and linear gradient elution is evaluated and analysed using Craig's cell model introduced in Chapter 3, the adsorption isotherm parameters described in Sections 9.2 and 9.3 and the ANN optimization technique described in Chapter 6.

Below, the theoretical optimum separation conditions are described. Finally results of experimental validations of these optimum conditions are discussed.

9.4.1. Theoretical analysis

In this section are discussed the results of the theoretical analysis devoted to optimize the separation of the middle component from a ternary mixture of cycloketones using different solvent gradients. In order to evaluate the potential of these solvent gradients, at first the isocratic optimum condition is evaluated (case1) as a bench mark. The estimated isotherm parameters (see Section 9.2) and corresponding coefficients correlating these parameters with the modifier concentration (see Section 9.3) are used in the numerical estimation of yield and productivities based on Craig's model.

9.4.1.1. Case 1

In reference to Section 8.2.1, the free parameters optimized in this case were the injection volume, V_{inj} , and the modifier concentration, C_{mod} .

The optimum condition for isocratic operation capable to maximize the objective function (Eq. 6.6) was found to be $V_{inj}=440 \mu\text{l}$ and $C_{mod}=30 \text{ vol. \%}$ with a productivity of isolating the target component $Pr_2=3807 \mu\text{g}/\text{cm}^2\text{min}$ and a maximum objective function $OF=3753 \mu\text{g}/\text{cm}^2\text{min}$ (Table 9.6). The optimum modifier concentration of this case, $C_{mod}=30 \text{ vol. \%}$ is the lower limit of the accessible optimization range (Table 8.2). Theoretically there might be a possibility to go below this limit. Unfortunately the column does not allow to work below a modifier concentration of 30 vol. %. These isocratic optimum operating conditions and the corresponding optimum yield and productivities were estimated to evaluate the potential of various optimum solvent gradients as discussed for the succeeding cases.

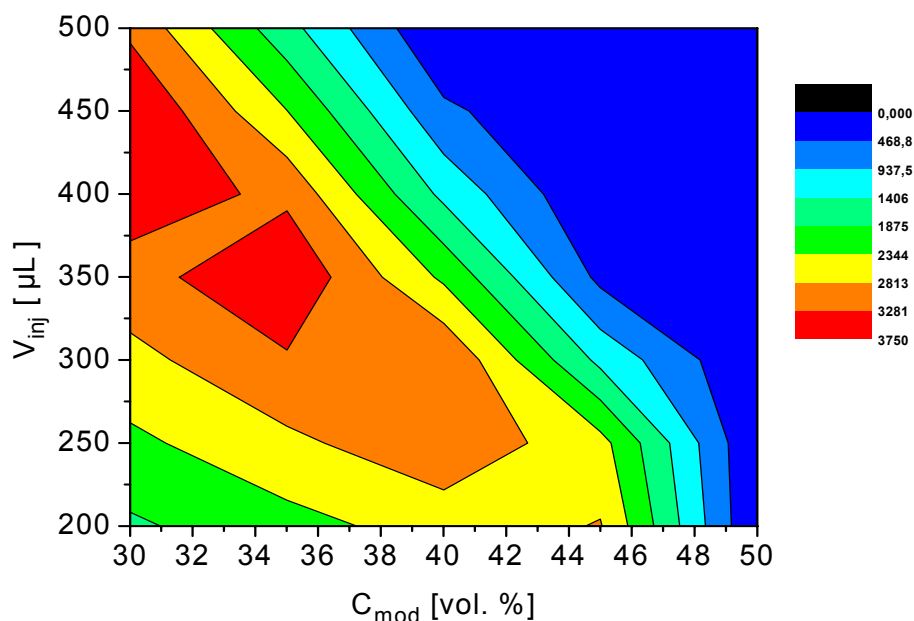


Figure. 9.16. Contour plot of the objective function OF vs. the injection volume V_{inj} and the modifier concentration C_{mod} (case 1).

From Figure 9.16, despite the overall optimum found at $C_{mod}=30 \text{ vol. \%}$ and $V_{inj}=440 \mu\text{l}$, another local optimum around modifier concentration of $C_{mod}=35 \text{ vol. \%}$ and

relatively lower injection volume of $V_{inj}=350 \mu\text{l}$ is observed. Which allows to achieve similar OF values.

9.4.1.2. Case 2

In this case, the objective was to maximize OF and to find the corresponding optimal operating conditions for three predefined gradient shape factors ($S=0.25$ referred as convex, $S=1$ referred as linear and $S=1.2$ referred as concave) at constant gradient time. These shape factors were selected because they represent different gradient types. In this case the three decision variables considered have been the injection volume, initial and final modifier concentrations (V_{inj} and C_{mod}^0 , and C_{mod}^f) respectively. The gradient time was kept to $t_g=4$ min which is the time for complete elution of the target component under isocratic conditions at $C_{mod}=30$ vol. % (Table 8.2). The result obtained is illustrated in Table 9.6. It is observed that there is an increase in productivity (or OF) if the value of the shape factor increases from 0.25 to 1.2. The nonlinear concave gradient with $S=1.2$ shows the best performance (OF=5240 $\mu\text{g}/\text{cm}^2\cdot\text{min}$). The maximum potential possible due to the constraints of a “step up” gradient was used (i.e. $C_{mod}^0=30$ vol. % and $C_{mod}^f=50$ vol. %) for $S=1$ and $S=1.2$. For $S=0.25$ C_{mod}^f was only 40 vol. %.

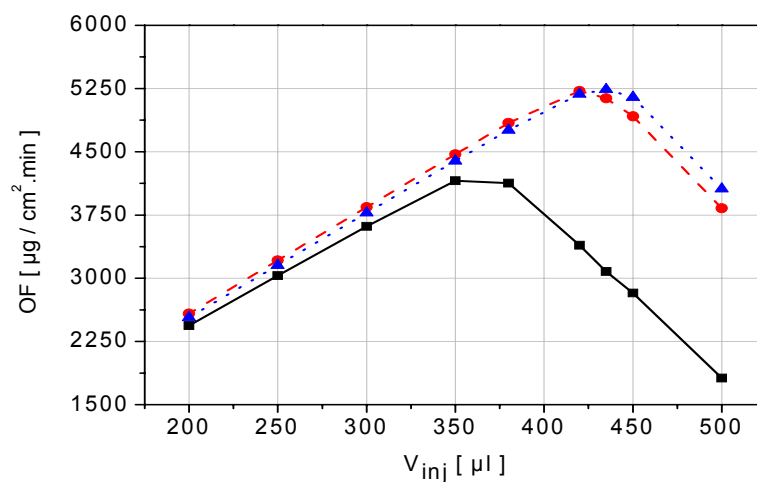


Figure 9.17. Comparison of OF vs. V_{inj} of case 2 for the three gradient shape profiles at the respective optimum modifier concentration shown in Table 7. Solid line for $S=0.25$, dashed line for $S=1$ and dotted line for $S=1.2$.

In Figure 9.17, the objective function is plotted for the three predefined S-values as a function of the injection volume for optimal gradient boundaries. In this figure can be also seen that the concave gradient mode outperforms convex and linear gradients. A gain in productivity of about 39 % is obtained compared to the isocratic operation even with slightly lower amount of sample injected in this case as shown in Table 9.6 ($V_{inj}=440$ for case 1 and $V_{inj}=435$ for the maximum OF of case 2). This gain clearly shows the potential of using solvent gradients for an optimized separation of ternary mixtures.

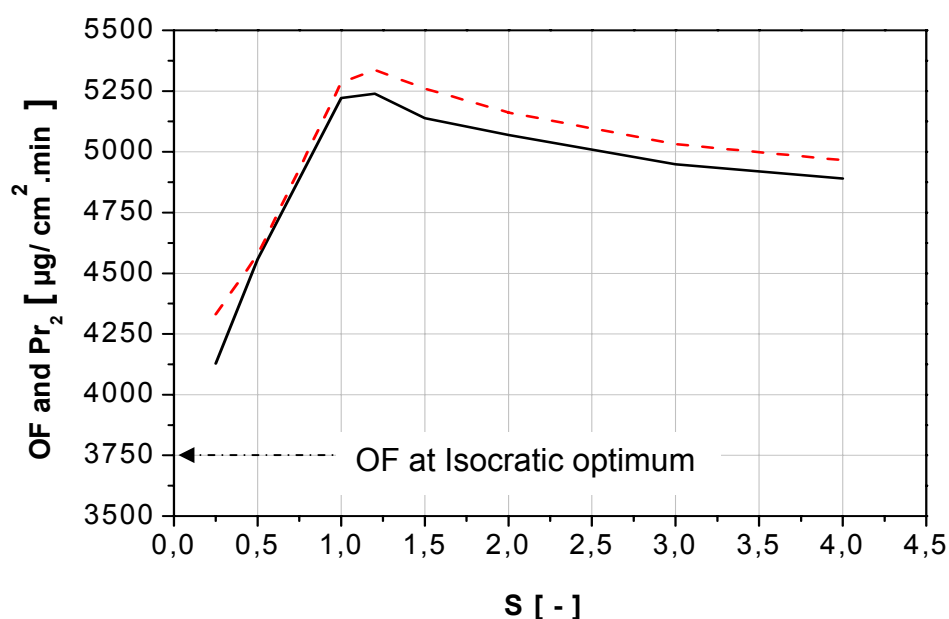


Figure 9.18. Objective function OF (solid line) and Productivity Pr_2 (dashed line) vs. gradient shape factor S at the respective optimum operating conditions of case 2 compared with the isocratic case (shown by the arrow).

From Figure 9.18, the objective function OF increases with the shape factor S at the respective optimum operating conditions until $S \approx 1.2$ and drops thereafter. That means even though a “step-up” concave gradient results in better separation, there might be loss of productivity if the gradient shape factor S is increased indefinitely beyond the optimum value.

9.4.1.3. Case 3

In this case, the gradient shape factor was kept constant at $S=1$ corresponding to a linear gradient and the other four free parameters were optimized: i.e. the initial modifier concentration, the final modifier concentration, the injection volume and also

the gradient time. The optimum objective function was found to be $OF=5730 \mu\text{g}/\text{cm}^2\cdot\text{min}$ (Table 9.6), which is higher than the respective optimum values determined for cases 1 and 2. This is essentially due to the adjustment of the gradient time. Again the maximum available potential of the “step up” gradient was fully used, (i.e. $C_{\text{mod}}^0=30 \text{ vol. } \%$ and $C_{\text{mod}}^f=50 \text{ vol. } \%$). In Table 9.6 can be seen, that the higher productivity in case 3 is achieved by injecting a smaller amount of feed compared to cases 1 and 2. Compared to case 2 and $S=1$, by optimizing in addition the gradient time, there is for case 3 a gain in productivity of 9 %.

Comparison of OF has been made for different shape factor values at these optimum operating conditions. In Figure 9.19, it can be seen that an increase in shape factor increases the productivity. Thus, a concave gradient ($S>1$) results in better separation of the middle (target) component. The shown differences in the OF for the concave gradient compared to the linear gradient are still rather small, because the productivity values for each shape factor were generated at the optimum operating conditions of the linear gradient profile.

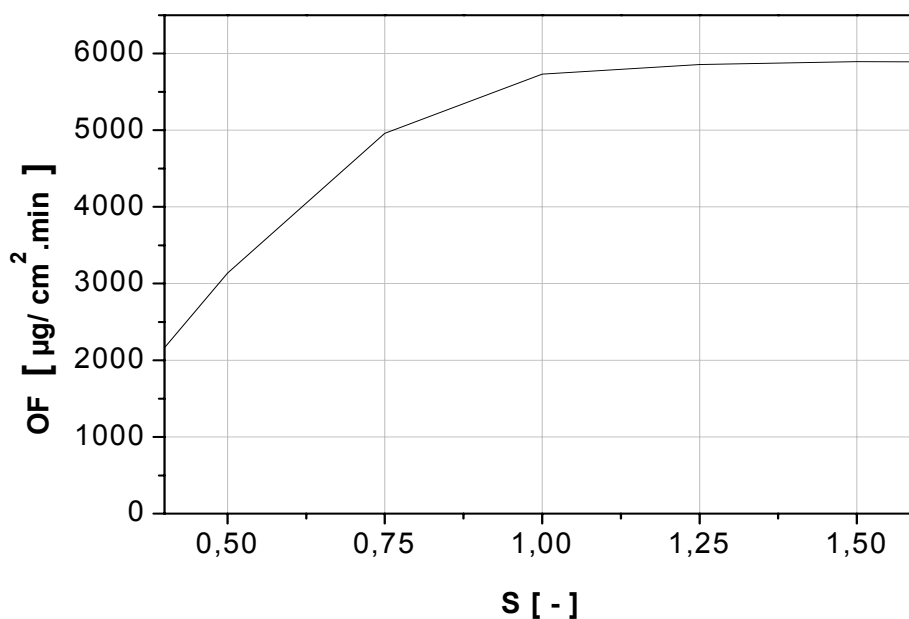


Figure 9.19. Objective functions OF vs. gradient shape factor S at the optimum operating conditions of case 3 ($V_{\text{inj}}=400 \mu\text{l}$, $C_{\text{mod}}^0=30 \text{ vol. } \%$, $C_{\text{mod}}^f=50 \text{ vol. } \%$ and $t_g=1.5 \text{ min}$) optimal for $S=1$ (Table 9.6).

9.4.1.4. Case 4

In the last case, all five free operating conditions have been optimized simultaneously to get the maximum objective function. I.e. the decision variables considered have been the injection volume, initial modifier concentration, final modifier concentration, gradient shape factor and gradient time (V_{inj} , C_{mod}^0 , C_{mod}^f , S and t_g). The optimum operating conditions and the corresponding optimum performance are shown in Table 9.6. The short gradient time of $t_g=1.1$ min and the high S value of 3.2 lead to a significant improvement in productivity. Again, the modifier concentration reached the available limits specified.

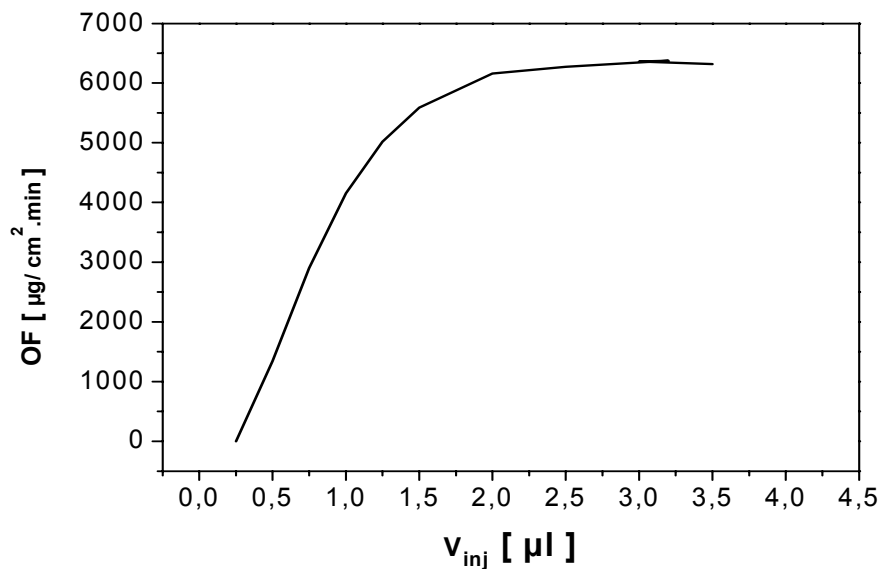


Figure 9.20. Sensitivity of objective function OF vs. injection volume V_{inj} at the optimum operating conditions of case 4 (i.e. $S=3.2$).

From Figure 9.20, the objective function OF increases with increasing shape factor indicating the general trend of getting higher productivities for concave ($S>1$) gradient shapes.

Where as in Figure 9.21, the objective function does not increase indefinitely with the increase in the amount injected, rather after some point the productivity drops after it reaches a maximum at a certain injection volume.

Compared to the conventional isocratic case (case 1), the objective function OF of this overall gradient optimum increases from 3753 $\mu\text{g}/\text{cm}^2 \cdot \text{min}$ to 6373 $\mu\text{g}/\text{cm}^2 \cdot \text{min}$ indicating a 70 % improvement. Similarly, the OF shows an increase by 22 % and 11

% compared to cases 2 and 3, respectively. In Table 9.6 can be seen, this gain is obtained for a slightly lower amount of injection volume than in case 1.

Thus, as expected, the optimization of all the five degrees of freedom provides the best performance. With the simple column model applied such optimization could be carried out efficiently.

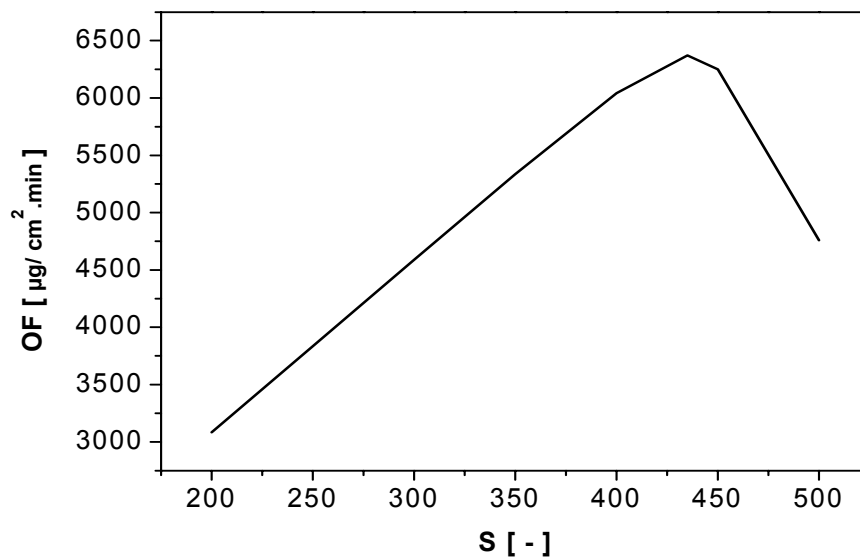


Figure 9.21 Sensitivity of objective function OF vs. gradient shape factor S at the optimum operating conditions of case 4 (i.e. for $V_{inj}=435 \mu\text{l}$).

		Case 1	Case 2			Case 3	Case 4
		Isocratic	a)convex gradient	b)linear gradient	c)concave gradient	Linear	Optimized gradient
Optimal parameters	$V_{inj.}$ [μ l]	440	380	420	435	400	435
	$C_{mod.}^0$ [vol.%]	30	30	30	30	30	30
	$C_{mod.}^f$ [vol.%]	30	40	50	50	50	50
	S [-]	n.a	0.25*	1.0*	1.20*	1.0*	3.20
	t_g [min]	n.a	4*	4*	4*	1.5	1.10
Performance	Y_2 [%]	98.6	95.31	98.81	98.56	97.76	98.18
	Pr_2 [μ g / cm^2 .min]	3807	4331	5284	5338	5861	6491
	OF [μ g/ cm^2 .min]	3753	4128	5221	5240	5730	6373
Illustration and exp. validation		Fig. 9.22	Fig. 9.23a	Fig. 9.23b	Fig. 9.23c		Fig. 9.24

*see Table 8.1

Table 9.6. Optimum operating conditions and performances at these conditions for the four cases.

9.4.2. Experimental validation

The experimental validation was performed for some of the conditions identified as promising in Section 9.4.1. Below the predicted chromatograms are compared with measured chromatograms for the optimum operating conditions. Additionally, for the gradient cases, the corresponding gradient profiles are also compared, i.e. the intended and the realized modulations of the modifier concentration.

9.4.1.1. Case 1

The simulated band profile for the conditions given in Table 9.6 is plotted on top of Fig. 9.22. In the figure is given below the measured chromatogram for the same conditions as a signal-time curve. No exact comparison of the two band profiles was intended here. Such a comparison would require highly precise calibration. Instead, we concentrate here on comparing general trends. It can be seen in Fig. 9.22 that the positions of the retention times and the shapes of the bands are represented relatively well by the model, although limitations are obvious regarding the exact position of the cut times. These discrepancies are certainly due to limitations of the simple Craig model, inaccuracies of the isotherm model and system dead volumes not considered exactly in the model.

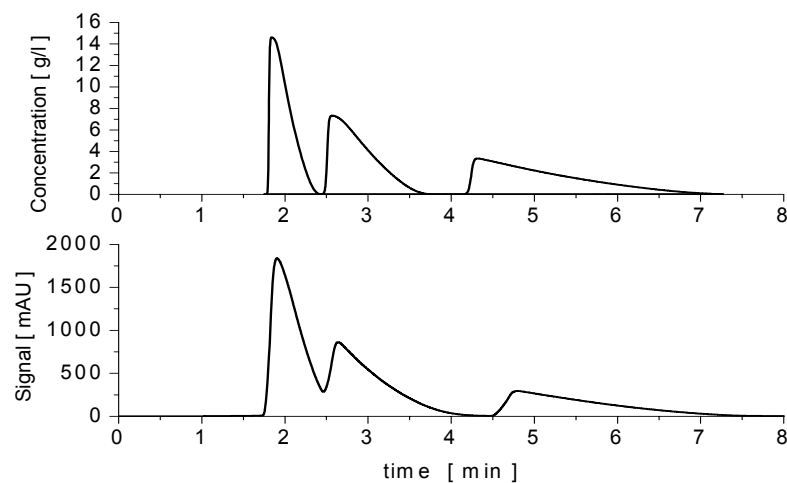


Figure 9.22. Simulated (upper) vs. experimental (lower) chromatograms at the optimum operating conditions of case 1, (see Table 9.6).

9.4.2.2. Case 2

Similar to case 1, comparison was made between the calculated and the measured band profiles for case 2. In Figs. 9.23a, 9.23b and 9.23c, are shown the results for the convex, linear and concave gradients, respectively.

For all conditions the calculated band profiles are again plotted on top and the measured elution profiles as signal-time curve in the bottom of each figure. The corresponding experimental and theoretical peak shapes and locations show a clear similarity. However, some deviations in the chromatogram shapes can be again seen due to the limitations mentioned. The relatively small shape factor difference ($S=0.25, 1, 1.2$) also makes it hard to differentiate between the gradient profiles also shown in Figs. 9.23.

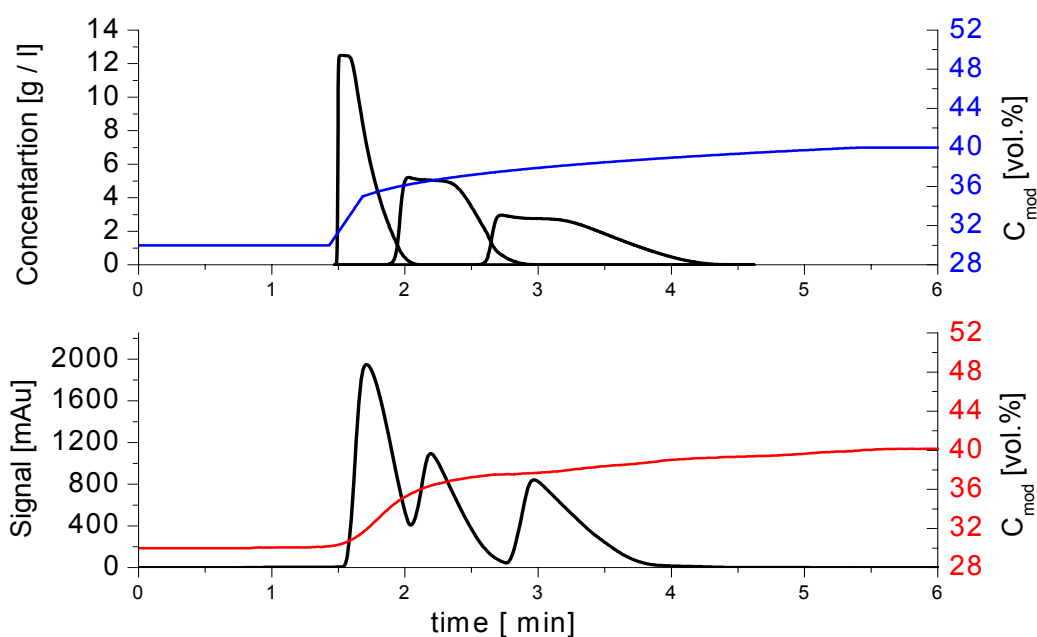


Figure 9.23a. Simulated (upper) vs. experimental (lower) chromatograms with the respective gradient profiles (at column exit) of case 2, for convex gradient shape of $S=0.25$, (see, Table 9.6).

In case of $S=0.25$, the concave gradient profile of Figure 9.23a uses only 50 % of the maximum potential of the available modifier concentration range.

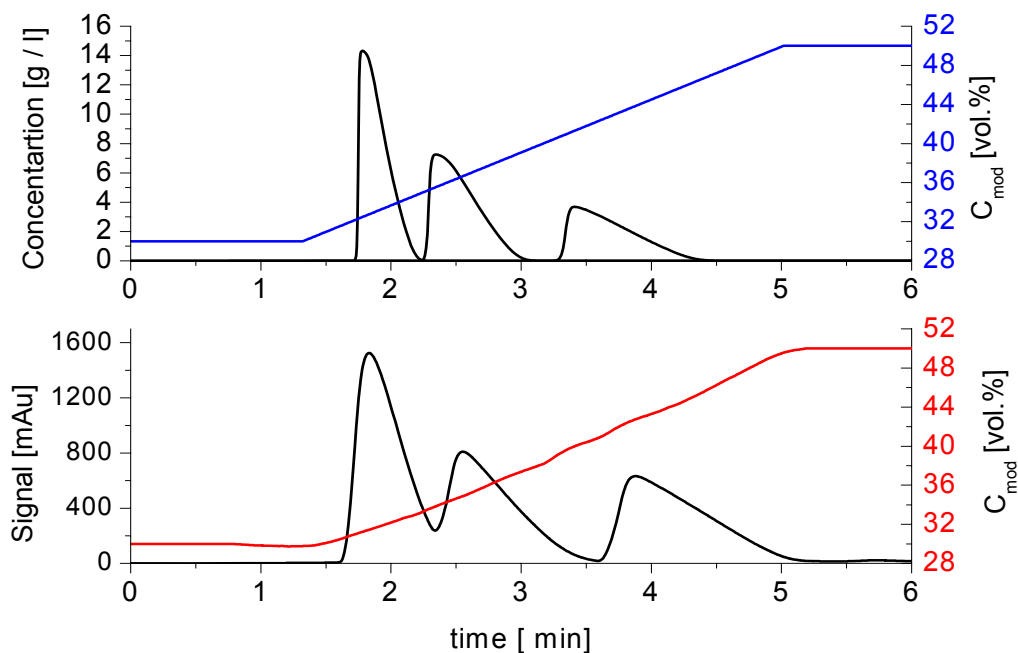


Figure 9.23b. Simulated (upper) vs. experimental (lower) chromatograms with the respective gradient profiles (at column exit) of case 2, for the linear gradient ($S=1$) as shown in Table 9.6.

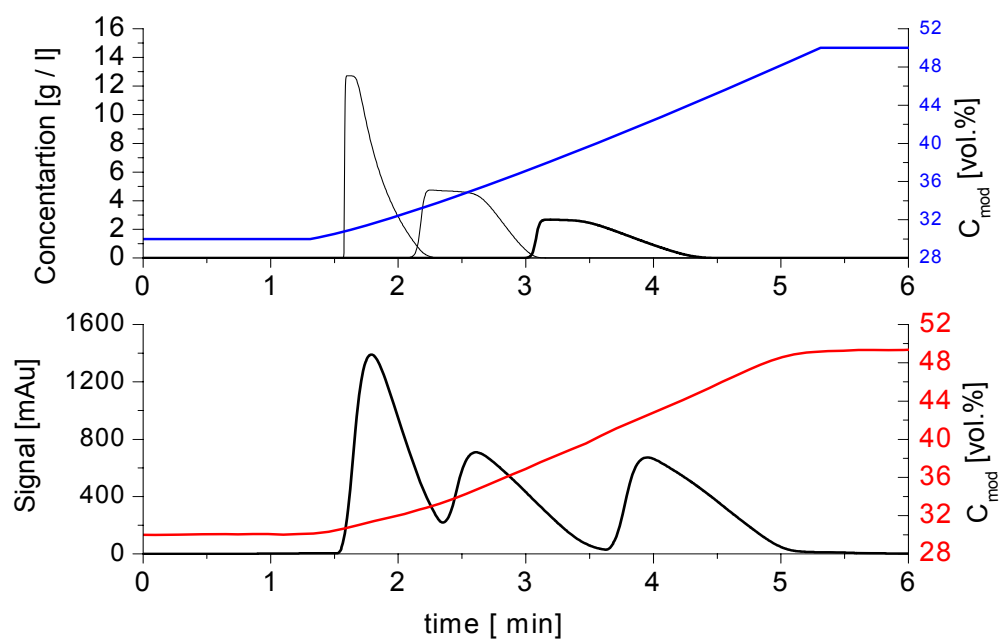


Figure 9.23c. Simulated (upper) vs. experimental (lower) chromatograms with the respective gradient profiles (at column exit) of case 2, for concave gradient shape $S=1.2$ as shown in Table 9.6.

9.4.2.3. Case 4

As shown in Fig. 9.24, the measured and calculated peaks show also for the optimum operating conditions corresponding to case 4 similar trends, despite visible shifts in cut-times. This cut time shifts are attributed again to the limitation of the cell model used, the assumptions made for the estimation of the isotherm parameters, possible flow rate fluctuations and unavoidable dead volumes. The strong nonlinearity of the applied concave gradient for $S=3.2$ is also illustrated in the figure. Due to the short gradient time the experimental implementation of the predicted gradient was more difficult and deviations to the theoretical identified gradient could not be avoided.

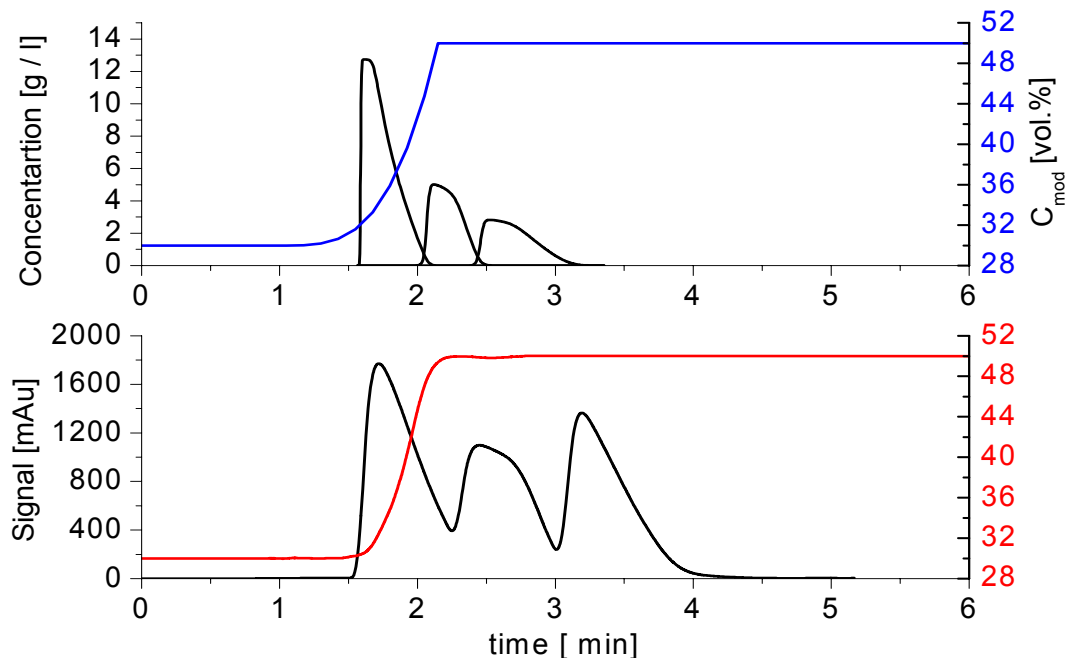


Figure 9.24. Simulated (upper) vs. experimental (lower) chromatograms with the associated optimal gradient profiles (at column exit) of case 4 (Table 9.6).

In Figure 9.24 the little deflections in the tails of the 2nd and 3rd components are due to effect of ending competition between neighbouring components for an adsorption site and indicating time for the total elution of a proceeding component.

In all the above chromatograms of cases 1, 2 and 4, the measured and calculated concentration profiles show significant similarity with small shift in the cut times. This indicates that the mathematical model applied to describe the concentration profile developing in the column (i.e. the Craig cell model, Eq. 3.16), the isotherm equations

used (Eq. 3.32) and the equations used to correlate the modifier concentration with time (Eq. 3.34) quantified relatively well the separation problem studied in this work.

10. Conclusions

In this study the potential of linear and nonlinear solvent gradients for the separation of ternary mixtures was evaluated. Gradient elution chromatography with the emphasis on nonlinear gradient processes was studied theoretically and experimentally considering the middle component of a ternary mixture as the target. Three cycloketones were considered as a model system. To quantify the development of band profiles in nonlinear preparative gradient chromatography, an equilibrium cell model proposed by Craig was used. Competitive isotherm equations were implemented in this model. Empirical equations were used to quantify the effect of the change in solvent composition on the isotherm parameters.

In a first part of the study the required adsorption isotherm parameters were determined for the three solutes on a reversed phase chromatographic system using methanol / water as mobile phase in a certain range of solvent compositions. A combination of the elution by characteristic point (ECP) and the inverse methods were used to estimate these parameters. Then, the effect of modifier concentration on the determined parameters was evaluated and described semi-empirically. For the three cycloketones, the estimated Langmuir isotherms decrease with increasing modifier concentration. The selectivities have shown a similar trend.

Subsequently linear and nonlinear gradients were analysed theoretically and experimentally. A gradient shape factor S was used to describe the gradients mathematically. In order to evaluate the potential of various forms of gradients and the effect of the gradient shape factor S on the separation, four scenarios were investigated. Optimum operating conditions, capable to separate the second eluting component, were determined for these four cases, which differed in the number of degrees of freedom. An artificial neural network method was used to determine the optimum operating conditions and the corresponding yields and productivities.

For the system studied, concave “step up” gradients (i.e. $S > 1$) outperformed conventional isocratic operation, linear gradients ($S = 1$) or convex gradients ($S < 1$). In

concave gradients, a low rate of increasing the initial modifier concentration improves the resolution of the target component whereas the high final modifier concentration shortens the cycle time and increase productivity. Table 9.6 summarizes the most important results. It shows that an increase in the number of free parameters (from two to five), increases the corresponding yields and productivities. In case 4 the highest productivity was obtained by adjusting five free parameters and using the maximum potential of the concave gradient. On the other hand the optimization of these five free parameters requires more computation time.

Selected optimized chromatograms as predicted by the Craig model were compared with experimental results. Although there was no perfect agreement found, the shapes of measured band profiles were relatively well predicted by the model. Thus, the concept and model applied can be used in optimization studies to specify optimal gradient shapes, provided the required thermodynamic functions are available. Nowadays this requires time consuming experimental work.

To summarize, gradient chromatography has a great potential to separate multi-component mixtures. To exploit the potential, a proper design of the gradient profiles and a high precision chromatographic unit are needed. The ternary mixture studied in this work can be considered as a general multi-component mixture. Thus, the results of this study can easily be extended to determine optimum operating conditions and the respective productivities of any multi-component mixture. Further work might concentrate also on investigating the potential of complex gradients working with more than two solvents.

Nomenclature

Latin Symbols

Symbol	Unit	Description
A	–	rectangular matrix assigned as orthogonal array
A_c	cm^2	column cross-sectional area
a_i	–	parameter of the Langmuir adsorption isotherm equation for component i
$a_{1,i}$	–	parameter of the bi-Langmuir adsorption isotherm equation for component i
$a_{2,i}$	–	parameter of the bi-Langmuir adsorption isotherm equation for component i
A^{peak}	mAu.ml	product of peak area and the flow rate
A^{peak^*}	mAu.min	peak area signal time curve
b_i	–	parameter of the Toth adsorption isotherm equation for component i
b_m	vol. \%^{-1}	parameter of the competitive Langmuir adsorption isotherm equation for component i
$b_{1,i}$	–	parameter of the bi-Langmuir adsorption isotherm equation for component i
$C_{i,\text{Feed}}$	vol. \%	concentration of component i in the injected mixture
C_{mod}	vol. \%	concentration of modifier
C_{mod}^0	vol. \%	initial modifier concentration
C_{mod}^f	vol. \%	final modifier concentration
$C_{\text{threshold}}$	vol. \%	threshold concentration for fractionation
$C_{i,j}^k$	vol. \%	concentration of component i in plate j and exchange time step k of the Craig model

C_i^{meas}	vol. %	measured concentration of component i
C_i^{sim}	vol. %	calculated concentration of component i
C_5	–	first component, i.e. Cyclopentanone (C_5H_8O)
C_6	–	second component, i.e. Cyclohexanone ($C_6H_{10}O$)
C_7	–	third component, i.e. Cycloheptanone ($C_7H_{12}O$)
Da_i	cm^2/s	the axial dispersion coefficient of component i
e	–	parameter of the Toth isotherm model
F	ml/min	volumetric flow rate of the mobile phase
F_R	–	phase ratio
G	–	gradient slope
H	–	height equivalent to theoretical plate
I	W/m^2	intensity of light entering detector cell
I_0	W/m^2	intensity of light leaving detector cell
K	–	total number of exchange time steps in Craig model
$K_{H,i}$	–	Henry's constant for component i
K'_i	–	capacity factor
L_c	cm	length of the column
$m_{i,\text{coll}}$	μl	amount of component i in the collected fraction
MeOH	–	methanol
m_{mob}	ml	mass fraction in the mobile phase
m_{sta}	ml	mass fraction in the stationary phase
m_{total}	ml	total mass
N	–	theoretical plate number
n	–	number of components in the sample
OF	$\mu\text{g}/\text{cm}^2\text{-min}$	objective function
P_A	–	pump A
P_B	–	pump B
$P_{1,i}$	–	parameter expressing effect of modifier on isotherms for reversed phase system
$P_{2,i}$	vol. % ⁻¹	parameter expressing effect of modifier on isotherms for reversed phase system

$P_{3,i}$	–	parameter expressing effect of modifier on isotherms for reversed phase system
$P_{4,i}$	vol. % ⁻¹	parameter expressing effect of modifier on isotherms for reversed phase system
Pr_i	$\mu\text{g}/\text{cm}^2\cdot\text{min}$	production rate of component i,
$Pur_{i,des}$	%	desired purity of component i
q_i	vol. %	concentration of component i in the stationary phase
$q_{sat,i}$	vol. %	saturation capacity of the column for component i
$q_{i,j}^k$	vol. %	concentration of component i in the stationary phase of plate j and exchange time step k of the Craig model
r	–	strength of orthogonal array
S	–	gradient shape factor
Sg	mAu	signal measured
t^{reg}	min	regeneration time
t_0	min	dead time of the column
t_g	min	duration of gradient
t_g^0	min	Initial gradient time
$t_{,g}^f$	min	final gradient time
t_{inj}	min	injection time
t_N^{end}	min	time when concentration of last eluting component drops below threshold
t_r	min	retention time
t_1^{begin}	min	time when concentration of first eluting component exceeds threshold
$t_{i,coll}^{end}$	min	end of collecting component i
$t_{i,coll}^{begin}$	min	begin of collecting component i
$t_{i,pur}^{begin}$	min	begin of time interval in which the local purity of component i is larger than desired purity
t_{dead}^{VD}	min	retention time measured to determine the dead volume between buffer selection valve and

		detector
$t_{\text{dead}}^{\text{ID}}$	min	retention time measured to determine the dead volume between injector and detector
$t_{i, \text{pur}}^{\text{end}}$	min	end of time interval in which the local purity of component i is larger than desired purity
Δt	min	residence time of the mobile phase in a plate
Δt_{c}	min	cycle time
u	cm/s	local average mobile phase velocity
$V_{\text{dead}}^{\text{ID}}$	ml	dead volume between injector and detector
$V_{\text{dead}}^{\text{VI}}$	ml	dead volume between buffer selection valve and detector
V_{c}	ml	volume of the column
V_{inj}	μl	injection volume
V_{int}	ml	interstitial volume
V_{j}	ml	volume of cell j
V_{m}	ml	volume of the mobile phase
V_{particle}	ml	particle volume
V_{pore}	ml	pore volume
V_{s}	ml	volume of the stationary phase
V_{solid}	ml	solid volume
$V_{\text{dead}}^{\text{VD}}$	ml	dead volume between buffer selection valve and detector
$W_{1/2}$	–	peak width at half height
Y_i	%	recovery yield of component i
z	cm	distance along the column
Δz	cm	slice of column thickness

Greek Symbols

Symbol	Unit	Description
$\alpha_{i,m}$	–	separation factor between components i and m
$\beta_{1,i}$	vol. % ⁻¹	parameter expressing effect of modifier on isotherms for normal phase system
$\beta_{2,i}$	–	parameter expressing effect of modifier on isotherms for normal phase system
$\beta_{3,i}$	vol. % ⁻¹	parameter expressing effect of modifier on isotherms for normal phase system
$\beta_{4,i}$	–	parameter expressing effect of modifier on isotherms for normal phase system
ε	–	porosity
λ	m ² /mol	molar absorptivity

Superscripts and Subscripts

Symbol	Description
c	column
coll	collected
des	desired
i	i th component
inj	injection
j	j th cell
k	k th time step
m	m th component
mob	mobile phase
mod	modifier
sta	stationary phase
pur	purity

References

- [Adam06] Adam P. Schellinger and Peter W. Carr, Isocratic and gradient elution chromatography: A comparison in terms of speed, retention reproducibility and quantitation. *Journal of Chromatography A*, **2006**, 1109, 253–266.
- [Alan52] R. S. Alan, R.J.P Williams and A. Tiselius, *Acta Chem. Scand.*, 1952, 6, 826.
- [Antia03] F. D. Antia, A Simple Approach to Design and Control of Simulated Moving Bed Chromatographs, Chromatographic Science Series, Scale-Up and Optimization in Preparative Chromatography, Principles and Biopharmaceutical Applications; Marcel Dekker, Inc.: USA, 2003.
- [Antos02] D. Antos and A. Seidel-Morgenstern, Two-step solvent gradients in simulated moving bed chromatography: Numerical study for linear equilibria. *Journal of Chromatography A*, **2002**, 944, 77-91.
- [Arne05] R. Arnella, P. Forsséna and T. Fornstedt, Accurate and rapid estimation of adsorption isotherms in liquid chromatography using the inverse method on plateaus. *Journal of Chromatography A*, **2005**, 1099, 167-174.
- [Atkin90] Peter W. Atkins and Julio de Paula, *Physikalische Chemie*; Wiley-VCH: Weinheim, Germany, 2005.
- [Berr89] J.C. Berridge, Simplex optimization of high-performance liquid chromatographic separations. *Journal of Chromatography A*, **1989**, 485, 3-14.
- [Borg87] K. H. Borgwardt, *The Simplex Method, A probabilistic Analysis*; Springer-Verlag: Berlin, Germany, 1978.
- [Brough84] D. B. Broughton, Production-Scale Adsorptive Separations of Liquid Mixtures by Simulated Moving-Bed Technology. *Separation Science and Technology*, **1984**, 19, 723-736.
- [Cela07] R. Cela, J. A. Martínez, C. González-Barreiro and M. Lores, Multi-objective optimisation using evolutionary algorithms: its application to HPLC separations. *Chem. Intel. Lab. Syst*, **2003**, 137-156.
- [Clar93] B. J. Clark, T. Frost, M. A. Russell, *UV spectroscopy techniques, instrumentation, data handling*; Chapman and Hall: London, UK, 1993.

- [Craig44] L. C Craig, Identification of Small Amounts of Organic Compounds by Distribution Studies. II. Separation By Counter-current Distribution. *Journal of Biol. Chem.* **1944**, 155, 519-534.
- [Crow90] J.A. Crow and J.P. Foley, Optimization of Separations in Supercritical Fluid Chromatography Using a Modified Simplex Algorithm and Short Capillary Columns. *Anal. Chem.*, **1990**, 378-386
- [Deem56] J. J. Van Deemter, F. J. Zuiderweg and A. Klinkenberg, longitudinal diffusion and resistance to mass transfer as causes of non-ideality in chromatography. *Chemical Engineering Science*, **1956**. 5, 271-289.
- [Ettre93] L. S. Ettre, Nomenclature For Chromatography, Pure and App. Chem. **1993**, 4, 819-872.
- [Feli96] A. Felinger, G. Guiochon, Optimizing preparative separations at high recovery yield. *Journal of Chromatography A*, **1996**, 752, 31-40.
- [Feli98] A. Felinger, G. Guiochon, Comparing the optimum performance of the different modes of preparative liquid chromatography. *Journal of Chromatography A*, **1998**, 796, 59-74.
- [Feli03] A. Felinger, A. Cavazzini and G. Guiochon, Numerical determination of the competitive isotherm of enantiomers. *Journal of Chromatography A*, **2003**, 986, 207-225.
- [Fiss04] D. Fissore, A.A. Barressi and D. Manca, Modelling of methanol synthesis in a network of forced unsteady-state ring reactors by artificial neural networks for control purposes. *Chem. Eng. Sci.*, **2004**, 59, 4033-4041.
- [Guio89] G. Guiochon, S. Ghodbane, S. Golshan-Shirazi, J. X. Huang, A. Katti, B. C. Lin and Z. Ma, Nonlinear chromatography Recent theoretical and experimental results. *Talanta*, **1988**, 36, 19-33.
- [Guio03] G. Guiochon, Bingchang Lin, Modeling for Preparative Chromatography; Academic Press: USA, 2003.
- [Guio06] G. Guiochon, A. Felinger, G. Shirazi, Anita M. Katti, Fundamentals of Preparative and Nonlinear Chromatography; Academic Press: USA, 2006.
- [Heda] A.S. Hedayat, N.J.A. Sloane, J. Stufken, Orthogonal Arrays: Theory and Applications, <http://www.research.att.com/~njas/oadir/oa.100.4.10.2.txt>.
- [Humph97] Jimmy L. Humphrey and George E. Keller, Separation Process Technology; McGraw-Hill: New York, USA, 1997.
- [Ingl88] J. D. Ingle and S. R. Crouch, Spechtrochemical Analysis; Prentice Hall: New Jersey, USA, 1988.

- [Jand85] P. Jandera, J. Churacek, Gradient Elution in Column Liquid Chromatography. Theory and Practice, Elsevier, Amsterdam, The Netherlands, 1985.
- [Jand99] P. Jandera, Simultaneous optimisation of gradient time, gradient shape and initial composition of the mobile phase in the high-performance liquid chromatography of homologous and oligomeric series. *Journal of Chromatography A*, **1999**, 845, 133–144.
- [Juza00] M. Juza, M. Mazzitti and M. Morbidelli, Simulated moving-bed chromatography and its application to chirotechnology. Trends in biotechnology, **2000**, 18, 108-118.
- [Lear07] R. Leardi, Genetic algorithms in chemistry. *Journal of Chromatography A*, **2007**, 1158, 226-233.
- [Lisec01] O. Lisec, P. Hugo and A. Seidel-Morgenstern, Frontal analysis method to determine competitive adsorption isotherms. *Journal of Chromatography A*, **2001**, 908, 19-34.
- [Matlab] [The MathWorks - MATLAB and Simulink for Technical Computing, www.mathworks.com](http://www.mathworks.com)
- [Mats91] R. Matsuda, Y. Hayashi, T. Suzuki and Y. Saito, Simplex optimization of liquid chromatography with the function of mutual information as a criterion. *Journal of Chromatography A*, **1993**, 585, 187-193.
- [Mett96] H. J. Metting and P. M. J. Coenegrach, Neural networks in high-performance liquid chromatography optimization: response surface modeling. *Journal of Chromatography A*, **1996**, 728, 47-53.
- [Mich94] Z. Michalewicz, Genetic Algorithms + Data Structures= Evolution Programs; Springer-Verlag: New York, USA, 1994.
- [Miller05] James M. Miller, Chromatography: Concepts and Contrasts; Wiley-Interscience: New Jersey, USA, 2005.
- [Morg04] A. S. Morgenstern, Experimental determination of single solute and competitive adsorption isotherms. *Journal of Chromatography A*, **2004**, 1037, 255-272.
- [Niki02] P. Nikitas, A. Pappa-Louisi, A. Papageorgiou and A. Zitrou, On the use of genetic algorithms for response surface modeling in high-performance liquid chromatography and their combination with the Microsoft Solver. *Journal of Chromatography A*, **2002**, 942, 93-105.
- [Niki07] P. Nikitas, A. Pappa-Louisi, A. Papageorgiou, Simple algorithms for fitting and optimisation for multilinear gradient elution in reversed-phase liquid chromatography. *Journal of Chromatography A*, **2007**, 1157, 178-186.

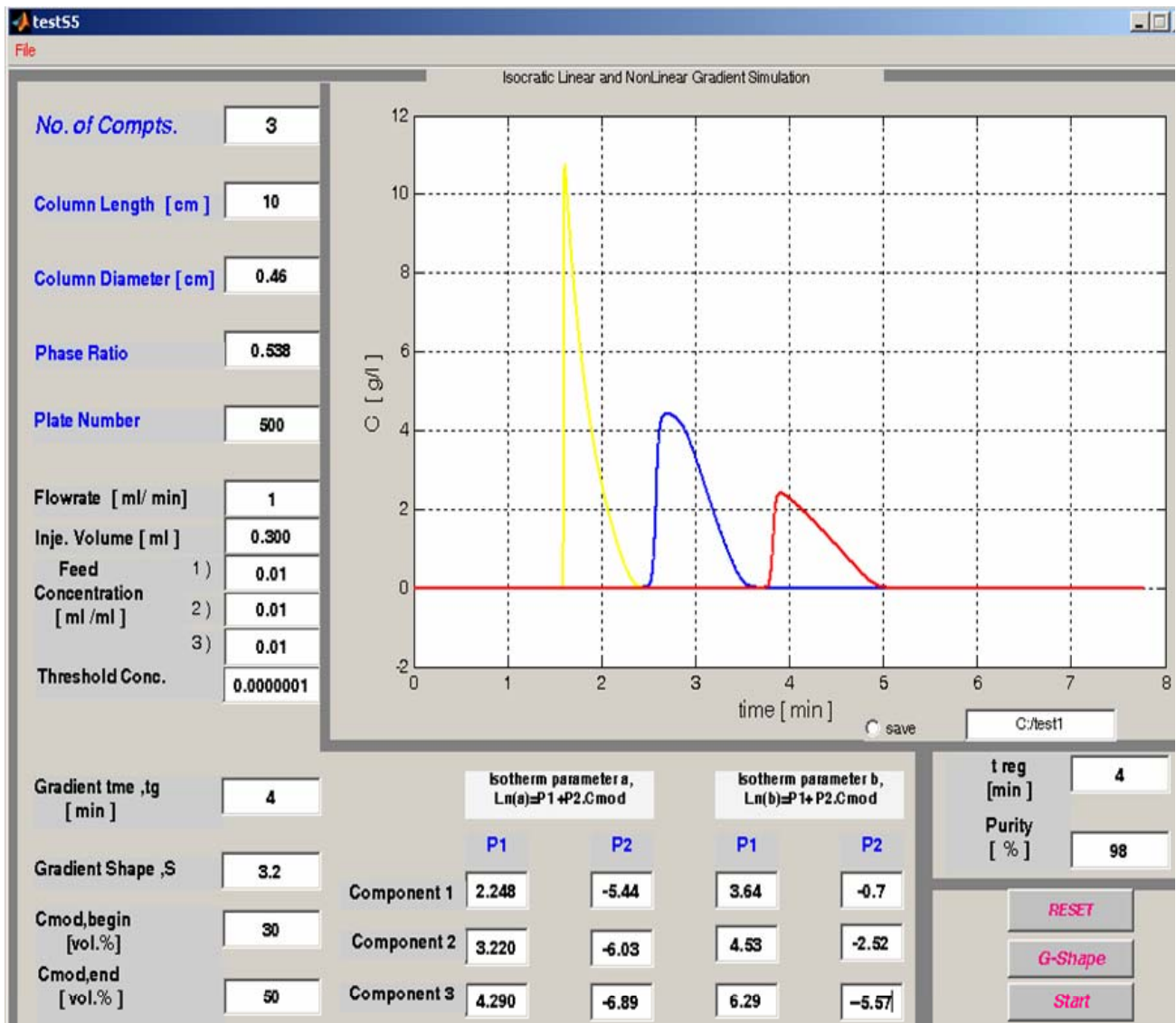
- [Perry97] Robert H. Perry and Don W. Green, Perry's Chemical Engineers' Handbook; McGraw-Hill: New York, USA, 1997.
- [Poole85] C.F. Poole, The Essence of Chromatography; Elsevier: Amsterdam, The Netherlands, 1985.
- [Poole03] Colin F. Poole, The essence of chromatography; Elsevier: Amsterdam, The Netherlands, 2003.
- [Press92] W.H. Press, S.A. Teukolsky, W.T. Vetterling and B.P. Flannery, Numerical Recipes in FORTRAN. The Art of Scientific Computing, Cambridge university press, UK, 1992.
- [Sakod72] K. Sakodynskii, The life and scientific works of Michael Tswett. *Journal of Chromatography A*, **1972**, 73, 303-360.
- [Shan04] Y. Shan, A. Seidel-Morgenstern, Analysis of the isolation of a target component using multicomponent isocratic preparative elution chromatography. *Journal of Chromatography A*, **2004**, 1041, 53-62.
- [Shan05] Yichu Shan and Andreas Seidel-Morgenstern, Optimization of gradient elution conditions in multi-component preparative liquid chromatography. *Journal of Chromatography A*, **2005**, 1093, 47–58.
- [Snyd68] L.R. Snyder, Principles of Adsorption Chromatography; Marcel Dekker: New York, USA, 1968.
- [Snyd07] L. R. Snyder and J. W. Dolan, High-Performance Gradient Elution; Wiley-Interscience: USA, 2006.
- [Socz69] E. Soczewinski, Solvent Composition Effects in Thin-Layer Chromatography Systems of the Type Silica Gel-Electron Donor Solvent. *Anal. Chem.*, **1969**, 41, 179-182.
- [Toth71] G. Tóth and J. Szabolcs, *Acta Chim. Acad. Sci Hung.* **1971**, 69, 311
- [Traub05] H. Schmidt-Traub, Preparative Chromatography; Wiley-VCH: Weinheim, Germany, 2005.
- [Well06] D. A. Wellings, A Practical Handbook of Preparative HPLC; Elsevier: The Netherlands, 2006.
- [Wrig88] A.G. Wright, A.F. Fell and J.C. Berridge, Strategies for automated optimisation of high-performance liquid chromatographic separations incorporating diode-array detection. *Journal of Chromatography A*, **1988**, 458, 335-353.
- [Zhan03] Z. Zhang, M. Mazzotti and M. Morbidelli, Multiobjective optimization of simulated moving bed and Varicol processes using a genetic algorithm. *Journal of Chromatography A*, **2003**, 989, 95-108.

- [Zhan04] Z. Zhang, M. Mazzotti, M. Morbidelli, Continuous Chromatographic Processes with a Small Number of Columns: Comparison of Simulated Moving Bed with Varicol, PowerFeed, and ModiCon. *Korean J. Chem. Eng*, **2004**, 21, 454-464.

Appendix A

Matlab codes used for simulations

Graphical user interface (GUI)



Matlab code

```

Cmod0=0.01*eval(get(handles.cmod0,'string'));
Cmodend=0.01*eval(get(handles.cmodend,'string'));
L=eval(get(handles.L,'string'));
d=eval(get(handles.d,'string'));
F=eval(get(handles.F,'string'));
N=eval(get(handles.NP,'string'));
VF=eval(get(handles.VF,'string'));
Vinj=eval(get(handles.Vinj,'string'));
p1a1=eval(get(handles.p1ofa1,'string'));
p2a1=eval(get(handles.p2ofa1,'string'));
p1a2=eval(get(handles.p1ofa2,'string'));
p2a2=eval(get(handles.p2ofa2,'string'));
p1a3=eval(get(handles.p1ofa3,'string'));
p2a3=eval(get(handles.p2ofa3,'string'));

p1b1=eval(get(handles.p1ofb1,'string'));
p2b1=eval(get(handles.p2ofb1,'string'));
p1b2=eval(get(handles.p1ofb2,'string'));
p2b2=eval(get(handles.p2ofb2,'string'));
p1b3=eval(get(handles.p1ofb3,'string'));
p2b3=eval(get(handles.p2ofb3,'string'));
cfeed1=eval(get(handles.cfeed1,'string'));
cfeed2=eval(get(handles.cfeed2,'string'));
cfeed3=eval(get(handles.cfeed3,'string'));
cthreshold=eval(get(handles.cthreshold,'string'));
tg=eval(get(handles.tgradient,'string'));
s=eval(get(handles.s,'string'));
% _____
Purity=0.01*eval(get(handles.purity,'string'));
treg=eval(get(handles.treg,'string'));
% _____

eta=1/(1+F);
a3=exp(p1a3+p2a3*Cmod0);
Vcol=(pi*d^2)*L/4;

to=Vcol*eta/VF;
tinj=Vinj/VF;
dt=to/N;
K1=round(tg/dt);
% _____
i=1;
tr=1.25*to*(1+F*a3);
K=round(tr/dt);
M=round(tinj/dt);
% _____
c1=zeros(K,N);
c2=zeros(K,N);
c3=zeros(K,N);
% i=1:1:M
c1(1:M,1)=cfeed1;
c2(1:M,1)=cfeed2;

```

```

c3(1:M,1)=cfeed3;
% i=M:1:K
c1(M+1:K+1,1)=0;
c2(M+1:K+1,1)=0;
c3(M+1:K+1,1)=0;
% j=2:1:N
c1(1,2:N)=0;
c2(1,2:N)=0;
c3(i,2:N)=0;
%
hh=waitbar(0,'Please wait a moment...');
%
part1=ones(K1,N).*Cmod0;
part2=ones(K-K1,N).*Cmodend;
Cmod=[part1;part2];
for j=1:N;
    for i=j:(K1+j);
        Cmod(i,j)=Cmod0+(Cmodend-Cmod0)*((i-j)/K1)^s;
    end
end
a1=exp(p1a1+p2a1*Cmod);
a2=exp(p1a2+p2a2*Cmod);
a3=exp(p1a3+p2a3*Cmod);
b1=exp(p1b1+p2b1*Cmod);
b2=exp(p1b2+p2b2*Cmod);
b3=exp(p1b3+p2b3*Cmod);
%

i=1;
j=2;
while i<(K+1);
    for j=2:N;
        x0=0.95*c1(i+1,j-1);
        y0=0.95*c2(i+1,j-1);
        z0=0.95*c3(i+1,j-1);
        fx=x0+F*a1(i,j)*x0/(1+b1(i,j)*x0+b2(i,j)*y0+b3(i,j)*z0)-c1(i,j-1)-
F*a1(i,j)*c1(i,j)/(1+b1(i,j)*c1(i,j)+b2(i,j)*c2(i,j)+b3(i,j)*c3(i,j));
        gx=y0+F*a2(i,j)*y0/(1+b1(i,j)*x0+b2(i,j)*y0+b3(i,j)*z0)-c2(i,j-1)-
F*a2(i,j)*c2(i,j)/(1+b1(i,j)*c1(i,j)+b2(i,j)*c2(i,j)+b3(i,j)*c3(i,j));
        hx=z0+F*a3(i,j)*z0/(1+b1(i,j)*x0+b2(i,j)*y0+b3(i,j)*z0)-c3(i,j-1)-
F*a3(i,j)*c3(i,j)/(1+b1(i,j)*c1(i,j)+b2(i,j)*c2(i,j)+b3(i,j)*c3(i,j));
        dfx=1+F*a1(i,j)/(1+b1(i,j)*x0+b2(i,j)*y0+b3(i,j)*z0)-
F*a1(i,j)*b1(i,j)*x0/(1+b1(i,j)*x0+b2(i,j)*y0+b3(i,j)*z0)^2;
        dgx=1+F*a2(i,j)/(1+b1(i,j)*x0+b2(i,j)*y0+b3(i,j)*z0)-
F*a2(i,j)*b2(i,j)*y0/(1+b1(i,j)*x0+b2(i,j)*y0+b3(i,j)*z0)^2;
        dhx=1+F*a3(i,j)/(1+b1(i,j)*x0+b2(i,j)*y0+b3(i,j)*z0)-
F*a3(i,j)*b3(i,j)*z0/(1+b1(i,j)*x0+b2(i,j)*y0+b3(i,j)*z0)^2;
        x1=x0-fx/dfx; y1=y0-gx/dgx; z1=z0-hx/dhx;
        while (abs(x1-x0)>cthreshold|abs(y1-y0)>cthreshold|abs(z1-z0)>cthreshold)
            x0=x1;y0=y1;z0=z1;
            fx=x0+F*a1(i,j)*x0/(1+b1(i,j)*x0+b2(i,j)*y0+b3(i,j)*z0)-c1(i,j-1)-
F*a1(i,j)*c1(i,j)/(1+b1(i,j)*c1(i,j)+b2(i,j)*c2(i,j)+b3(i,j)*c3(i,j));
            gx=y0+F*a2(i,j)*y0/(1+b1(i,j)*x0+b2(i,j)*y0+b3(i,j)*z0)-c2(i,j-1)-
F*a2(i,j)*c2(i,j)/(1+b1(i,j)*c1(i,j)+b2(i,j)*c2(i,j)+b3(i,j)*c3(i,j));
            hx=z0+F*a3(i,j)*z0/(1+b1(i,j)*x0+b2(i,j)*y0+b3(i,j)*z0)-c3(i,j-1)-
F*a3(i,j)*c3(i,j)/(1+b1(i,j)*c1(i,j)+b2(i,j)*c2(i,j)+b3(i,j)*c3(i,j));

```



```

    dfx=1+F*a1(i,j)/(1+b1(i,j)*x0+b2(i,j)*y0+b3(i,j)*z0)-
F*a1(i,j)*b1(i,j)*x0/(1+b1(i,j)*x0+b2(i,j)*y0+b3(i,j)*z0)^2;
    dgx=1+F*a2(i,j)/(1+b1(i,j)*x0+b2(i,j)*y0+b3(i,j)*z0)-
F*a2(i,j)*b2(i,j)*y0/(1+b1(i,j)*x0+b2(i,j)*y0+b3(i,j)*z0)^2;
    dhx=1+F*a3(i,j)/(1+b1(i,j)*x0+b2(i,j)*y0+b3(i,j)*z0)-
F*a3(i,j)*b3(i,j)*z0/(1+b1(i,j)*x0+b2(i,j)*y0+b3(i,j)*z0)^2;
    x1=x0-fx/dfx;
    y1=y0-gx/dgx;
    z1=z0-hx/dhx;
end
    c1(i+1,j)=x1;c2(i+1,j)=y1;c3(i+1,j)=z1;
end
waitbar(i/K)
i=i+1;
end
close(hh)

%_____

i=1:K;

plot(i*dt,948*c1(i,N),'y',i*dt,950*c2(i,N),'b',i*dt,951*c3(i,N),'r','LineWidth',2);
grid on;
xlabel('time [ min ]','FontSize',12);
ylabel('C [ g/l ]','FontSize',12);
itdmin2=1;
while (c2(itdmin2,N)<cthreshold);
    itdmin2=itdmin2+1;
end
itdmin2;
itdmin1=1;
while (c1(itdmin1,N)<cthreshold);
    itdmin1=itdmin1+1;
end
itdmin1;

itdmin3=1;
while (c3(itdmin3,N)<cthreshold);
    itdmin3=itdmin3+1;
end
itdmin3;

%_____
% 2nd Maximum threshold point of the target component
itdmax2=K;
while (c2(itdmax2,N)<cthreshold);
    itdmax2=itdmax2-1;
end
itdmax2;
%_____
itdmax1=K;
while (c1(itdmax1,N)<cthreshold);
    itdmax1=itdmax1-1;
end
itdmax1;

```

```

cmax1=max(c1(i,N));
cmax2=max(c2(i,N));
cmax3=max(c3(i,N));
i=1;
%finding the ,time at the max concentration
while i<K+1;
    if cmax2-c2(i,N)==0;
        imax2=i;
    end
    i=i+1;
end
imax2;
%
if imax2<itdmax1;
    i=itdmax1+5;im=itdmax1+5;
elseif imax2==itdmax1|imax2>itdmax1;
    i=imax2+5;im=imax2+5;
end
sum1=0;
while i<(itdmax2+1); % right side area of the target component
    sum1=sum1+c2(i+1,N)*dt;
    i=i+1;
end
if imax2<itdmax1;
    i=itdmax1+5;im=itdmax1+5;
elseif imax2==itdmax1|imax2>itdmax1;
    i=imax2+5;im=imax2+5;
end
%40;
sum2=0; %left side area of the target component
while i>(itdmin2-1);
    sum2=sum2+c2(i-1,N)*dt;
    i=i-1;
end
pkarea=sum1+sum2;
%
% adding the yields
s1=c2(im+1,N)*dt;
s1t=c1(im+1,N)*dt+c2(im+1,N)*dt+c3(im+1,N)*dt;
sumr=s1;
sumt=s1t;
p=sumr/sumt;
x=2;
if p>Purity
    while (p>Purity & (x+im)<K);
        sumr =sumr+c2(im+x,N)*dt;
        sumt =sumt+c2(im+x,N)*dt+c1(im+x,N)*dt+c3(im+x,N)*dt;
        p=sumr/sumt;
        x=x+1;
    end
    x=x-1;
    sumr =sumr-c2(im+x,N)*dt;
    sumt =sumt-c2(im+x,N)*dt-c1(im+x,N)*dt-c3(im+x,N)*dt;
    p=sumr/sumt;

% adding the left side
p=sumr/sumt;

```

```

y=1;
while (p>Purity & (im-y)>0);
    sumr=sumr+c2(im-y,N)*dt;
    sumt=sumt+c1(im-y,N)*dt+c2(im-y,N)*dt+c3(im-y,N)*dt;
    p=sumr/sumt;
    y=y+1;
end
p;
sum1;
sum2;
sumr;
yield=sumr*100/pkarea
%'
else
    ' zero yield for the required purity';
    yield=0
end
%-----Calculating cycle time-----
itdmax3=K;
while (c3(itdmax3,N)<cthreshold);
    itdmax3=itdmax3-1;
end
%_____dotnettool_____
prod=(yield/100)*Vinj*cfeed2*rho*1000/(((pi*d^2)/4)*eta*cycletime)
OF=yield*prod/100
dt
function pushbutton2_Callback(hObject, eventdata, handles)
    eta=0.65;
    L=10;d=0.46;
    Vcol=(pi*d^2)*L/4;
    tg=eval(get(handles.tgradient,'string'));
    VF=eval(get(handles.VF,'string')); %input ('flow rate ml / min');
    N=eval(get(handles.NP,'string'));
    Cmod0=0.01*eval(get(handles.cmod0,'string'));
    Cmodend=0.01*eval(get(handles.cmodend,'string'));
    to=Vcol*eta/VF;dt=to/N;
    F=(1-eta)/eta;
    a3=exp(4.171-6.710*Cmod0)
    tr=1.5*to*(1+F*a3);
    K=round(tr/dt);TG=round(tg/dt);
    s=eval(get(handles.s,'string'));

y=round(to/dt);
i=1:y-1;
Cmodifier(i,1)=Cmod0;
i=y:TG+y-1;
Cmodifier(i,1)=Cmod0+(Cmodend-Cmod0)*((i-y)/(TG-1)).^(s);
% subplot(2,1,2);
i=TG+y:1.25*(TG+y);
Cmodifier(i,1)=Cmodend;
i=1:(1.25*(y+TG));
plot(i*dt,100*Cmodifier(i,1),'b','LineWidth',2);grid on;
% text((TG+y)*dt/2,40,' G-shape for S= ',num2str(s))
xlabel('time [ min ]','FontSize',12);
ylabel('C modifier [ vol. % ]','FontSize',12);

```

Appendix B

Programming gradient profiles

I. Convex gradient $S=0.25$

Pump A: 30:70, Methanol: water
Pump B: 40:60, Methanol: water
Gradient time $t_g=4$ min.

Time	Module	Device	Value
0.01	Pump	Pump A	1
0.01	Pump	Pump B	0
0.01	SCL-10Avp	SV	0
0.01	Pump	Pump A	0.6
0.01	Pump	Pump B	0.4
0.01	SCL-10Avp	SV	0
0.52	Pump	Pump A	0.4
0.52	Pump	Pump B	0.6
0.52	SCL-10Avp	SV	0
1.63	Pump	Pump A	0.8
1.63	Pump	Pump B	0.2
1.63	SCL-10Avp	SV	0
4.00	Pump	Pump A	0
4.00	Pump	Pump B	1
4.00	SCL-10Avp	SV	0

II. Linear gradient $S=1$

Pump A: 30:70, Methanol: water
Pump B: 40:50, Methanol: water
Gradient time $t_g=4$ min.

Time	Module	Device	Value
0.01	Pump	Pump A	1
0.01	Pump	Pump B	0
0.01	SCL-10Avp	SV	0
4.00	Pump	Pump A	0
4.00	Pump	Pump B	1
4.00	SCL-10Avp	SV	0

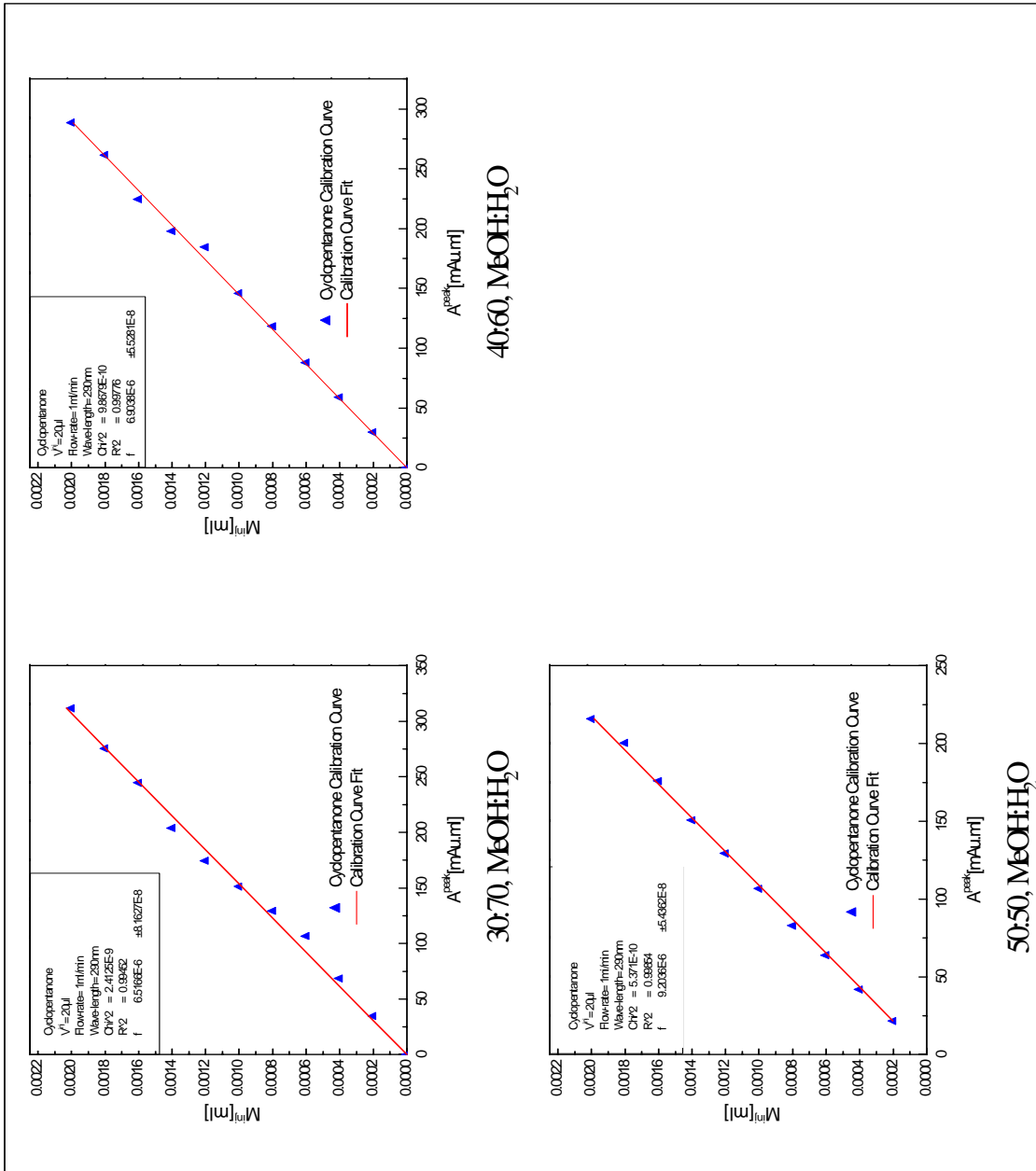
III. Concave gradient $S=3.2$

Pump A: 30:70, Methanol: water
 Pump B: 40:50, Methanol: water
 Gradient time $t_g=1.1$ min.

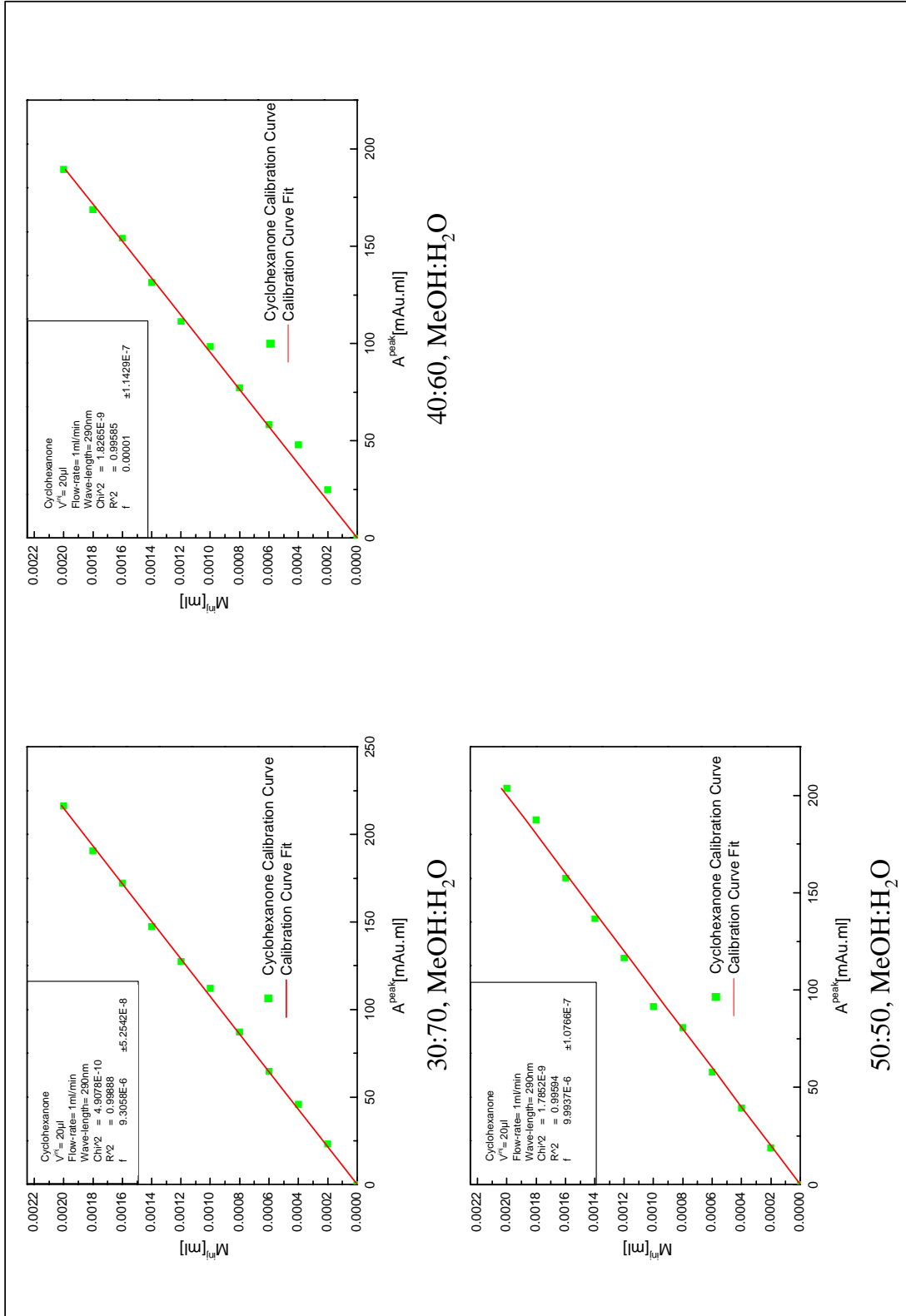
Time	Module	Device	Value
0.01	Pump	Pump A	1
0.01	Pump	Pump B	0
0.01	SCL-10Avp	SV	0
0.30	Pump	Pump A	1
0.30	Pump	Pump B	0
0.30	SCL-10Avp	SV	0
0.54	Pump	Pump A	0.9
0.54	Pump	Pump B	0.1
0.54	SCL-10Avp	SV	0
0.66	Pump	Pump A	0.8
0.66	Pump	Pump B	0.2
0.66	SCL-10Avp	SV	0
0.83	Pump	Pump A	0.6
0.83	Pump	Pump B	0.4
0.83	SCL-10Avp	SV	0
0.98	Pump	Pump A	0.3
0.98	Pump	Pump B	0.7
0.98	SCL-10Avp	SV	0
1.10	Pump	Pump A	0
1.10	Pump	Pump B	1
1.10	SCL-10Avp	SV	0

Appendix C

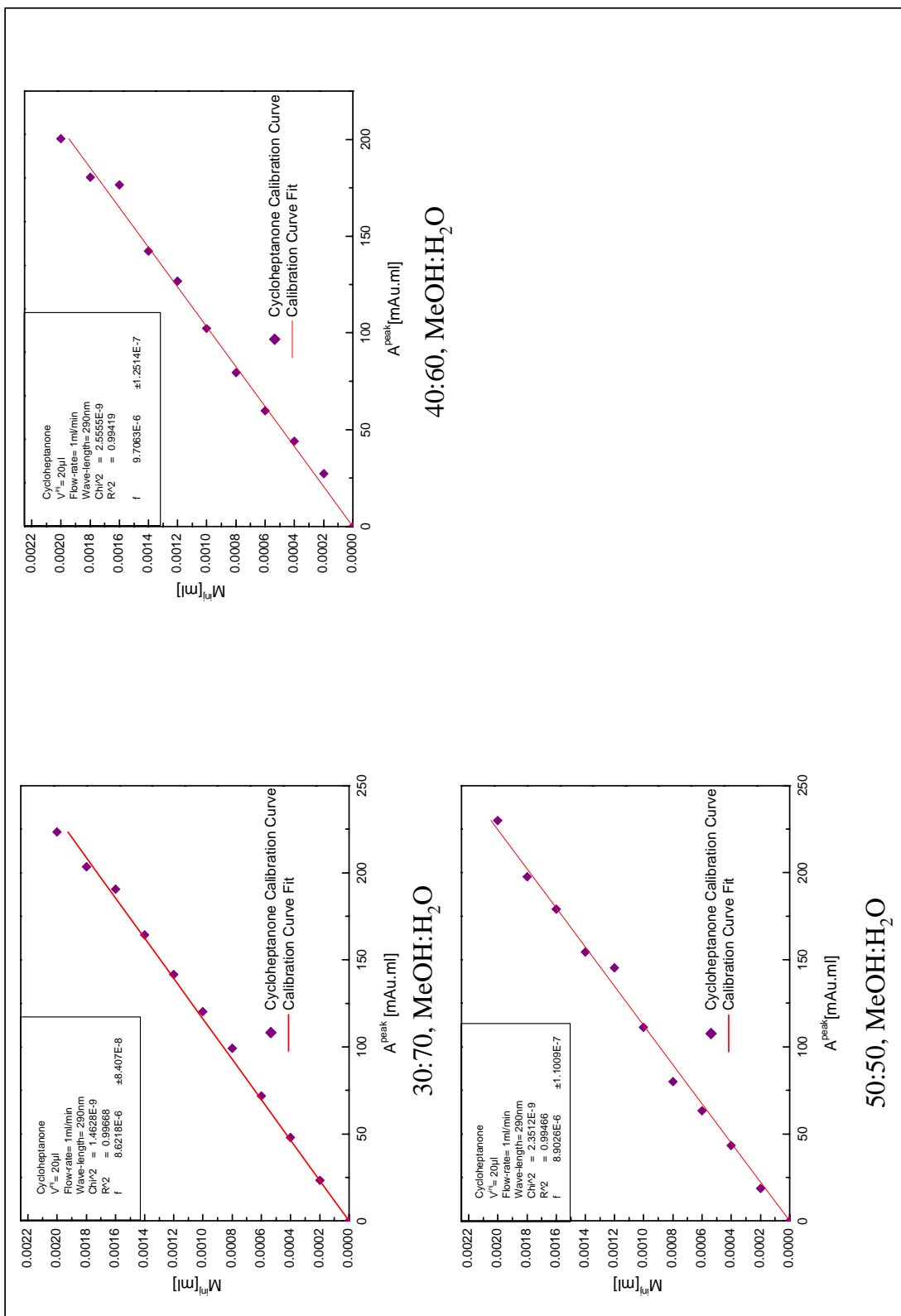
Calibration curves



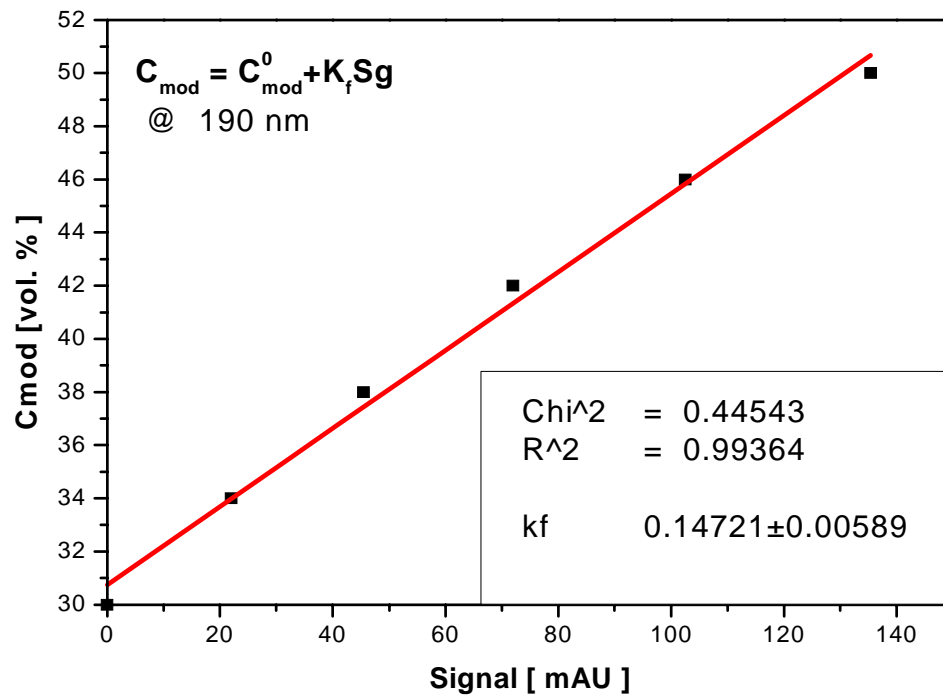
Cyclopentanone



Cyclohexanone



Cycloheptanone



Methanol

Appendix D

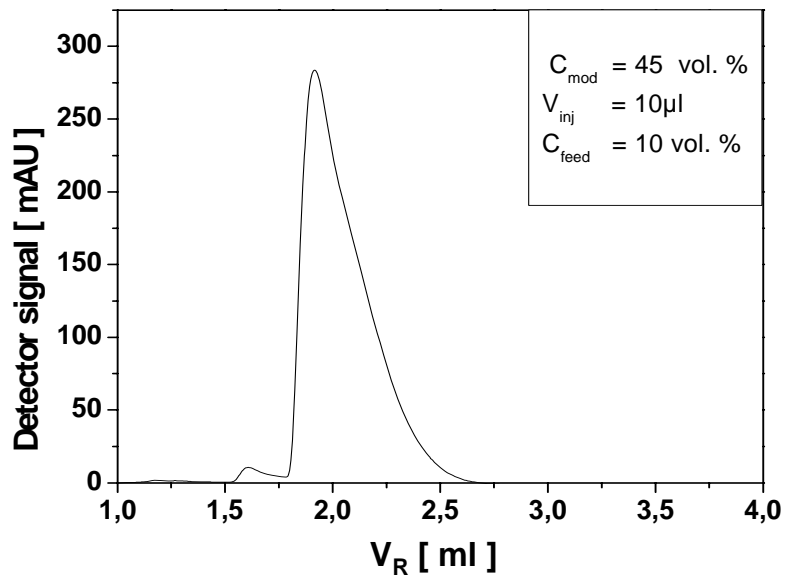
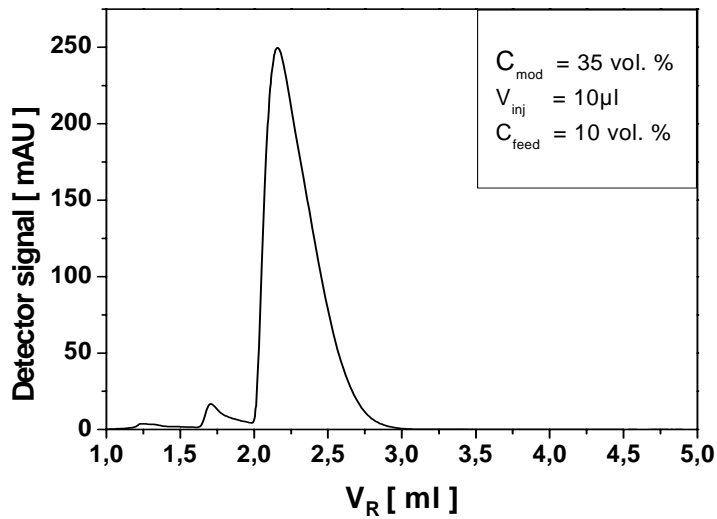
Theoretical plate numbers

Component	Solvent composition Methanol: Water [vol. %]	Plate Number, N
Cyclopentanone	30:70	316.73
	40:60	246.05
	50:50	242.85
Cyclohexanone	30:70	369.58
	40:60	282.88
	50:50	245.32
Cycloheptanone	30:70	661.54
	40:60	389.69
	50:50	371.52

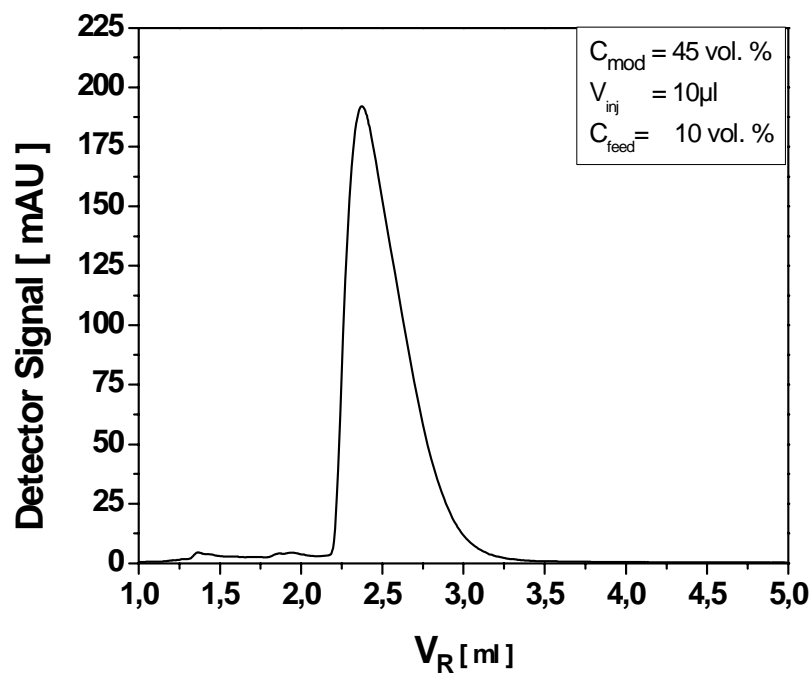
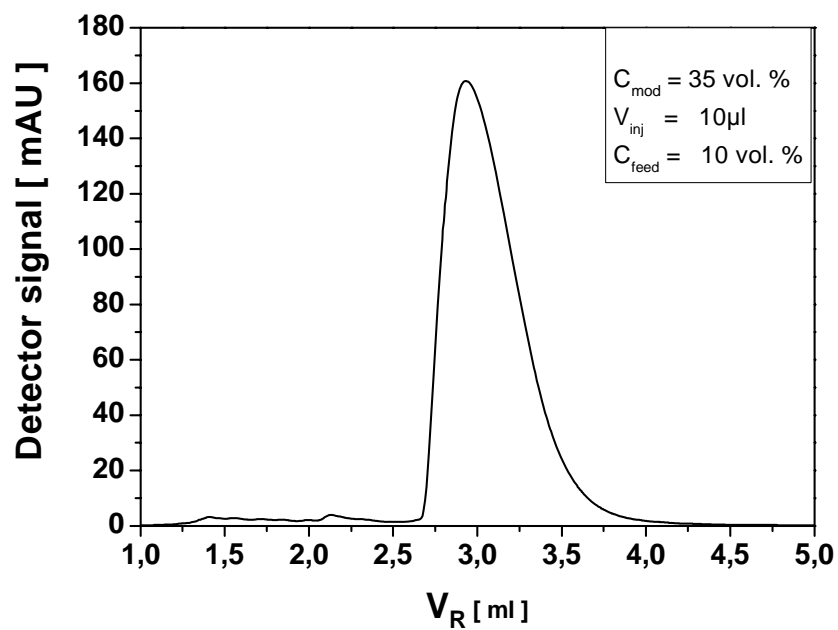
Average plate numbers

Appendix E

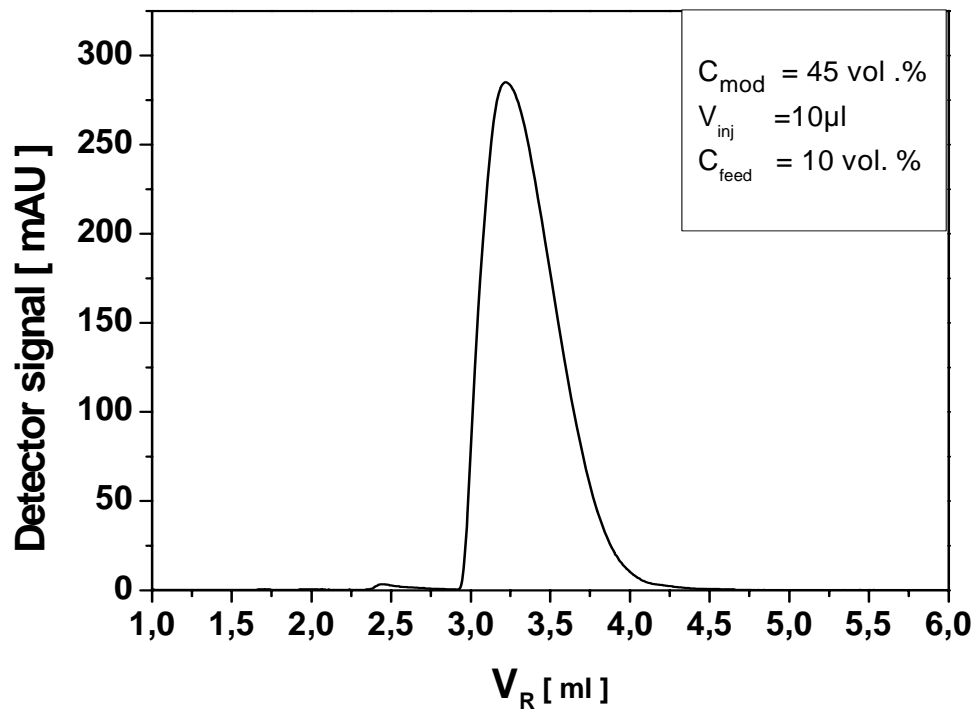
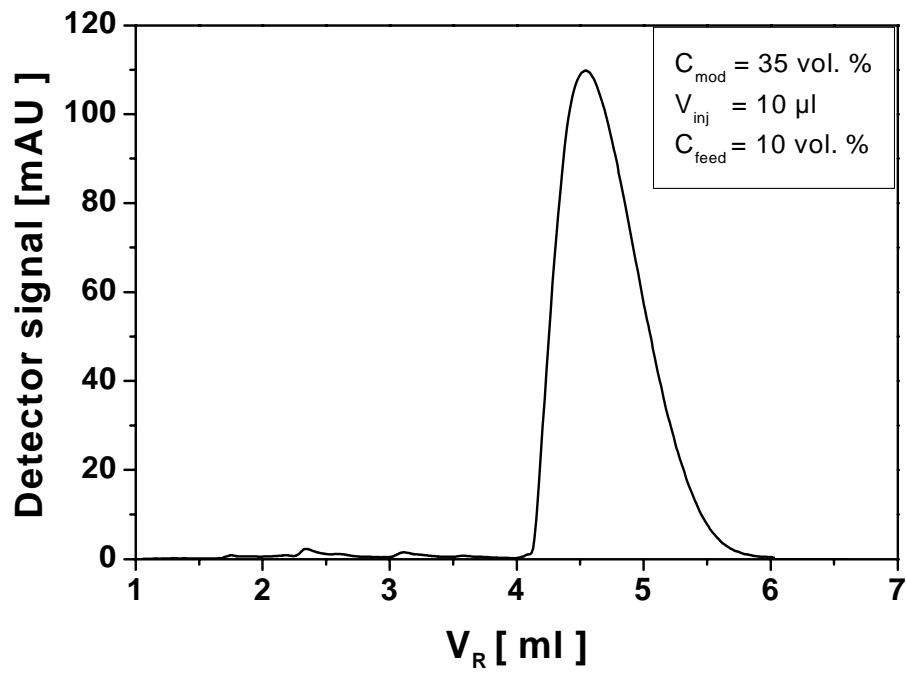
Overloaded peaks



Cyclopentanone



Cyclohexanone



Cycloheptanone

CURRICULUM VITAE

Personal Information:

First Name: Andualem

Last Name: Damtew Hamza

Address:

Rögatzer str 5A, 4.18
39106 Magdeburg Germany

Telephone:

+49 (0) 176 / 82165392 (mobile)
+49 (0) 391 / 2428442 (home)
+49 (0) 391 / 6712198 (Office)

E-mail:

anduex@yahoo.com
andualem.damtew@st.ovgu.de

Date of Birth: August 17, 1975

Nationality: Ethiopian

Language Proficiency:

English – (fluent)
German - (basic)
Amharic – (Mother tongue)

Education:

January 2006 - present

Otto-von-Guericke-Universität Magdeburg and Max Planck Institute of Magdeburg, Magdeburg, Germany

PhD student in the Faculty of Process and Chemical Engineering

Institute of Chemical Process Engineering

Title of Dissertation

“Analysis of the potential of nonlinear solvent gradients in preparative chromatography”

February 2004 – December 2005

Otto-von-Guericke-Universität Magdeburg, Magdeburg, Germany

Research assistant in the Faculty of Process and Chemical Engineering

Institute of Chemical Process Engineering

October 2002- October 2003

Otto-von-Guericke-Universität Magdeburg, Magdeburg, Germany

M.Sc. In Quality and Safety and Environment

Title of the master's thesis

“Safety analysis of pressurized storage of hydrogen”

September 1994 – July 1999
Addis Ababa University, Addis Ababa, Ethiopia
B.Sc. in Chemical Engineering

Professional Experience:

February, 2000 – July, 2002 as Chemical Engineer of the Plant
ELICO-Awash Tannery, Addis Ababa, Ethiopia

September, 1999 – February, 2000 as Quality Control Chemist
Nefas Silk Paints Factory, Addis Ababa, Ethiopia

Certificates and Trainings:

Certificate of German language attended for 180 hours

Certificate of participation in introductory training program on Cleaner Production

Certificate of participation in advanced training program on Cleaner Production

IT Skills:

Programming Languages:

Pascal, Matlab, html basics

Platforms & software:

Windows 95/98/NT/2K/XP, MS Office